EVALUATION OF TANTALUM/316 STAINLESS STEEL TRANSITION JOINTS

BY

D. R. STONER

WESTINGHOUSE ASTRONUCLEAR LABORATORY

prepared for

NATIONAL AERONAUTICS AND SPACE ADMINISTRATION

NASA Lewis Research Center

NOTICE

This report was prepared as an account of Government-sponsored work. Neither the United States, nor the National Aeronautics and Space Administration (NASA), nor any person acting on behalf of NASA:

A.)   Makes any warranty or representation, expressed or implied, with respect to the accuracy, completeness, or usefulness of the information contained in this report, or that the use of any information, apparatus, method, or process disclosed in this report may not infringe privately-owned rights; or

B.)   Assumes any liabilities with respect to the use of, or for damages resulting from the use of, any information, apparatus, method or process disclosed in this report.

As used above, "person acting on behalf of NASA" includes any employee or contractor of NASA, or employee of such contractor, to the extent that such employee or contractor of NASA or employee of such contractor prepares, disseminates, or provides access to any information pursuant to his employment or contract with NASA, or his employment with such contractor.

Request for copies of this report should be referred to

    National Aeronautics and Space Administration
    Scientific and Technical Information Facility
    P. O. Box 33
    College Park, Maryland 20740

1. Report No. NASA CR-121111	2. Government Accession No.	3. Recipient's Catalog No.
4. Title and Subtitle Evaluation of Tantalum/316 Stainless Steel Transition Joints		5. Report Date December, 1972
		6. Performing Organization Code
7. Author(s) D. R. Stoner		8. Performing Organization Report No. WANL-M-FR-72-006
		10. Work Unit No.
9. Performing Organization Name and Address Westinghouse Astronuclear Laboratory P. O. Box 10864 Pittsburgh, Pa. 15236		11. Contract or Grant No. NAS 3-13444
12. Sponsoring Agency Name and Address NASA Lewis Research Center 21000 Brookpark Road Cleveland, Ohio 44135		13. Type of Report and Period Covered Contractor Report
		14. Sponsoring Agency Code

15. Supplementary Notes

NASA Project Manager: Phillip L. Stone, Materials & Structures Division

16. Abstract

Tubular transition joints providing a metallurgically bonded connection between tantalum and 316 stainless steel pipe sections were comparatively evaluated for durability under thermal cycling conditions approximating the operation of a SNAP-8 mercury boiler. Both coextruded and vacuum brazed transition joints of 50 mm (2 inch) diameter were tested by thermal cycling 100 times between 730°C and 120°C (1350°F and 250°F) in a high vacuum environment. The twelve evaluated transition joints survived the full test sequence without developing leaks, although liquid penetrant bond line indications eventually developed in all specimens. The brazed transition joints exhibited the best dimensional stability and bond line durability.

17. Key Words (Suggested by Author(s)) Bimetal joints Co-extrusion	18. Distribution Statement

19. Security Classif. (of this report) Unclassified	20. Security Classif. (of this page) Unclassified	21. No. of Pages	22. Price*

FOREWORD

This report describes work performed under Contract NAS 3-13444 during the period of July, 1969 to July, 1971. The experimental program was administered under the Lewis Research Center of the National Aeronautics and Space Administration with Mr. Phillip L. Stone acting as the project manager.

This work was administered at the Astronuclear Laboratory by Mr. R. W. Buckman with Mr. D. R. Stoner serving as the principal investigator.

The author gratefully acknowledges the contribution of the following people to the successful completion of the program.

> Metallography – K. Galbraith
> Thermal Cycle Apparatus and
> Control Circuit Design and Construction – R. E. Sabolcik
> Ultrasonic Testing – M. Demczyk
> Electron Beam Microprobe – R. W. Conlin, A. Danko

TABLE OF CONTENTS

LIST OF TABLES

LIST OF FIGURES

LIST OF FIGURES (CONTINUED)

LIST OF FIGURES (CONTINUED)

SUMMARY

Tubular transition joints providing a metallurgically bonded connection between tantalum and 316 stainless steel pipe sections were compared for as-fabricated quality and for resistance to thermal cycling. Three types of transition joints were evaluated: a cobalt-base brazed tongue-in-groove design and two variations of a coextruded design. Of the co-extruded pair, one was a sleeve design which was basically a heavy walled bimetallic tube later machined to a tube-to-header joint configuration, and the other was a tandem or tapered interface design.

The 50 mm (2 inch) diameter transition joints were thermal cycled 100 times between 730°C and 120°C (1350 to 250°F). The thermal cycling, which included a total exposure time of up to 1600 hours at 730°C (1350°F), was designed to simulate the operating conditions of a SNAP-8 mercury boiler. An ion pumped, high vacuum test environment was used, to prevent contamination of the tantalum section of the transition joints during thermal cycling and thermal exposure.

All three types of transition joints survived the full test sequence and remained helium leak tight although the two types of coextruded transition joints developed bond line fissures as the thermal cycle tests progressed. The coextruded transition joints also experienced severe diametral contraction in the bimetal butt joint area. In view of these results, the brazed transition joint is recommended for service in applications similar to that of the SNAP-8 mercury boiler.

I. INTRODUCTION

The purpose of this investigation was to make a comparative evaluation of the bond durability of three types of tantalum to stainless steel transition joint   The test conditions were keyed to the mercury boiler requirements of the SNAP-8[1] nuclear power system, and the prime intent was to select the best bimetallic joint for this mercury boiler.

The tubular transition joints were designed to provide a leak tight, metallurgically bonded tube joint between tantalum and 316 stainless steel.   Tantalum is required for corrosion resistance in a 730°C (1350°F) tube-in-tube mercury boiler which must be joined to an iron base alloy turbine loop.   The use of prefabricated tubular transition joints thus permits conventional tantalum and stainless steel welding techniques to be used at either side of the transition area.

Of the several processes which are capable of providing a sound, metallurgically bonded joint between tantalum and 316 stainless steel, hot coextrusion and cobalt base alloy brazing were selected for evaluation because of previous favorable fabrication experience.   Two types of coextruded joints were evaluated: a tube within a tube sleeve joint and a butt joint with a tapered interface.

Thermal cycling over the expected SNAP-8 boiler operating range 120°C to 730°C (250°F to 1350°F) was selected as the basic durability test because it was felt that the large difference in coefficient of thermal expansion between tantalum and 316 stainless steel (about 2-1/2 to 1) could lead to bond deterioration.

The relatively slow heating and cooling rate thermal cycle test (2 hours heating, 2 hours cooling, 10 hours hold at temperature) was designed to simulate the normal operating mode of the SNAP-8 system. A clean, ion pumped high vacuum environment of 10^{-7} to 10^{-9} torr

was used in conjunction with a low thermal inertia hot wall furnace for the thermal cycle test. The joints were tested in an open and in a sealed, internally pressurized condition. The evaluation included as-fabricated dimensional inspection to determine the process control provided by the various techniques.

Since the primary function of the transition joint was the containment of boiling mercury, the sensitive helium leak test was used as the primary inspection mode both for the as-fabricated transition joints and for the sequential thermal cycle test. The 100 cycle exposure was interrupted after 5, 10, 30, and 50 cycles, and nondestructive inspection was performed to follow gradual degrading modes of joint failure.

Ultrasonic inspection techniques were developed both to determine the as-fabricated bond integrity and to follow bond degradation as the thermal cycle tests progressed.

During the fabrication of refractory metal to stainless steel transition joints, care must be taken to avoid the formation of extensive diffusion zones between the dissimilar metals. The diffusion zones are characterized by brittle intermetallic compounds which may lead to joint failure. A marked decrease in bimetal joint strength when the interdiffusion zone reaches a thickness of 12.7 μm (0.5 x 10^{-3} inches) had been observed in a previous evaluation[2]. Bimetal transition joints are commonly used at elevated temperature where interdiffusion may enlarge a thin as-fabricated diffusion zone to troublesome proportions. The growth of the brittle intermetallic during service will be a function of the operating temperature and time, which, in the case of the SNAP-8 boiler, is approximately 730°C (1350°F) and at least five years. The interdiffusion zone dimensions were measured in the as-fabricated condition and following 1600 hours of 730°C (1350°F) thermal cycling. Five year growth predictions were made based on the short time test data.

In summary, this program was intended to compare the durability of three types of bimetal transition joints (sleeve joint-hot extrusion, tandem joint-hot extrusion, and brazed joints), and to select the best process for the SNAP-8 mercury boiler. The hot extruded transition joints were made for NASA by the Nuclear Metals Division of Whittaker Corporation, and the brazed joints were made by Nuclear Systems Programs, Space Division of the General Electric Company.

II. BACKGROUND

The SNAP-8 nuclear power system was designed by NASA to use a nuclear reactor heat source to power a mercury turbo-electric generator[1]. A NaK primary coolant loop transfers the reactor heat to vaporize mercury in a once-through tube-in-tube mercury boiler. Though the entire mercury-NaK heat transfer system was designed to use conventional iron base stainless steels and superalloys, component tests indicated severe corrosion problems on the mercury side of the mercury boiler. Unalloyed tantalum was identified as having excellent corrosion resistance to mercury, but not to the NaK primary coolant so two boiler designs evolved which interfaced tantalum to mercury and 316 stainless steel to NaK. The initial design utilized tantalum lined stainless steel tubing. Several fabrication development programs were completed in which small diameter 1.9 cm (3/4 inch) bimetal boiler tubes were made by explosive bonding, hot extrusion and cold drawing, and direct hot extrusion to final size[3]. Results of fabrication and welding studies assured that hardware could be made from double layer stainless-tantalum tubing[4]. Adequate resistance to thermal cycle unbonding was only provided by hot extruding directly to final size, and a successful process was identified[3].

The final boiler design utilized a double containment concept wherein tantalum boiler tubes were isolated from the flowing primary loop NaK by a larger diameter stainless steel tube. The annulus between the stainless steel and tantalum tubes was filled with nonflowing NaK to satisfy the heat transfer requirements. In order to contain all tantalum surfaces within a protective stainless steel boiler shell, large diameter transition joints from tantalum to 316 stainless steel were required which are the subject of this evaluation program. A complete description of the double containment boiler, which was fabricated and operated successfully for 15,000 hours, is provided in a SNAP-8 report[5].

To provide sufficient hardware for boiler fabrication immediately after an optimum fabrication process was selected, thirty-six (36) transition joints were prepared; twelve (12) each by three different techniques. Two variations of hot extrusion and a cobalt base alloy brazing technique were chosen as the three processes. Each of the 36 transition joints were nondestructively evaluated to assess the as-fabricated quality. Four transition joints were selected from each lot and were destructively and nondestructively evaluated to provide a measure of process reproducibility.

In parallel with this program, thermal shock tests, using high flow velocity mercury systems, were made on similar brazed and tandem transition joints[6]. A 10 cm (2.5 inch) diameter braze joint survived 150 thermal shocks without apparent damage while a tandem joint developed leaks at the bimetal interface. Failures during high temperature (730°C/1300°F) tensile tests of brazed joint configurations occurred in either parent metal (tantalum or stainless steel) depending on joint design and adequacy of the braze[7]. In addition to the specific tensile and shock tests, J-8400 brazed joints have been employed in mercury boiler tests with good results both from a corrosion and structural standpoint.

Outside of the direct SNAP-8 experience, tandem transition joints of a wide range of materials and sizes have been made for nuclear, chemical, and aerospace applications. At the Westinghouse Astronuclear Laboratory, tandem transition joints of Ta-10w/oW and 316 stainless steel have been in service for over one year in thermoelectric modules with excellent results[8]. These 2.5 cm (1 inch) diameter joints were hot coextruded by the Nuclear Metals Division of the Whittaker Corporation. Four thermoelectric modules, each containing two tandem transition joints as a NaK containment and structural member, have been in operation from 9000 to 12,000 hours at 605°C (1125°F) including 50 rapid thermal cycles from 605 to 260°C (1125 to 500°F) without a single leak-through failure. Although the transition joints could not be examined for signs of progressive bond failures until the test program is complete, an identical tandem transition joint was tested for 2500 hours at 605°C (1125°F) and thermal cycled 50 times with no evidence of diametral contraction or bond line fissuring.

III. MATERIALS EVALUATED

Three types of 316 stainless steel to tantalum transition joints were evaluated for thermal cycle durability. Figure 1 shows the open and pressure sealed versions of the 50.0 mm (2.00 inch) diameter transition joints. From left to right in Figure 1 the transition joints are a sleeve joint, with a header plate simulating flange welded in place, a tandem joint, and a tongue and groove brazed joint. The sleeve joint and tandem joint were made by hot extrusion over a fixed mandrel, and the brazed joint was vacuum brazed using a high temperature cobalt base alloy. Although all three types of transition joints were in competition to provide a leak tight union between 316 stainless steel and tantalum, the sleeve joint was also useful as a header joint for a heat exchanger; hence, the welded flange simulating the header plate stress conditions.

Hot Coextruded Joints – The hot coextruded joints were made by the Nuclear Metals Division of the Whittaker Corporation for NASA Lewis under Contract No. NAS 3-11847, and the complete fabrication details are described in NASA CR 72761[9]. The tantalum lined sleeve joints were made by assembling a tantalum cylinder inside a stainless steel cylinder, canning the assembly in a carbon steel container, evacuating, and hot extruding over a tool steel mandrel. The tandem joints were made by butting a tantalum cylinder to a stainless steel cylinder and similarly vacuum canning the assembly in carbon steel and hot extruding over a mandrel. To provide the completed tapered transition length of 3.8 cm (1-1/2 inches), an initial bevel was provided between the tantalum and stainless steel components. The extrusion details are summarized in Table 1. Following extrusion, the carbon steel cladding was removed by selective pickling, and the transition joints were machined.

Previous bimetal tubing evaluation programs[3] had indicated that the final metal working operation should be high temperature deformation to maintain acceptable bimetal bonding, and consequently no cold working operations were performed following extrusion.
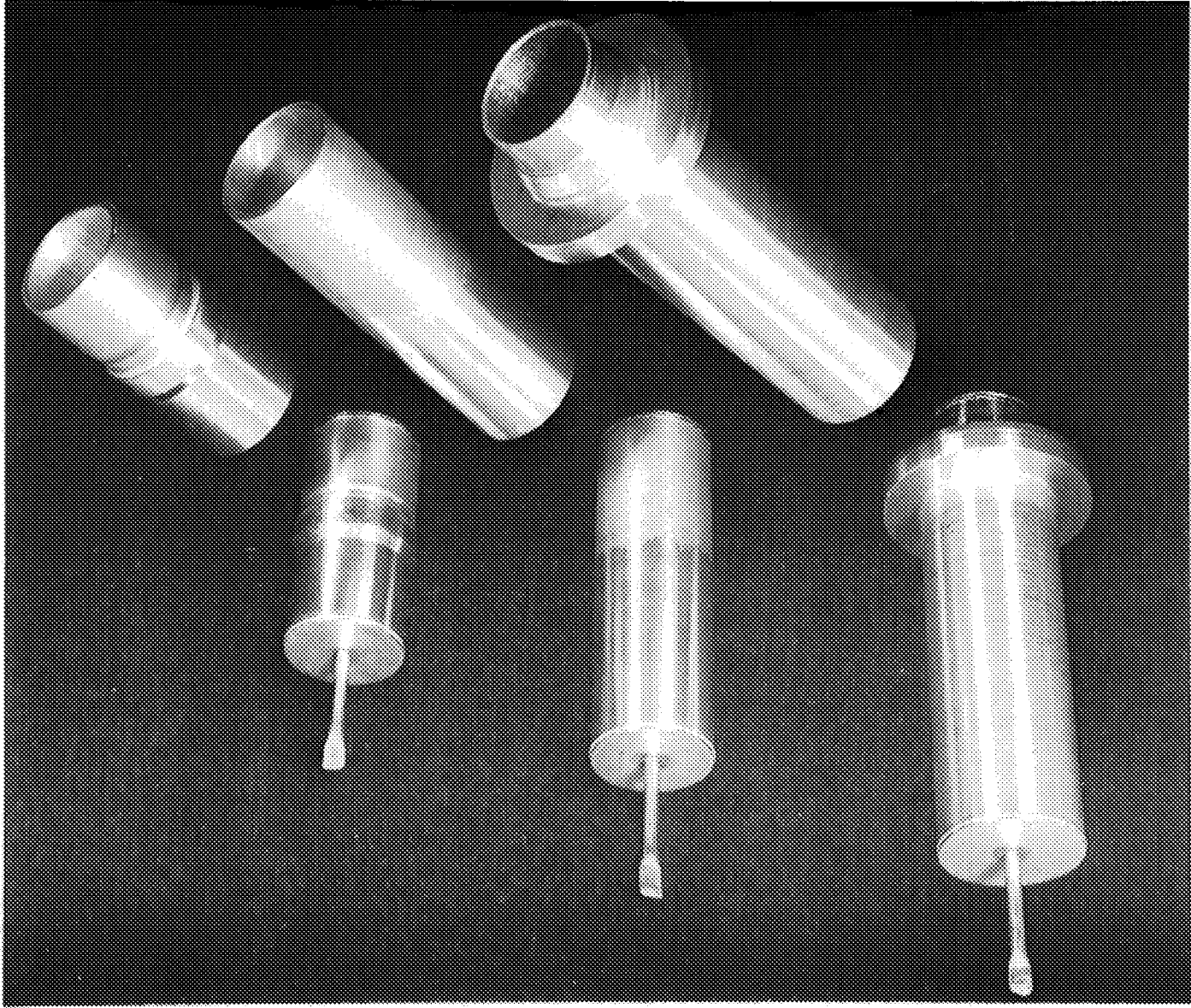
FIGURE 1. From Left to Right, Open and Closed Versions of Sleeve,
Tandem, and Brazed Bimetal Transition Joints

TABLE 1. Extrusion Conditions for Co-extruded Joints

	Reduction Ratio	Temperature (^{o}C)	Temperature (^{o}F)
Large Diameter Sleeve	8:1	1065	1950
Small Diameter Sleeve	8:1	1065	1950
Tandem Joints	5:1	995	1825

Sleeve Joints

Figure 2 compares full scale transverse ring sections from the as-extruded sleeve joints. The inside diameter surface, which in the clad state was extruded over a mandrel, was smooth. The inside layer of tantalum and the outside layer of 316 stainless steel were concentric.

Microstructure and Hardness — A discussion of the microstructure and hardness is deferred to the experimental results section where a direct before and after comparison is made between the as-extruded and thermal cycled joints.

Dimensions — Six of the eight sleeve joint extrusions were cut in two, and the outside diameter was machined. One of the pair of sleeve joints from each extrusion then had a heavy stainless steel flange electron beam welded to the wall to simulate the stresses expected in service as a tube to header joint. Table 2 compares the dimensions of the six flange-welded sleeve joints, and Figure 3 is a sketch which clarifies the dimension location. The great variation in center wall thickness, shown in Table 2 is not a product of the extrusion process but is due to the outside diameter machining of the cambered or bent bimetal sleeves. Had the tube lengths been press straightened prior to machining, considerably more uniform dimensions would have been obtained. The full section views of the as-extruded sleeve joints shown in Figure 2 are more indicative of the concentricity of the extrusion process.

Tandem Joints

Tandem transition joints are best observed in full longitudinal section as shown in Figure 4. The tapered transition joint is designed to distribute the dissimilar thermal expansion stresses and to prevent rupture during thermal cycling. To estimate the variation in taper length,
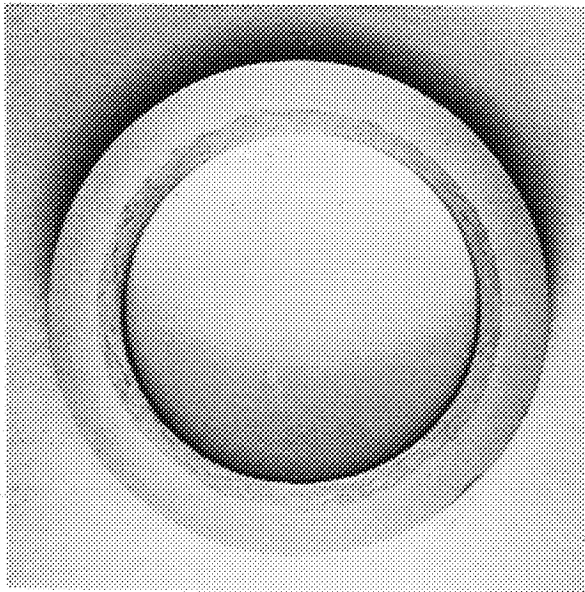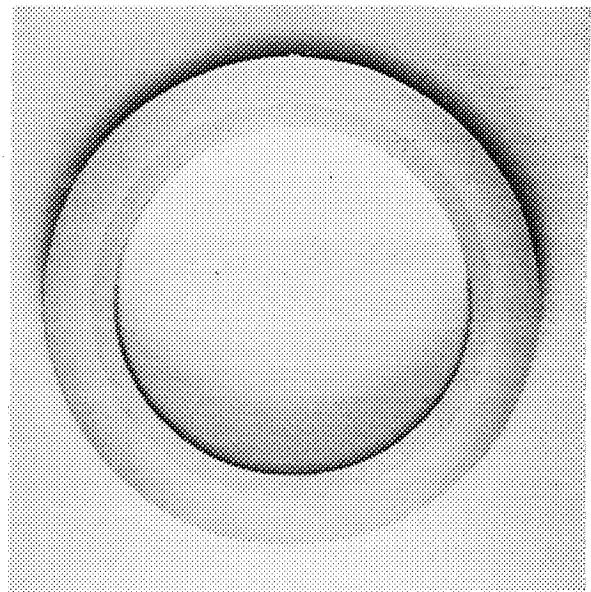
No. 1 (center)   1X   No. 2 (front center)   1X
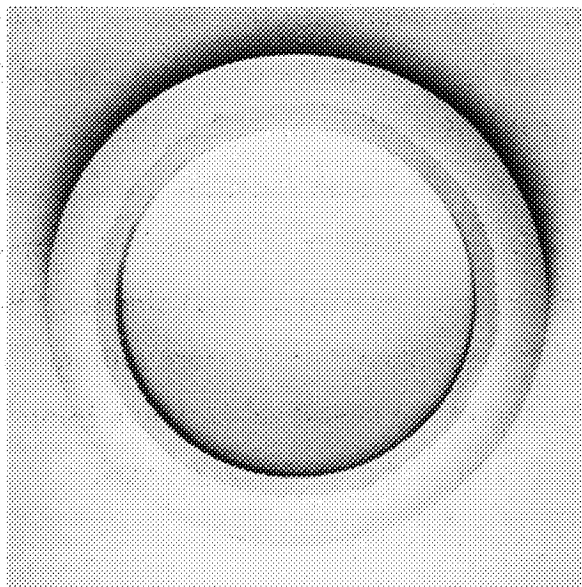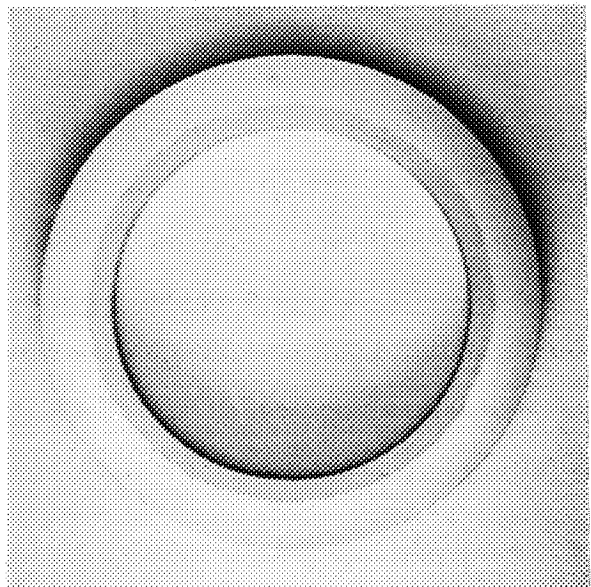
No. 5 (front center)   1X   No. 8 (front center)   1X

2.54 cm (1.0 inches)

FIGURE 2.   Transverse Sections of Sleeve Joint Extrusions As-extruded

TABLE 2. Flanged Sleeve Joint Dimensions

No.	Overall length (inches)	Weight (pounds)	SN End 316 S.S. OD^A (inches)	ID^A (inches)	Wall Thick. (in.) Max.	Min.	Center Wall Thickness (in.) Max.	Min.	Opposite End Tantalum OD^A (inches)	ID^A (inches)	Wall Thick. (in.) Max.	Min.
2	8.00	5.113	2.254	2.001	.129	.123	.267	.253	1.886	1.723	.080	.074
4	7.98	5.228	2.252	2.000	.126	.123	.268	.249	1.970	1.762	.107	.104
5	8.00	5.021	2.237	1.998	.119	.114	.302	.203	1.883	1.728	.082	.068
6	7.63	5.014	2.254	1.998	.127	.125	.261	.255	1.954	1.746	.104	.102
7	7.27	4.760	2.250	1.998	.124	.123	.263	.255	1.959	1.749	.106	.104
8	7.83	5.100	2.256	1.998	.129	.123	.271	.249	1.869	1.723	.072	.069

SI UNITS

No.	Overall length (mm)	Mass (kg)	SN End 316 S.S. OD^A (mm)	ID^A (mm)	Wall Thick. (mm) Max.	Min.	Center Wall Thickness (mm) Max.	Min.	Opposite End Tantalum OD^A (mm)	ID^A (mm)	Wall Thick. (mm) Max.	Min.
2	203	2.319	57.25	50.82	3.28	3.12	6.78	6.43	47.90	43.76	2.03	1.88
4	203	2.371	57.21	50.80	3.20	3.12	6.80	6.32	50.04	44.75	2.72	2.64
5	203	2.278	56.82	50.75	3.02	2.90	7.67	5.16	47.83	43.89	2.08	1.73
6	194	2.274	57.25	50.75	3.22	3.18	6.63	6.48	49.63	44.35	2.64	2.59
7	185	2.159	57.15	50.75	3.15	3.12	6.68	6.48	49.76	44.42	2.69	2.64
8	199	2.313	52.30	50.75	3.28	3.12	6.88	6.32	47.47	43.76	1.83	1.75

A – Average of 0° and 90° readings

B – Maximum and minimum of 4 readings
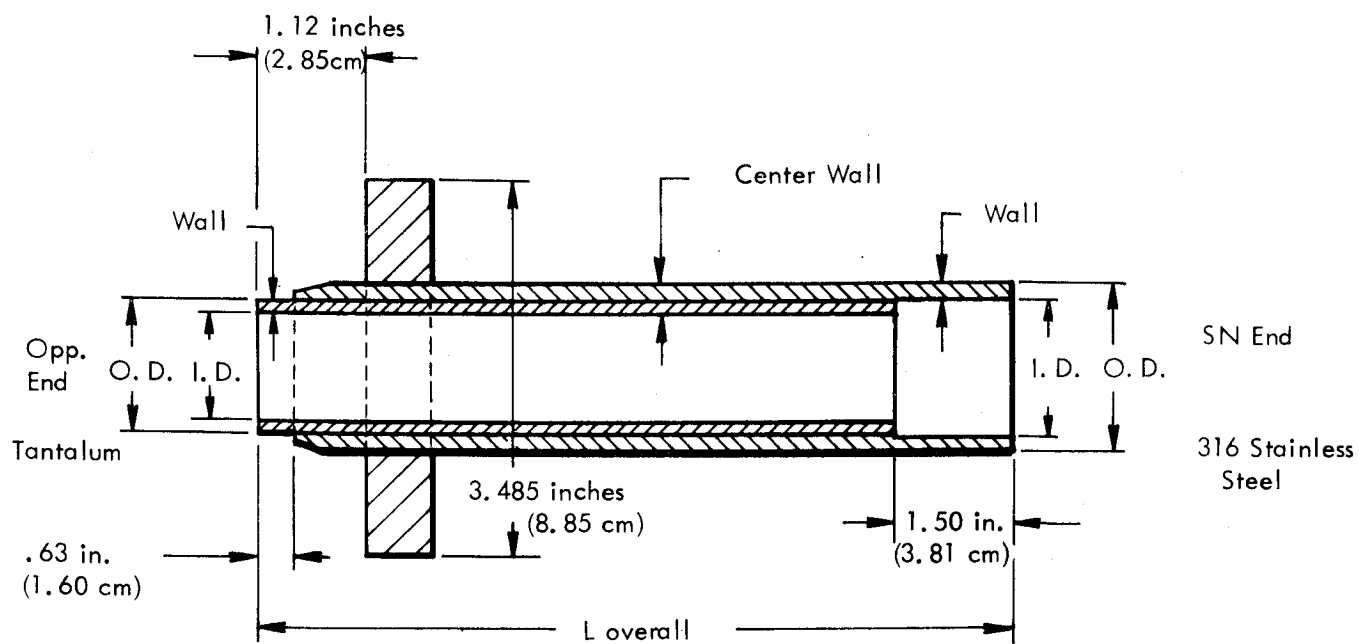
FIGURE 3.   Dimension Locations of Flanged Sleeve Joints

22,488   0°

22,489   72°

22,490   144°

216°

22,491   288°

22,492

2X

2.54 mm
(0.1 inch)
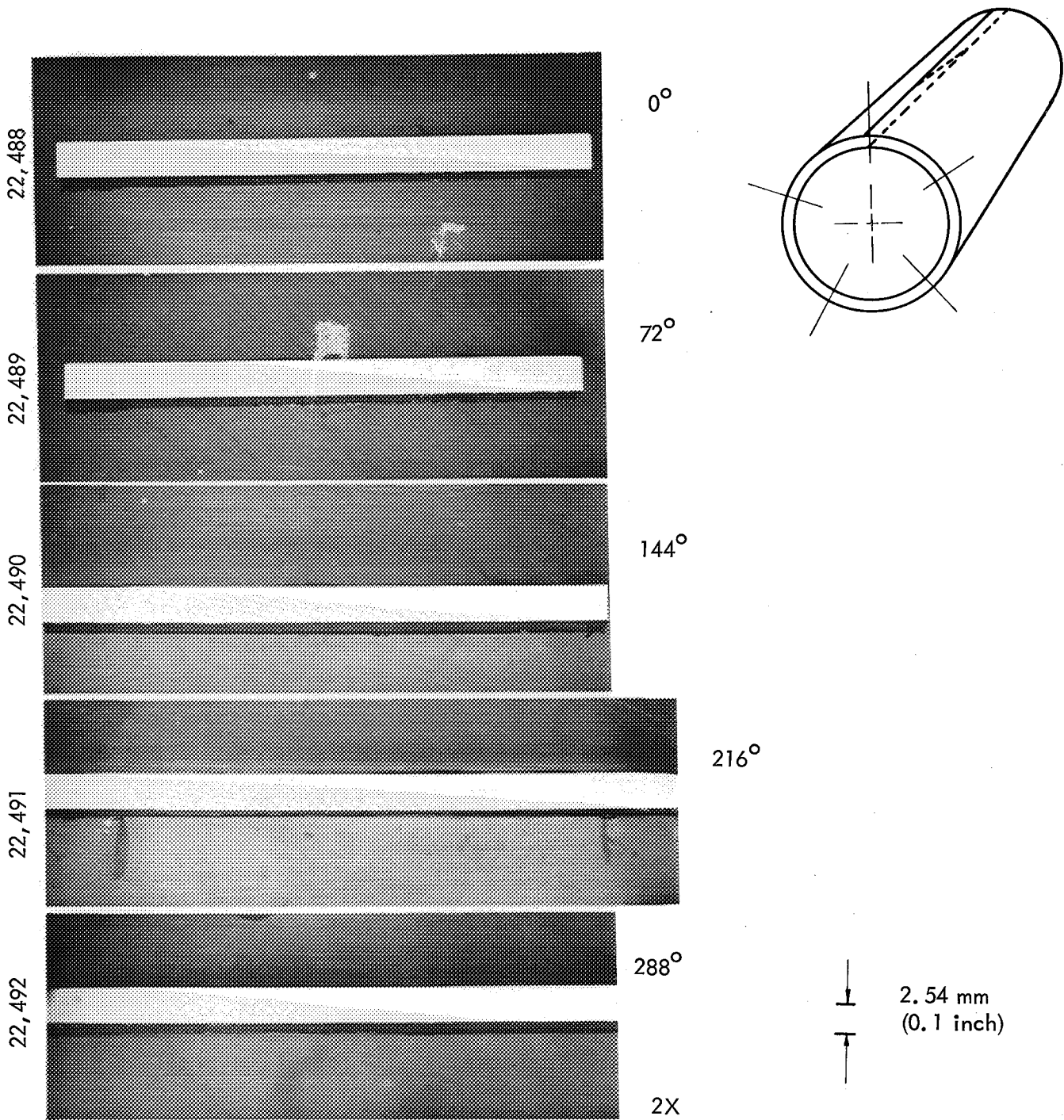
FIGURE 4.   Longitudinal Sections from Joint No. 3
in the As-Extruded Condition

five longitudinal sections were obtained spaced 72° apart around a single transition joint. The sectioned taper length of joint No. 3 varied from 4.76 cm to 2.67 cm (1.875 inches to 1.060 inches) which compares favorably to the 4.80 cm to 3.7 cm (1.89 inches to 1.455 inches) variation measured by radiograph. Figure 5 lists the machined dimensions of the tandem joints including the only piece to piece variable dimension, the radiographically determined taper length. The taper lengths shown in Figure 5, although generally less than the target value of 3.8 cm (1.5 inches)[9], are considered acceptable for a durable, leak tight transition joint of this diameter and wall thickness. A 1.02 cm (0.4 inch) bevel had been machined on the extrusion blanks to purposely increase the taper length of the 5:1 ratio extrusion.

Microstructure and Hardness – A discussion of the microstructure and hardness is deferred to the experimental results section where a comparison is made between the as-extruded and thermal cycled transition joints.

Brazed Joint

The brazed joints were designed and made by the Space Systems Division of the General Electric Company, Cincinnati, Ohio, for NASA Lewis under Contract NAS 3-11846, and the complete fabrication details are described in NASA CR-72746[10].

The brazed joint tongue and groove design is shown in Figure 6. The tantalum side of the transition joint was machined to a tongue to fit the stainless steel groove. Previous successful joints had been made at General Electric with a stainless steel tongue and a tantalum groove, but the present configuration was considered to be more favorable. A cobalt-base alloy, J-8400*, also developed by General Electric, was used for the fluxless vacuum brazing operation. A brazing temperature of approximately $1200^\circ C$ ($2200^\circ F$) was required, and generally from 2 to 3 brazing cycles at successively higher temperatures were required to produce an acceptable braze as determined by ultrasonic inspection. Table 3 lists the brazing

---

* 45 w/o Co – 21 w/o Cr – 21 w/o Ni – 8 w/o Si – 3.5 w/o W – 0.8 w/o B – 0.4 w/o C

Weight – 2.70 lbs.
Mass – (1.22 kg)

Tantalum

Taper Length

.122 inches
(.310 cm)

SN End

1.760 inches
(4.470 cm)

2.007 inches
(5.098 cm)

8.00 inches
(20.3 cm)

No.	Average* Taper Length		Special Characteristics
	inches	cm	
1	1.22	3.10	
2	1.44	3.66	
3	1.67	4.24	ID Unbond – Single Point
4	1.35	3.43	
5	1.06	2.69	
6	1.30	3.30	OD Defect – Dye Pen. – Single Point
7	1.01	2.56	
8	1.47	3.73	OD Defect – Dye Pen. – Line
9	1.33	3.38	
10	1.44	3.66	
11	1.35	3.43	
12	1.18	3.00	

* – Average of four locations measured by radiography

FIGURE 5. Tandem Transition Joint Dimensions and Special Characteristics
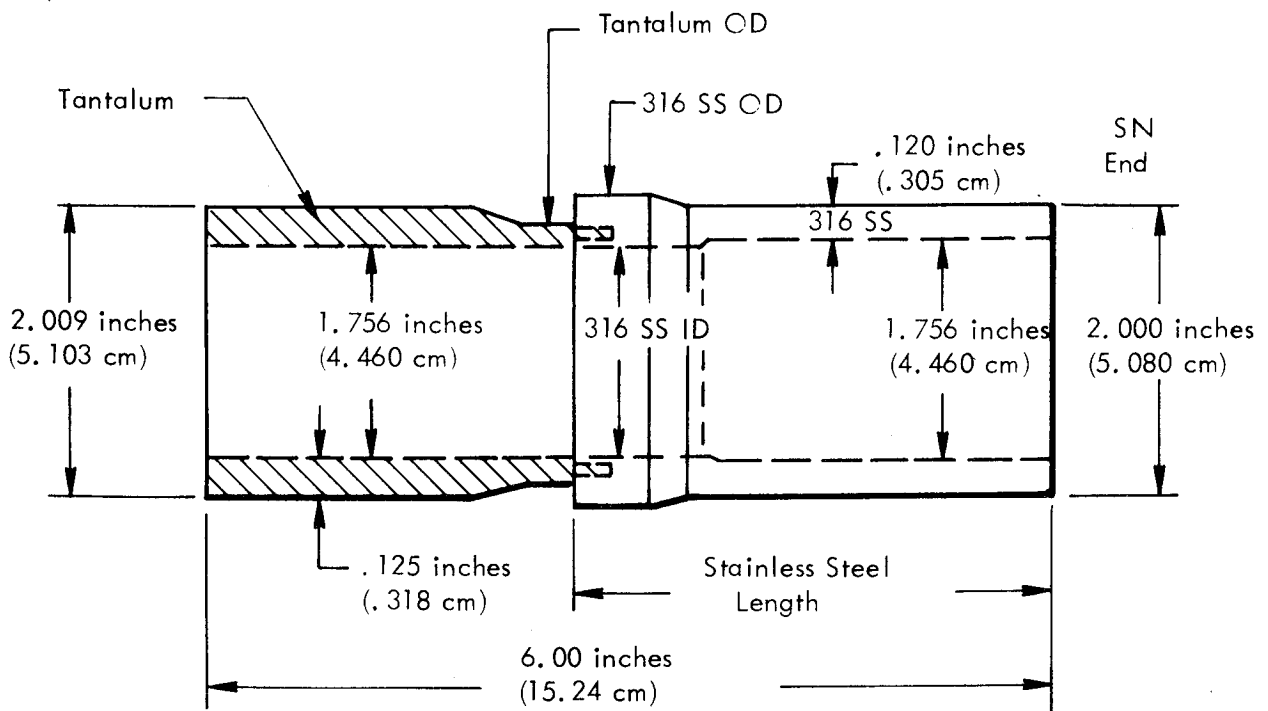
FIGURE 6. Brazed Transition Joint Dimensions

cycles and the maximum brazing temperature for each of the 12 brazed joints. On the same table an ultrasonic inspection rating column compares the relative braze quality as determined by G. E. and WANL. A good rating by G. E. should correspond to a low number of defects as inspected by WANL, but consistent inspection results were not obtained. The ultrasonic inspection results are discussed in greater detail for all three types of transition joints in the experimental results section, and more quantitative results are presented.

Dimensions — The dimensions shown in Figure 6 are common to all twelve brazed joints and did not differ significantly. Several machined dimensions in the area of the braze did differ, and these are shown in Table 4.

Microstructure and Hardness — A discussion of the microstructure and hardness is deferred to the experimental results section where a comparison is made between the as-extruded and thermal cycled transition joints.
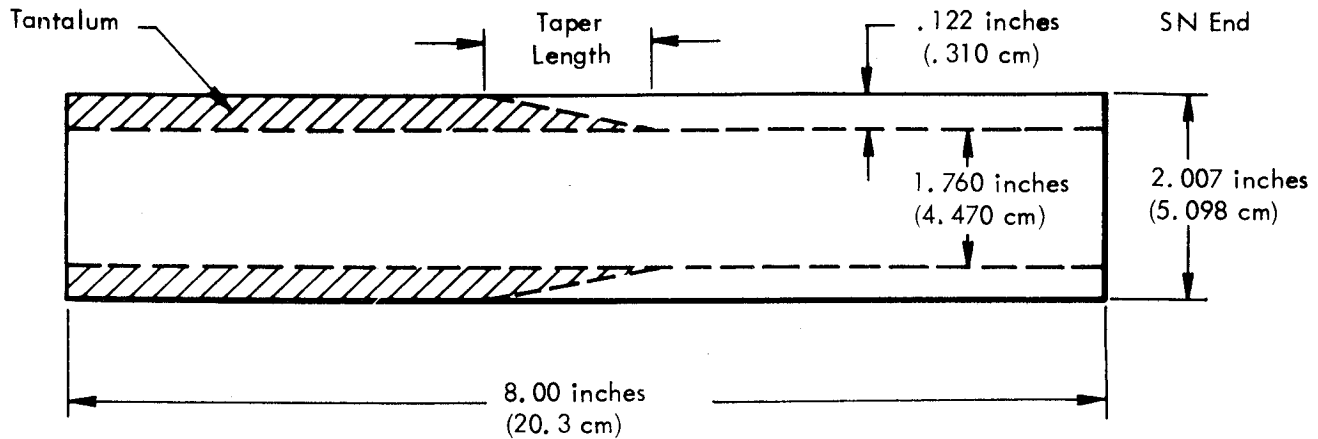
TABLE 3. Braze Joint Fabrication History

| Specimen No. | Date Brazed | Total Braze Cycles | Maximum Braze Temp. | | Ultrasonic Rating | |
			(°C)	(°F)	G. E.	WANL No. of Defects
8	8-14-69	1	1182	2160	Good	0
9	7-14-69	1	1182	2160	Good	Poor Signal Return
10	7-14-69	2	1204	2200	Poor Signal Return	1
11	2-14-70	2	1232	2250	Average	8
13	2-28-70	2	1232	2250	Good	3
15	10-30-69	2	1199	2190	Bad	0
16	3-6-70	2	1211	2212	Good	0
17	2-21-70	2	1232	2250	Average	1
18	12-13-69	3	1232	2250	Good	0
19	2-15-70	2	1232	2250	Bad	0
20	2-14-70	2	1232	2250	Bad	4
22	12-13-69	3	1232	2250	Average	0

TABLE 4. Brazed Joint Dimensions

Number	Weight (lbs.)	Mass (kg)	Stainless Steel Length (in.)	Stainless Steel Length (cm)	Stainless Steel OD (in.)	Stainless Steel OD (cm)	Tantalum OD (in.)	Tantalum OD (cm)	Stainless Steel ID (in.)	Stainless Steel ID (cm)
8	1.925	.8732	3.250	8.26	2.130	5.410	1.940	4.928	1.740	4.420
9	1.936	.8782	3.23	8.20	2.128	5.405	1.942	4.933	1.740	4.420
10	1.925	.8732	3.16	8.03	2.126	5.400	1.928	4.897	1.738	4.414
11	1.973	.8950	3.69	9.37	2.127	5.402	1.950	4.953	1.726	4.384
13	2.086	.9462	3.22	8.18	2.126	5.400	1.946	4.943	1.724	4.379
15	1.850	.8392	3.67	9.32	2.128	5.405	1.941	4.930	1.723	4.376
16	1.973	.8950	3.69	9.37	2.126	5.400	1.944	4.938	1.724	4.379
17	2.114	.9589	3.23	8.20	2.126	5.400	1.952	4.958	1.724	4.379
18	1.971	.8940	3.25	8.26	2.128	5.405	1.944	4.938	1.724	4.379
19	1.956	.8872	3.69	9.37	2.126	5.400	1.946	4.943	1.726	4.384
20	2.092	.9489	3.25	8.26	2.126	5.400	1.945	4.940	1.725	4.382
22	1.987	.9013	3.25	8.26	2.126	5.400	1.944	4.938	1.722	4.374

IV. TEST APPARATUS

The durability test used for the transition joints consisted of thermal cycling 100 times from 730°C (1350°F) to 120°C (250°F) in high vacuum. The heating and cooling rates were low, as this was required to simulate the normal expected thermal transient for the transition joints. Figure 7 shows a typical thermal cycle which required approximately 2 hours for heating and 2 hours for cooling. As the program continued, the hold time at temperature was reduced from an initial 10 hours to 5 hours and finally to 2 hours for the last thermal cycle. The hold time was reduced to complete the test program more quickly since it was believed that the hold times had little affect on the test severity.

To provide a symmetrical thermal environment for six large transition joints, a long, small diameter, 316 stainless steel hot wall vacuum furnace was used. Had more rapid heating and cooling rates been required, the high thermal inertia of the hot wall furnace could not have been tolerated, and an internally heated ultra-high vacuum system would have been used.

Figure 8 is a drawing of the hot wall furnace and the specimen array. The specimens were supported by a stainless steel rack. The temperature was monitored at three locations in the furnace interior, and the hot wall furnace was controlled by an external thermocouple adjacent to the furnace tube. The hot wall furnace was pumped by a titanium sublimation pump chamber and three small sputter ion pumps. The combined pumping capacity was approximately 900 l/sec for nitrogen. To provide the initial roughing vacuum and to aid the ion and sublimation pumps during bakeout, a 250 l/sec turbo-molecular pump was used. Furnace vacuum was monitored by a nude ion gage at the roughing end and by a cold cathode gage and the ion pump current at the sublimation chamber end. The pressures obtained were 2×10^{-7} torr with the furnace hot to 5×10^{-9} torr with the furnace cold. Figure 9 is a photograph of the hot wall furnace and associated control system.
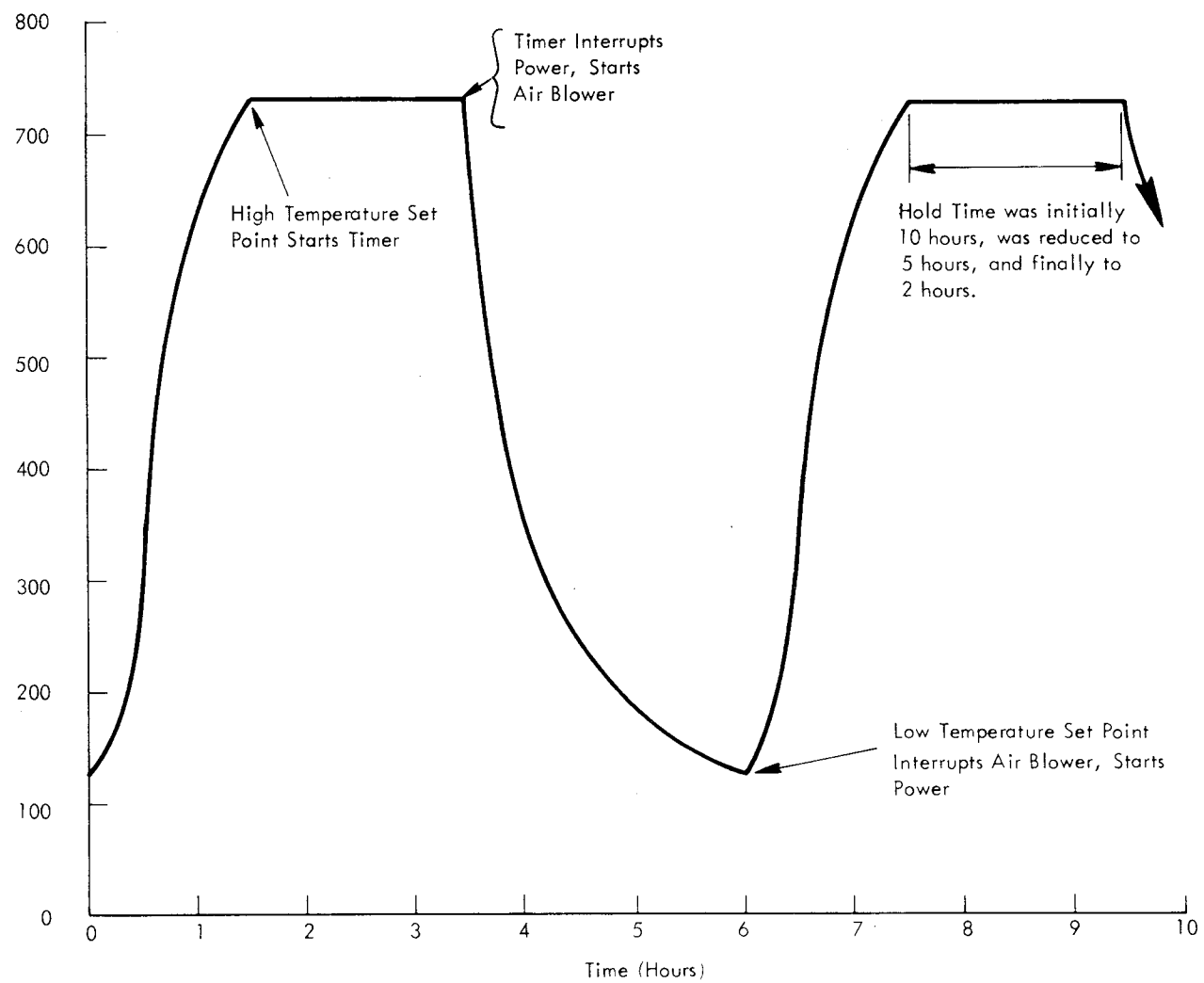
FIGURE 7. Thermal Cycle Test for Transition Joints

Sputter Ion Pumps
2 - 15 l/sec
1 - 30 l/sec

24 KWClamshell Resistance Furnace
42 inches, 4* Zone Active Length

8 inch UHV Flange

Flanged Sleeve
Joint

Cooling
Annulus
Exhaust

TSP Filaments

10 inch UHV Flange

Tandem Joint
(darkened areas are pressurized)

Brazed Joint

Nude Ion Gage

36 inch Specimen Zone

Air Cooling
Annulus Inlet

12 inch diameter x 24 inches long
Titanium Sublimation Pump Chamber
Estimated pumping speed 850 l/sec.

Main Retort Tube,
3.5 inches OD x
0.120 inch wall
316 SS

Roughing System
250 l/sec
Turbomolecular Pump

* Two end zones and two center zones separately controlled.

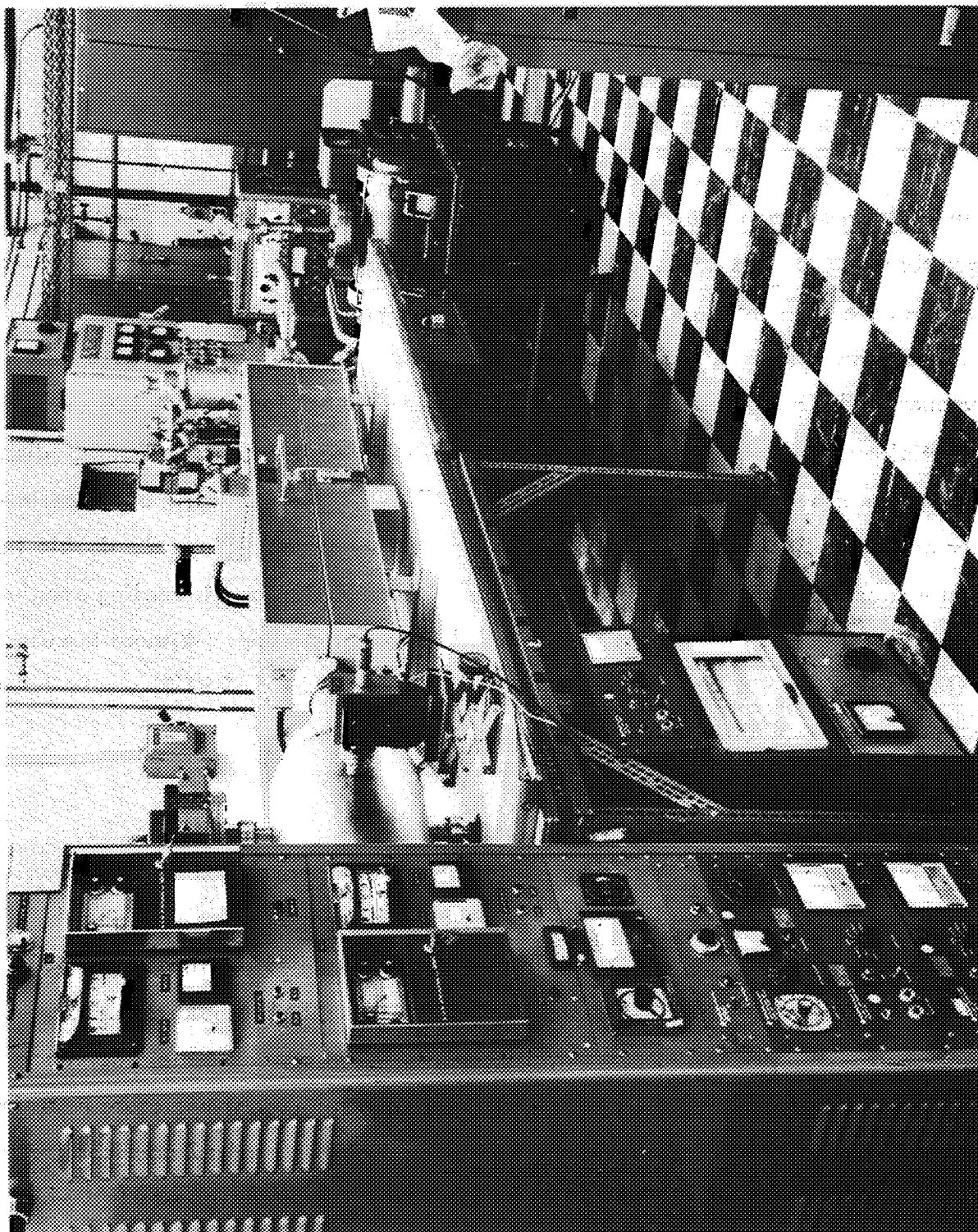FIGURE 8. High Vacuum Thermal Cycling Furnace (1350°F) (730°C)

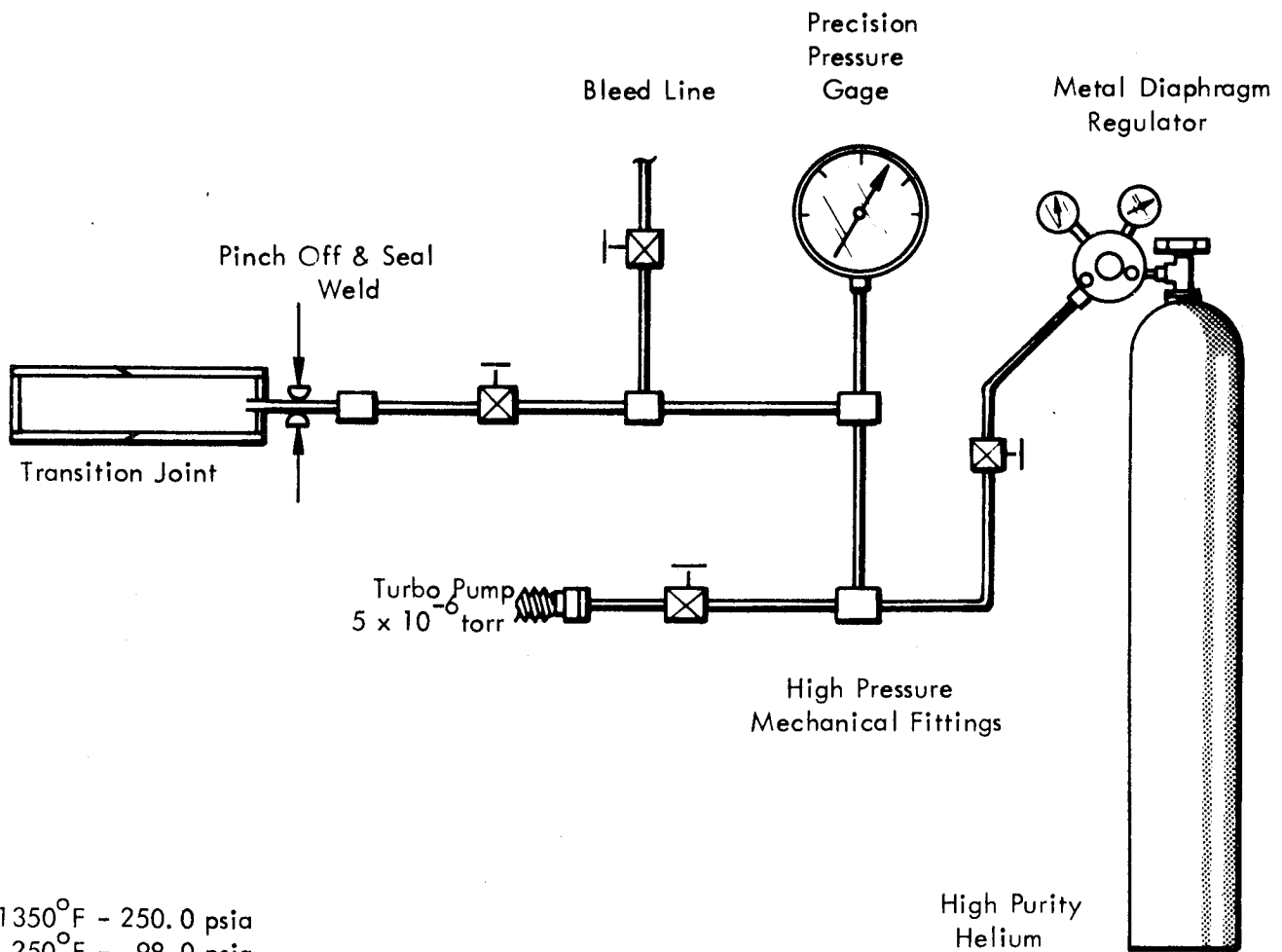FIGURE 9. Photograph of Thermal Cycling Apparatus

As an added precaution to prevent contamination, the transition joints were wrapped in tantalum foil during thermal cycling. Chemical analyses of sections of tantalum from the thermal cycled specimens indicated no contamination had occurred as discussed in a later section. Also, no significant interstitial element difference was observed between the sealed (pressurized) and open transition joints.

The double wall furnace construction was initially designed to prevent the diffusion of hydrogen through the hot stainless steel furnace wall. The outer wall was to be evacuated to a modest pressure (10^{-3} torr) to reduce the partial pressure of the contaminant. Preliminary experiments with a small scale double wall stainless steel system indicated that double evacuation did not improve the internal vacuum of the hot furnace. A 100 mm hydrogen partial pressure in the outer annulus led to a rapid rise in internal pressure indicating the rapid diffusion of hydrogen through the hot 730°C (1350°F) furnace wall, but experiments with helium and air indicated that no appreciable diffusion occurred. Since the double wall construction was not required to obtain low pressures, it was used as an air cooling annulus to increase the cooling rate of the specimen during the thermal cycling. Without the use of forced air cooling, the cooling time from 730°C (1350°F) to 120°C (250°F) would have been increased from the required 2 hours to 5 hours.

Automatic Control – The thermal cycle automatic controls were designed to provide an accurate high and low temperature and a uniform hold time at temperature. During the heating ramp, current limiters were adjusted to provide a 2 hour heating time. At 730°C (1350°F) a high set point switch started a timer to provide the required hold time at temperature. Proportional, SCR two-zone controllers were used to provide a rapid approach to temperature without an overshoot. At the end of the required high temperature hold time, the timer interrupted the furnace power and turned on an air blower for a 2 hour cooling ramp to 120°C (250°F). At 120°C (250°F) a low temperature set point turned off the air

blower and restored the furnace power for a second heating cycle. Both thermocouple
break and a separate over temperature set point were provided to prevent high temper-
ature excursions. The sputter ion pump current controlled an over-pressure relay which
would permanently interrupt furnace power in the event of vacuum failure. With the built
in safeguards, no damaging temperature excursions occurred over the 6 months of operation
and a total of 200 thermal cycles. Continuous recordings were maintained of the specimen
temperature.

Pressurized Specimens – Each six specimen thermal cycle load was composed of two
specimens of each type of transition joint, one of which was open and one was seal welded
and pressurized with helium. The helium pressure at room temperature was adjusted to pro-
vide a calculated 1.70 MN/m^2 (250 psig) pressure at 730°C (1350°F), which is the expected
service environment for the transition joints. Figure 1 shows the open and pressurized
versions of the three types of transition joints. Figure 10 shows the technique used to pres-
surize the transition joints with high purity helium. End caps of like material were electron
beam welded to both ends of the transition joint, and a .635 cm (1/4 inch) stainless steel
tube was welded to the stainless steel end cap. The seal welded transition joint was helium
leak checked and evacuated with a turbomolecular pump as shown in Figure 10. Following
a two hour evacuation, which also evacuated the precision pressure gage and the gas
supply lines back to the metal diaphragm regulator, the transition joints were filled to
0.42 MN/m^2 (62 psig) high purity helium. The gas supply tube was then heated to 755°C
(1400°F), and squeezed flat with a 22,300 N (5000 lb.) hydraulic pinch-off tool. The flat-
tened tube was then cut with sharp bolt cutter, and the sheared edge was immediately GTA
welded. The seal welded transition joints were then helium leak checked. This method
of pressurizing permitted easy thermal cycle loading and unloading and ultrasonic inspection
as compared to alternate methods employing dynamic pressurizing connections. Following
the 100 thermal cycle tests, the pressurized specimens were drilled open in a sealed vacuum
chamber of a known small volume, and the pressure rise of the sealed system was measured

Precision
Pressure
Gage

Bleed Line

Metal Diaphragm
Regulator

Pinch Off & Seal
Weld

Transition Joint

Turbo Pump
5×10^{-6} torr

High Pressure
Mechanical Fittings

High Purity
Helium

1350°F – 250.0 psia
250°F – 98.0 psia
75°F – 73.9 psia – Specimen filled and sealed at 75°F

+ 3.4% Correction for Volume Change of 316 SS Specimen from 75°F to 1350°F.

73.9 psia
2.5 psia – Volume Change Correction
76.4 psia
14.4 psia – Atmospheric Pressure
62.0 psig – Gage pressure

FIGURE 10. Static Pressure Sealing Technique

and compared to calculated values to determine if leaks had occurred during thermal cycling.
No leaks were observed in any of the pressurized specimens indicating the process was suc-
cessful.

Aging Furnace – Sections of a brazed joint were exposed for 3000 hours at $730^{\circ}C$ ($1350^{\circ}F$) to
determine the effect of extended service time on the complex, cobalt base, braze alloy.
A vertical sputter ion pumped furnace was used as shown in Figure 11. Pressures measured
in the pumping area of the furnace varied from 6×10^{-8} torr at temperature to 4×10^{-9} torr
cold, following the 3000 hour run. The pressure at the beginning of the exposure was
1×10^{-6} torr. This type of hot wall quartz tube furnace had previously been used in high
vacuum heat treating with good results[2]. As an added precaution, the bimetal specimens
were wrapped in tantalum foil. Figure 9, the photograph of the thermal cycling furnace,
also shows the sputter ion pump top section of the thermal exposure furnace in the background.
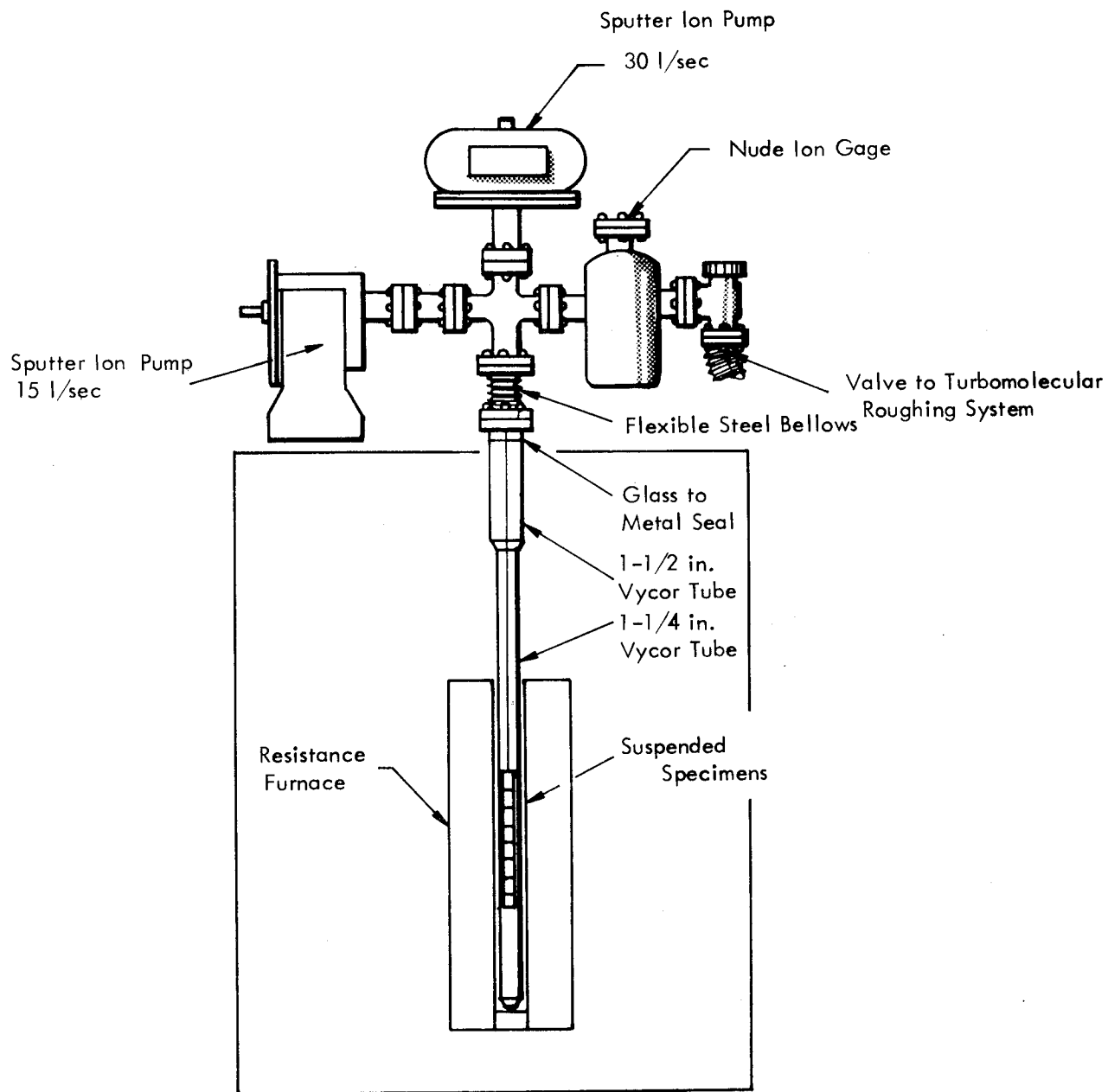The turbomolecular pump was used to rough pump the system to ion pump starting pressure.

FIGURE 11. Vertical High Vacuum Aging Furnace

V. TEST PROCEDURES

The basic performance evaluation for the transition joints was a relatively slow thermal cycling exposure from 730°C (1350°F) to 120°C (250°F) in high vacuum. A total of four of each type of transition joint was fully evaluated which provided a reasonable measure of performance for the three types of specimens. Each specimen was subjected to 100 thermal cycles with from 2 hours to 10 hours of dwell time at 730°C (1350°F) between each cycle. One half of the specimens were tested in the open condition, and one half were tested internally pressurized with helium to duplicate the 1.70 MN/m^2 (250 psig) service pressure at 730°C (1350°F). As shown in Table 5, which details the entire thermal cycling test and inspection plan, the 12 transition joints were separated into two test lots in which a different soak time-thermal cycle sequence was used although each lot eventually received a total of 100 thermal cycles. The basic difference between the two lots was that a group of six designated as Plan A was immediately raised to 730°C (1350°F) to begin a series of five thermal cycles; whereas, Plan B was first soaked at temperature for 100 hours before starting the same five thermal cycles. These differing test modes were an attempt to simulate SNAP-8 startup conditions. Originally, the general opinion was that the 100 hour soak at 730°C (1350°F), preceding the thermal cycling would be the more severe test condition. Plan· B also included a 1000 hour hold at temperature before a final 10 thermal cycles.

As is shown in Table 5, the transition joints were thoroughly evaluated following increasingly larger numbers of thermal cycles to establish the thermal cycle effect on joint deterioration. As more confidence was obtained in the transition joint performance, the number of thermal cycles between evaluations was increased from 5 to 10 to 30 and finally to 53 to complete the full 100 cycles. In addition, any bond failures in the pressurized specimens would have produced an unmanageable pressure rise and consequent test interruption in the high vacuum system since the titanium sublimation pump and the sputter ion pumps have a negligible pumping speed for helium.

The intercycle leak checking, ultrasonic inspection, and liquid penetrant inspection added considerably to the time and cost of running the thermal cycles since the ion pumped high vacuum system required approximately two days to load, evacuate and bakeout, and bring up to temperature. Prior to the test program, however, it was not known if any of the transition joints would survive the full 100 cycle test, and a measure of which type of transition joint lasted the longest would have been important.

To prevent contamination of the tantalum components of the transition joints, all thermal cycling was done in a clean, sputter ion and sublimation pumped vacuum system. The vacuum obtained in the hot wall test furnace was modest compared to most ion pumped systems, (10^{-7} torr hot to 10^{-9} torr cold) but was more than adequate to prevent interstitial contamination of the tantalum as determined by before and after chemical analysis shown on Table 6.

TABLE 6. Interstitial Chemical Analyses of Tantalum
Sections of Bimetal Transition Joints

	As-fabricated			PLAN A			PLAN B		
				100 Thermal Cycles			100 Thermal Cycles Plus 1000 Hour Soak		
				(Interstitial Content in ppm)					
	Oxygen	Nitrogen	Carbon	Oxygen	Nitrogen	Carbon	Oxygen	Nitrogen	Carbon
Brazed Joint	33	4	6						
Open				24	6	3	58	10	5
Pressurized				15	4	5	50	3	3
Sleeve Joint	53	31	12						
Open				39	28	10			
Pressurized				69	31	11			
Tandem Joint	34	23	14						
Open							34	30	12
Pressurized							30	26	14

VI. TEST RESULTS

General – The test results for all of the transition joints are presented in the following sequence.

      A.   Helium Leak Test and Liquid Penetrant Inspection

      B.   Ultrasonic Inspection

      C.   Microprobe Analyses

      D.   Microstructure and Hardness

      E.   Dimensional Changes

A. Helium Leak Test

A helium leak test served as the functional appraisal of bond durability since liquid metal containment was the primary function of the bimetal transition joints and associated tubing.

At the beginning and end of the full 100 cycle thermal cycle evaluation all of the specimens were helium leak tested with the inside directly connected to a helium mass spectrometer and spraying helium on the exterior surface. In practice, one end of the open tube was inserted into the leak detector "O" ring sealed adaptor and the other open end of the tube was plugged with a rubber stopper. A VEECO Model MS-9-AB leak detector was used which was calibrated by a standard leak to a sensitivity level of less than 3.2×10^{-8} std. cc/sec. During the inter-thermal cycle testing, the sealed specimens were leak tested using a helium pressurizing and evac-uation cycle in a small retort connected to a helium mass spectrometer.

Results – All 12 of the thermal cycled transition joints remained leak tight throughout the testing program, Also, no leaks were observed in the entire group of 36 as-fabricated transition joints prior to specimen selection and thermal cycling.

Liquid Penetrant Inspection

The dissimilar metal joint area was liquid penetrant inspected using Spotcheck SKL-HF red dye and SKD-NF developer. Fluorescent dye ZL-22 was evaluated, but the rough braze area and the severe fissures developed in the thermal cycled joints produced excessive bleeding, and the less sensitive red dye was used. Table 7 shows the gradual increase in dye penetrant indications as the thermal cycle test progressed.

B.   Ultrasonic Inspection

A considerable effort was made to develop ultrasonic inspection of the dissimilar metal bond to the point where deteriorating bond quality could be accurately followed. Constant checks with other bond measurements techniques such as dye penetrant inspection and helium leak testing were provided. A final comparison of bond quality measurement techniques was provided by destructive sectioning following the test program.

To provide an accurate measurement record, an automatic "C" scan inspection process was developed using immersion testing and water couplant. Figure 12 shows the test apparatus with the small water tank and recorder-coupled transducer drive. In general, through transmission techniques were used for the initial inspection and the final inspection following the 100 cycle thermal cycle exposure, but pulse echo techniques were also used on the sealed and pressurized specimens when through transmission techniques could not be used.

Results - Severe distortion and concentricity problems were encountered with the extruded transition joints, both the tandem and the sleeve joint. The sleeve joints were initially machined non-concentric, and the varying thickness of stainless and tantalum around the diameter played havoc with test sensitivity, especially the modified and gated pulse echo techniques. Also, as the thermal cycle tests progressed, the severe camber and diameter changes

			Serial No.	Base OD	Base ID	1st Test OD	1st Test ID	2nd Test OD	2nd Test ID	3rd Test OD	3rd Test ID	4th Test OD	4th Test ID	5th Test OD	5th Test ID
PLAN B	Brazed Joint	Press.	15												O(1)
		Open	10	O	O	O	O	O	O	O	O	O	O	O	O
	Sleeve Joint	Open	2	O(f)		O(f)		O(f)	O	O(f)	O	O(f)	O	O(f)	O
		Press.	8							O(f)		O(f)		O(f)	O(1)
	Tandem Joint	Open	8	O		O		O		O	O	O	O	O	O
		Press.	11												O(1)
						5 Cycles		10 Cycles		30 Cycles		43/53 Cycles		10 Cycles	
PLAN A	Brazed Joint	Press	8									O(1)			
		Open	20		O		O		O		O		O		
	Sleeve Joint	Open	4					O(f)		O(f)	O	O(f)	O		
		Press.	6	O(f)		O(f)		O(f)		O(f)		O(f)	O(1)		
	Tandem Joint	Open	7						O		O	O			
		Press.	6										O(1)		

Top soak labels: 100 Hour Soak, 100 Hour Soak, 1000 Hour Soak
Bottom soak labels: 100 Hour Soak, 100 Hour Soak

O = Defect
(f) = Flange End
(1) = Cut open for final inspection
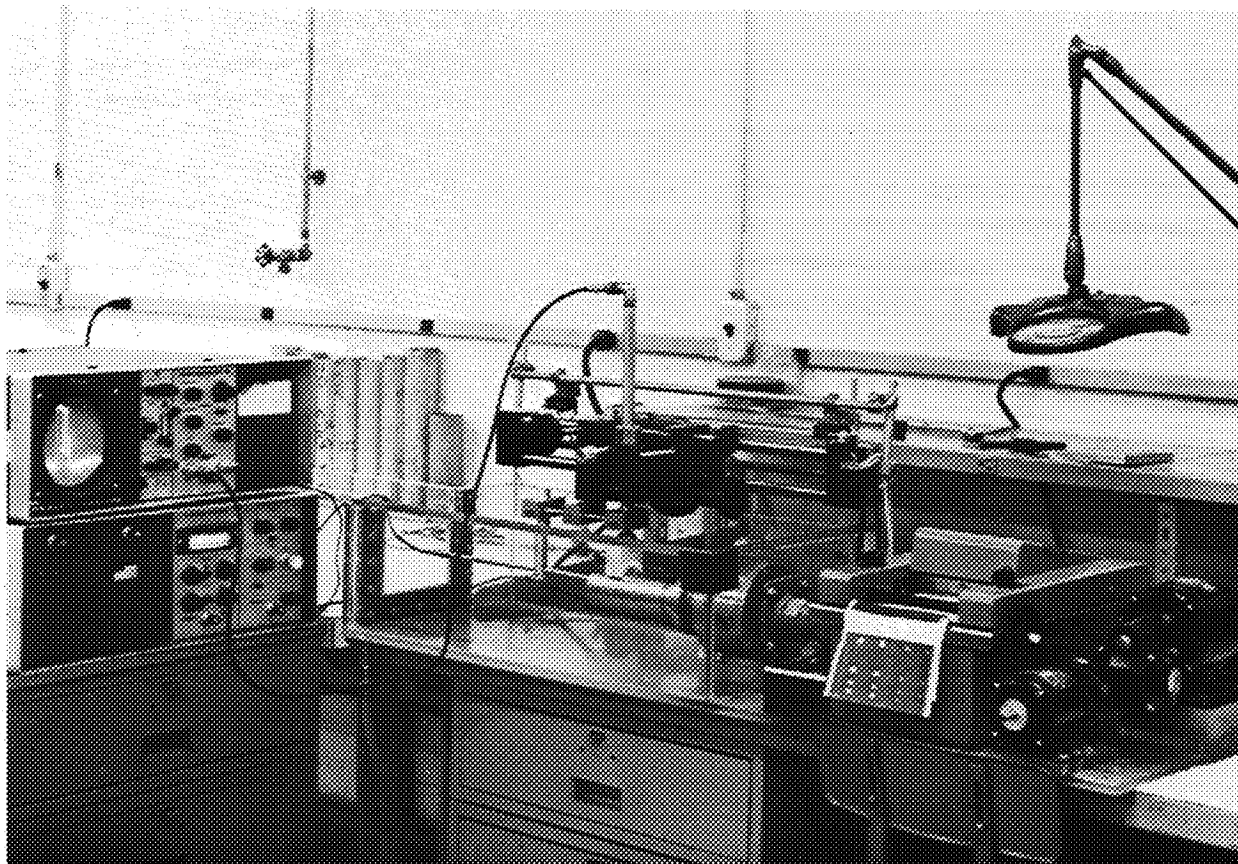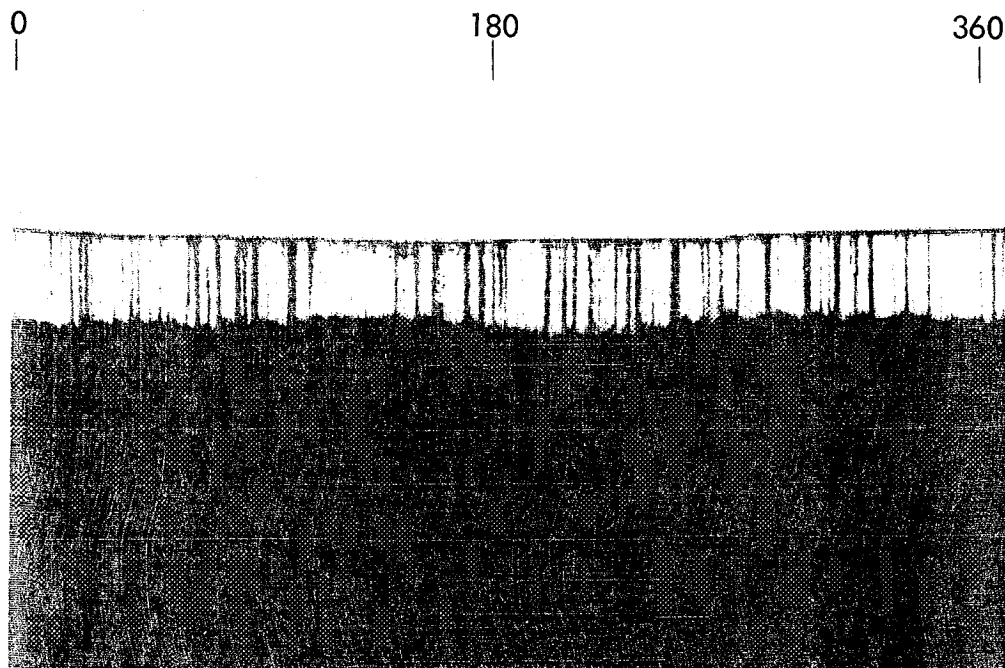
Table 7. Liquid Penetrant Inspection Results

FIGURE 12. Water Immersion Automatic Traversing Transducer Head
for Ultrasonic Testing and "C" Scan Recording

in the sleeve and tandem tests made transducer coupling a problem even with the spring loaded teflon stand-off block which was used. Testing was completed, however, although at some sacrifice in sensitivity.

Sleeve Joint – Figure 13 shows an ultrasonic "C" scan of the counterbored end of sleeve joint No. 4 following the thermal cycle exposure. An electronic gated pulse-echo technique was used and shown on the same figure is the flat bottom hole standard, which was run sequentially and at the same sensitivity level as joint No. 4. Liquid penetrant inspection also identified the defect which was measured by metallographic sectioning to be 0.86 cm (0.340 inches) long as shown in Figure 14. The off-set observed between the tantalum and 316 stainless steel at the free surface of the fissure, Figure 14, top, gives some indication of the thermal strains involved in the dissimilar metal joint. Other than a similar exposure edge unbond at the opposite or flanged end of the sleeve joint, no other ultrasonic defects were observed in the sleeve joint. A pulse-echo technique was also used to inspect the area under the flange with the transducer mounted on the flange edge, but no unbonds were observed in the supposedly high stressed region under the flange. Weld defects in the electron beam tube-to-flange weld were detected using this method. Typical exposed edge unbond areas are also presented in Figures 28 and 29 in a following metallographic section.

Tandem Joint – The continuously tapering interface region of the tandem joint caused difficulty in ultrasonic inspection techniques especially the pulse-echo techniques which were required for the sealed specimens. Through transmission inspection was more successful as shown in Figure 15, a "C" scan of thermal cycled joint No. 7, which was tested sequentially with a tape and flat bottom hole standard. The inside diameter ultrasonic unbond indications were verified by dye penetrant inspection and by metallographic sectioning. Figure 31 from the metallography section shows the longitudinal sections of ultrasonically detected defects in tandem joints No. 7 and No. 8.
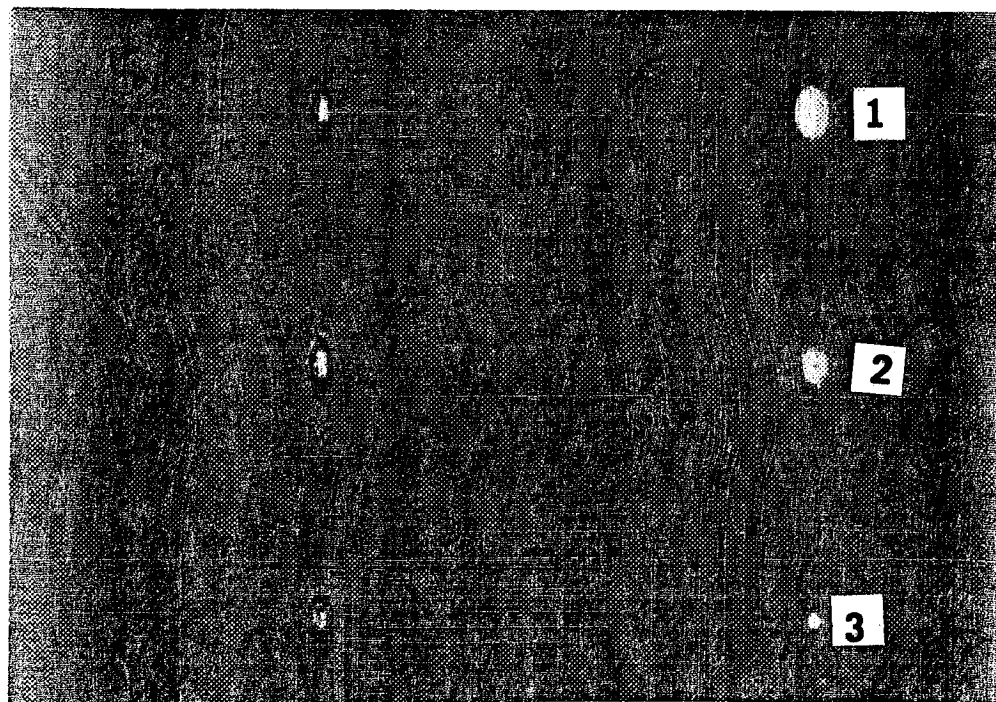
0   180   360

Stainless
Steel

Unbond

Good
Bond
                                                         316
                                                         SS

Tantalum

Tube No. 4 Following 100 Thermal Cycles,Counterbored End
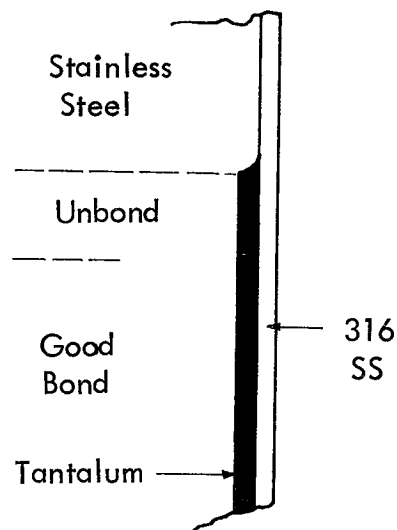
Wall Cross Section

"C" Scan Orientation

360°

0°

Longitudinal

1

2

3

(1) = (0. 190")
(2) = (0. 125")
(3) = (0. 062")

Ultrasonic Standard
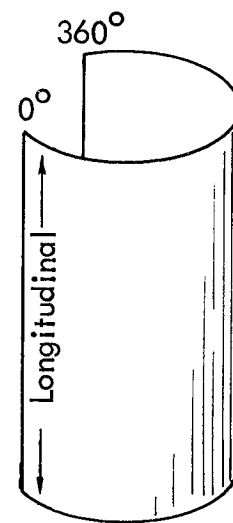
Flat Bottomed Holes

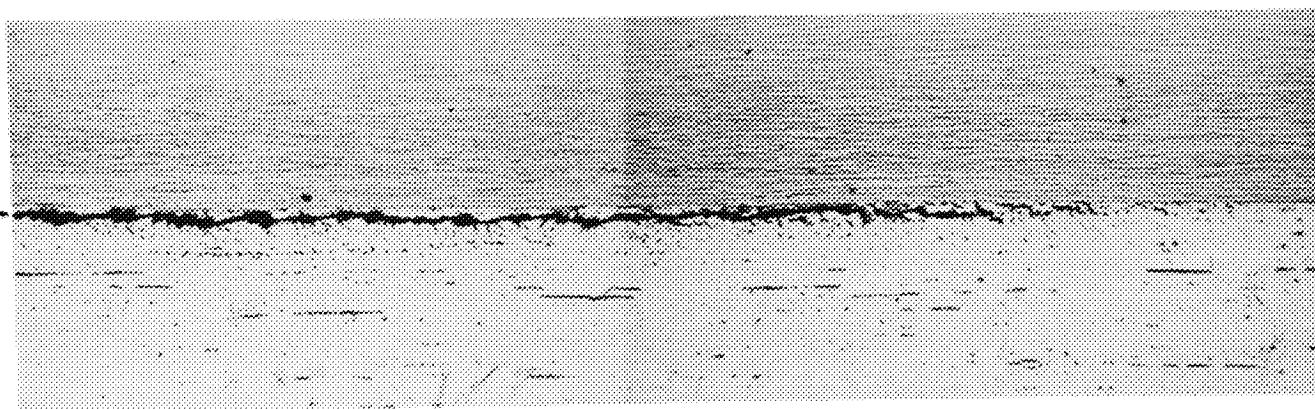FIGURE 13.   15 MHZ Gated Pulse Echo "C" Scans of Unbond
in Thermal Cycled Sleeve Joint No. 4
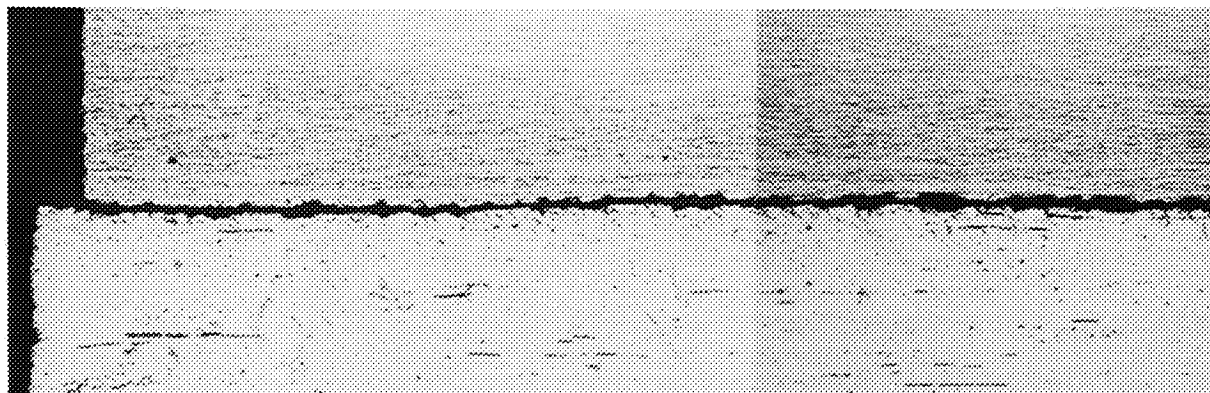
Tantalum
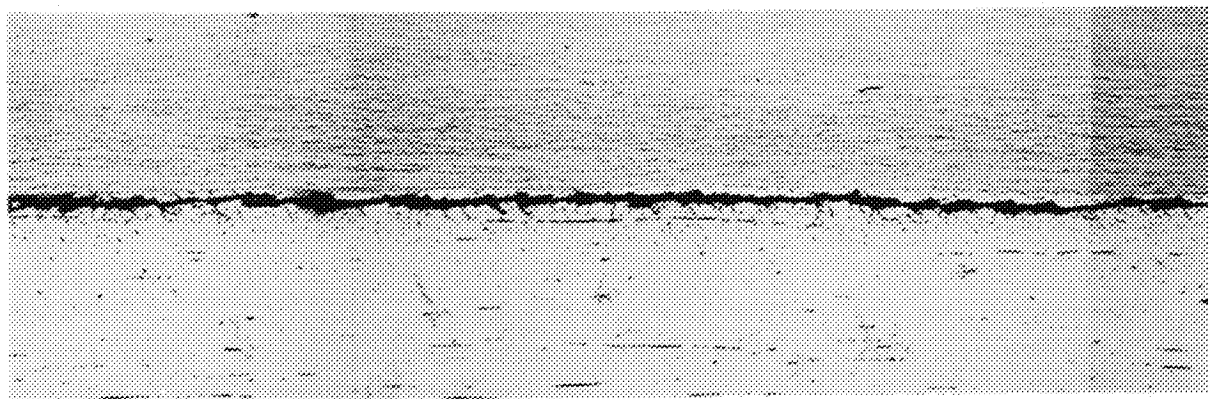
316 SS

23,335   50X

FIGURE 14.   Longitudinal Section of 8.6 mm (0.340 in) Fissure Ultrasonically
Detected in the Counterbored End of Thermal Cycled Sleeve Joint No. 4

0° 180° 360°

Tantalum →

316 SS →
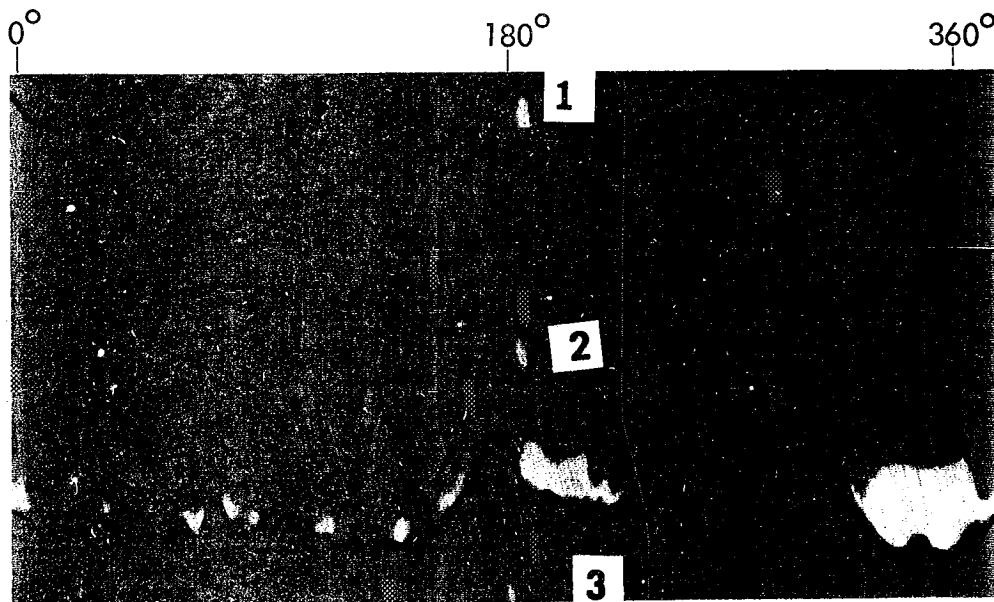
Tube No. 7 Following 100 Thermal Cycles

Wall Cross Section

360°

0°

Longitudinal
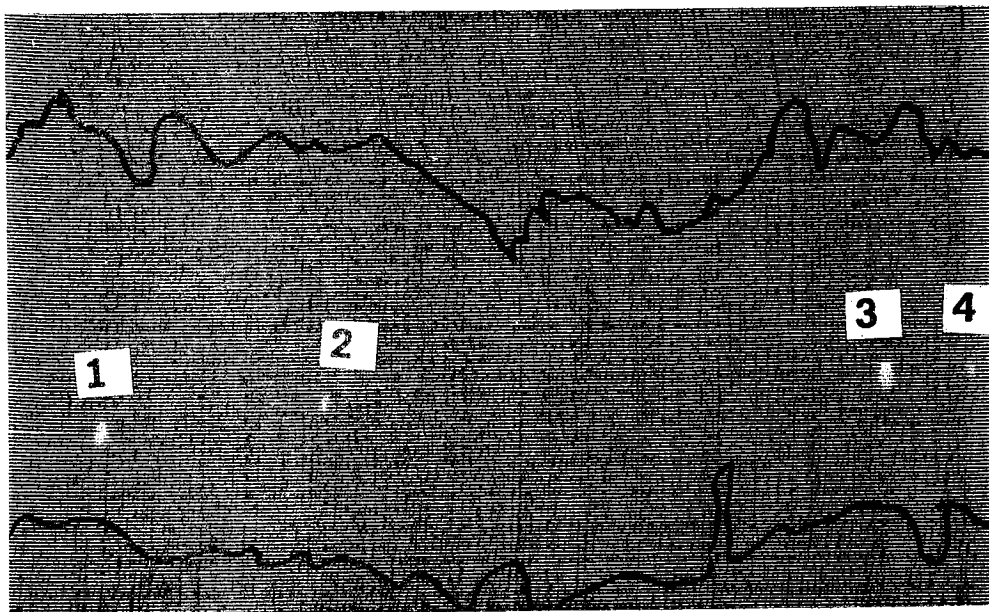
"C" Scan
Orientation

Tandem Ultrasonic Standard No. 4

1 - 1/16" Tape I. D.
2 - 1/16" Tape I. D.
3 - 1/16" Flat Bottomed Hole
4 - 1/32" Flat Bottomed Hole

FIGURE 15. 5 MHZ Thru-Transmission "C" Scans in
Thermal Cycled Tandem Joint No. 7

Brazed Joint - The small overall length of the brazed joint 0.51 cm (0.200 inches) made inspection difficult. In addition, two braze areas, called an outside diameter braze and an inside diameter braze as shown in cross section view in Figure 16, are traversed by the sound beam. Two techniques were used, pulse echo and through transmission with pulse echo having the advantage of discriminating between the inner and outer braze.
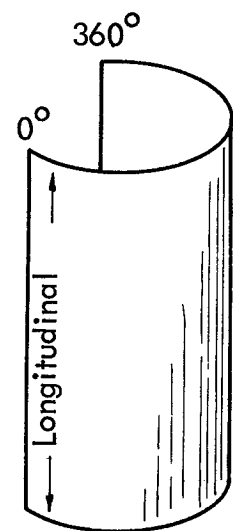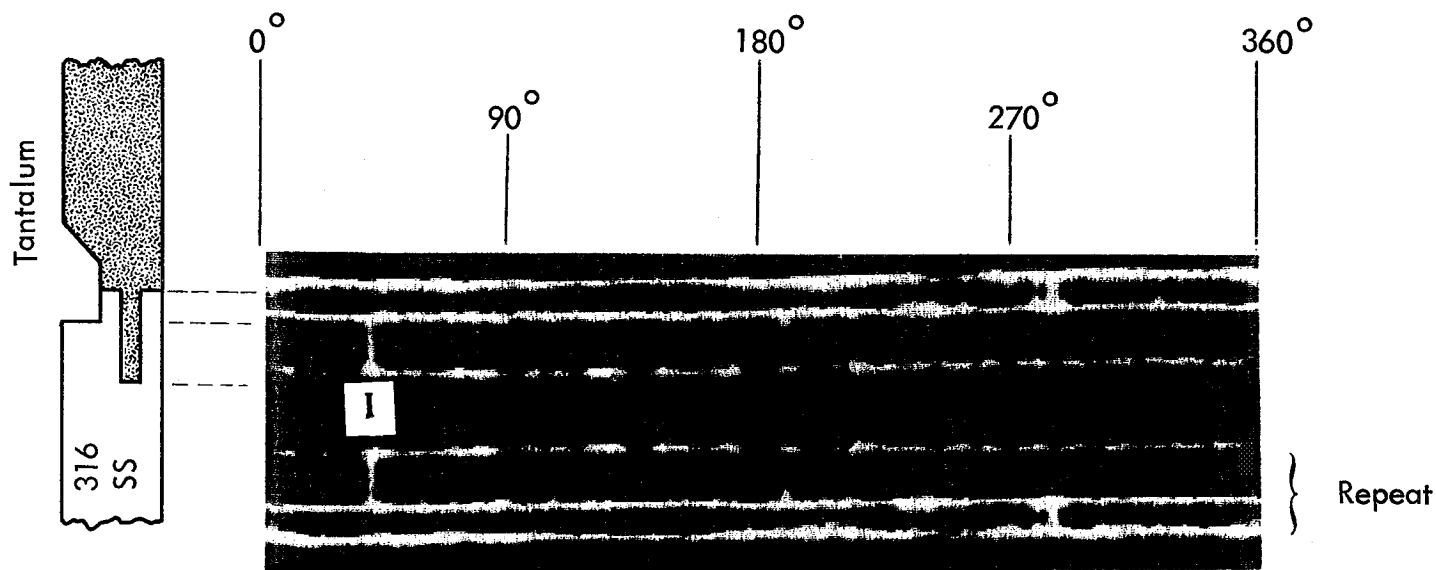
Figure 16 shows "C" scans of through transmission inspection of thermal cycled braze joint No. 10 and the ultrasonic standard. In general, a progressive deterioration of the braze joint could not be followed by intercycle ultrasonic inspection.

C.   Microprobe Analyses

An Applied Research Labs AMX electron beam microprobe scan was used to measure the dissimilar metal interdiffusion zones in the bimetal transition joints. The interdiffusion zone width determined by the microprobe analysis was compared to the similar width determined by optical metallography. The zone width from 1% to 99% of an element concentration as determined by microprobe analysis was larger than that determined optically since only single phase areas will be delineated metallographically. The total diffusion zone widths encountered in this program were very small, 1.2 μm (0.05 x 10^{-3} inches) maximum, which though considered excellent for transition joint durability, made accurate measurement of zone growth difficult.

Since approximately 80% of the diffusion zone growth occurred during the high temperature extrusion of the sleeve and tandem joints, and since the very critical time at temperature prior to extrusion was not precisely known, the diffusion constants for zone growth could only be estimated. The estimates, however, based on one hour at temperature prior to extrusion, compare favorably with previously determined data on dissimilar metal joints[2]. To illustrate the

Braze Joint No. 10 Following 100 Thermal Cycles

1 = 2.0 mm (0.080") Tape Defect
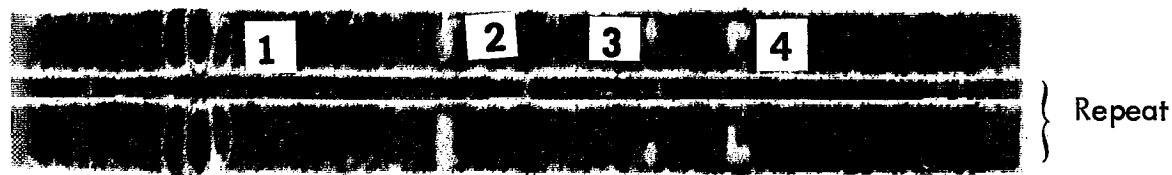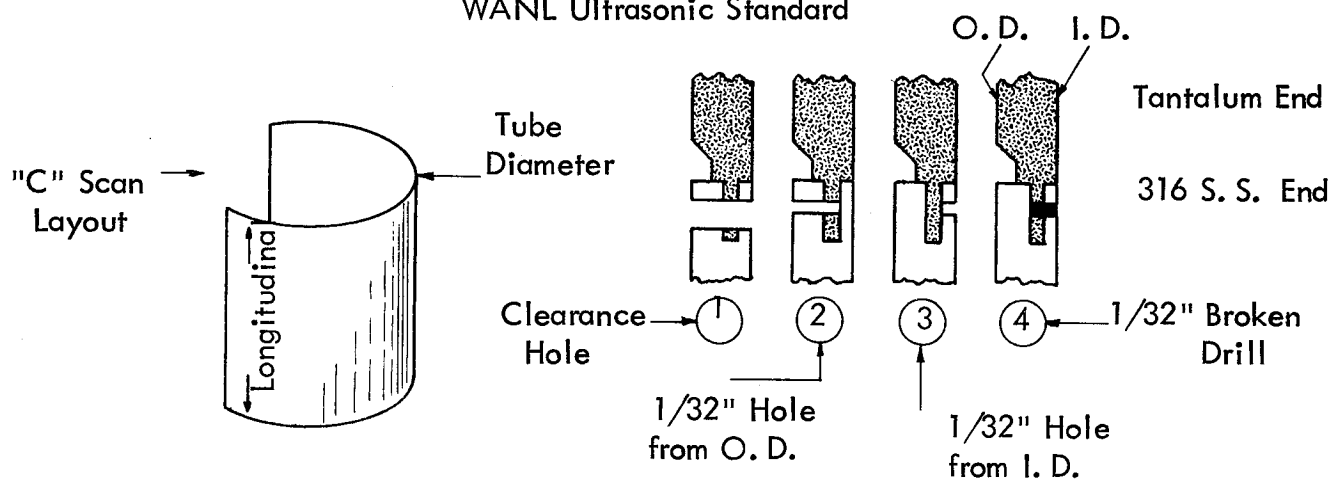
WANL Ultrasonic Standard

FIGURE 16. 5 MHZ Through Transmission "C" Scans of
Thermal Cycled Brazed Joint and Standard

preponderance of diffusion zone growth during the fabrication process, calculations are presented in Table 8 for sleeve joints. The Table 8 calculations were based on diffusion zone growth rates for bimetal couples shown in Figure 17. The comparison of calculated and measured diffusion zone widths presented in Table 8 is within the margin of error observed for heating time prior to extrusion. For instance, if the billets were at temperatures somewhat less than one hour, the calculated diffusion zone width of 1.34 μm (0.053×10^{-3} inches) would be very close to the 0.84 μm (0.033×10^{-3} inches) measured optically.

Figure 18 shows the concentration scans for iron for sleeve joints No. 7 and No. 8 which correspond to the as-extruded joint and 1600 hours additional exposure to 730°C (1350°F), respectively. The very small diffusion distance includes a "smearing" or broadening effect caused by the 1 μm effective spot size of the microprobe. In other words, an "S" shaped apparent concentration gradient twice the spot size or 2 μm would be produced on a traverse across a perfectly abrupt interface. Thus, the measured 1% to 99% concentration gradients must be reduced or corrected by 2 μm as shown in Table 9. For more extensive diffusion zones, the spot size correction would be insignificant, but for the small diffusion zones obtained in this program, the uncertainty in measurement technique was half or better of the total diffusion zone thickness. As also shown in Figure 18, the expected step transition in concentration, corresponding to single phase areas of intermetallic compounds, was not observed for any of the element scans, probably because of the measurement limitations. Several areas tentatively identified as Ta (Fe, Cr, Ni) and Ta_8 (Fe Ni) have been observed in more extensive diffusion zones in Ta/321 stainless steel exposed at 865°C (1600°F) for 2700 hours[2].

Table 9 is a summary of the linear microprobe scans for the three types of transition joints. The tandem and sleeve joints were similar with the tandem joints having the smaller diffusion

TABLE 8

Relative Contribution of Extrusion and Test Exposure to Diffusion Zone Growth in Sleeve Joints

	Extrusion Contribution	Total Thermal Cycle Exposure Contribution
Temperature	(1950°F) 1338°K	(1350°F) (1005°K)
Time	1 hour	1600 hours
Parabolic Growth Rate[1] K	(1.5×10^{-4} in/hr $1/2$), (3.8 μm/hr $1/2$)	(2.0×10^{-7} in/hr $1/2$), (5.08×10^{-3} μm/hr $1/2$)
Width $D = K t^{1/2}$	$D = K (1 \text{ hr})^{1/2}$ 3.8 μm (0.15×10^{-3} in.)	$D = K (1600 \text{ hrs})^{1/2}$ 0.2 μm, (0.008×10^{-3} inches)
Extrusion Reduction in Area Ratio	8:1 $\sqrt{8} = 2.84$ is reduction in dia.	No extrusion related reduction in thickness involved
Reduction in size of diffusion zone due to extrusion	3.8 μm/$2.84 = 1.34$ μm (0.15×10^{-3} in/$2.84 = 0.053 \times 10^{-3}$ in.)	Total change in thickness to be observed is: 0.2 μm/1.34 μm $= 15\%$ 0.008 in./0.053 in. $= 15\%$
Measured Diffusion Zone Metallographic Microprobe (1% to 99%)	0.84 μm (0.033×10^{-3} in.) 3.6 μm (0.14×10^{-3} in.)	Measured change is less than specimen to specimen variation

1×10^{-2} 254

O   Data of Ferry and Page
(Ref. 11) for Cb/316 Bimetal

Data of Buckman and
Goodspeed, Ref. 2

1×10^{-3} 25.4

⬢   Cb/321
◆   Ta/321
▲   T-222/347
●   Cb/Inconel 600

1×10^{-4} 2.54

+   Used for the calculations,
Table 8

$K \ (in - hr^{-1/2})$

$K \ (\mu m - hr^{-1/2})$

1×10^{-5} 2.54×10^{-1}

1×10^{-6} 2.54×10^{-2}

$1600^{\circ}F$ $1500^{\circ}F$ $1400^{\circ}F$

1×10^{-7} 2.54×10^{-3}

7.0   7.5   8.0   8.5   9.0   9.5   10.0

$1/T \times 10^{4} \ (^{\circ}K^{-1})$ 612324-11B
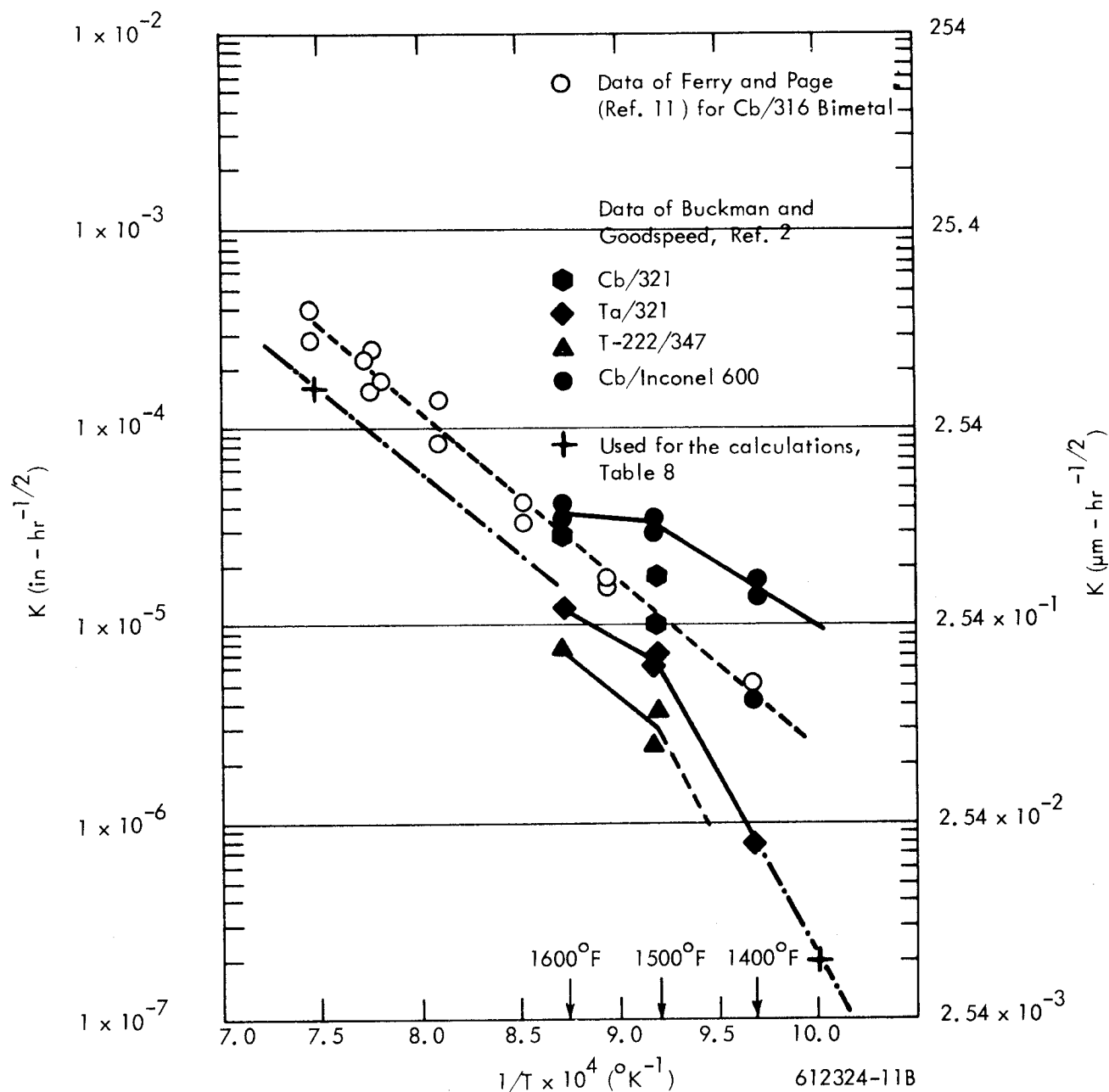
FIGURE 17. The Parabolic Reaction Rate of Interdiffusion Zone Growth as a
Function of Reciprocal Temperature for Selected Refractory/
Austenitic Bimetal Composites
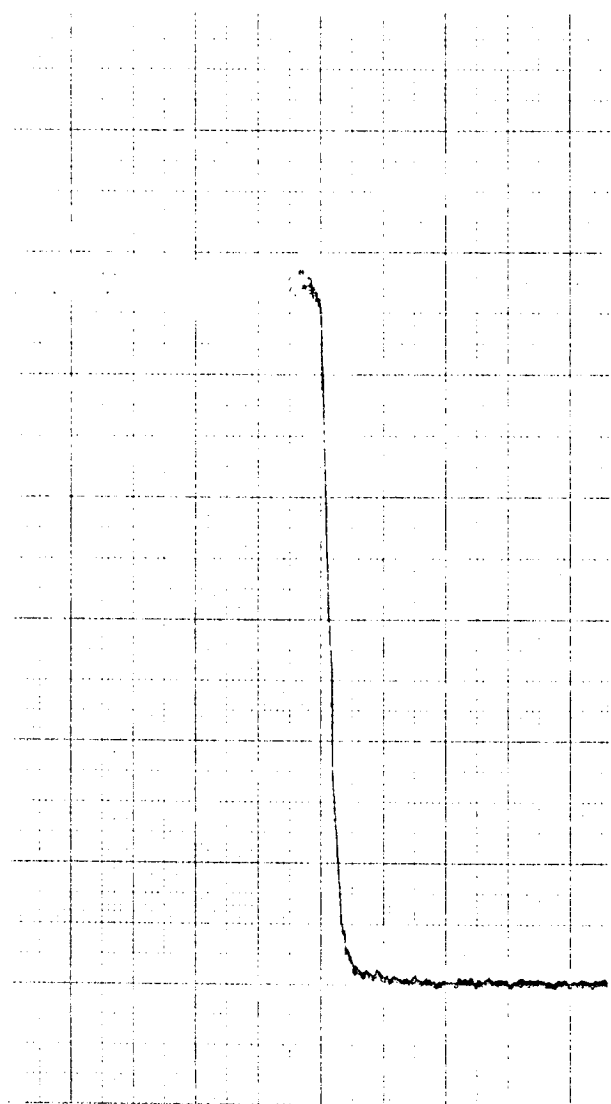
316 SS ⟶| |⟵ Tantalum

3.0 μm
(0.12 x 10⁻³ inches)

S-7 As-extruded Sleeve Joint
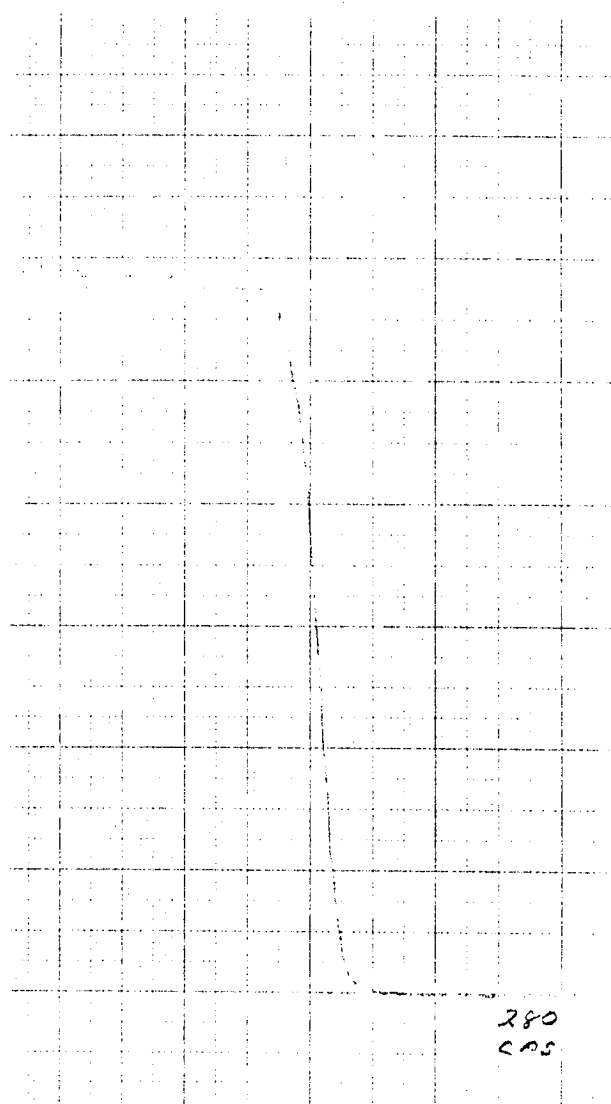
316 SS ⟶| |⟵ Tantalum

5.8 μm
(0.23 x 10⁻³ inches)

S-8-B Thermal Cycled Sleeve Joint
1600 Hours at 1350°F

FIGURE 18. High Magnification Electron Microprobe Linear Scans for Iron Over Bimetal Interface in 316 SS/Tantalum Sleeve Joints

TABLE 9

Diffusion Zone Widths Determined by Microprobe Perpendicular Traverse

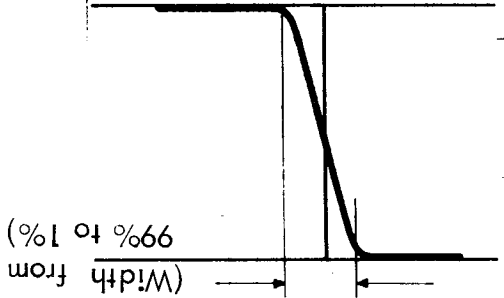|		Sleeve				Tandem				Ta/Braze				Braze/Stainless Steel			
		S-7		S-8B		T-3		T-11B		B-11 As-brazed		B-11 2000 hrs at 732°C		B-11 As-brazed		B-11 2000 hrs at 732°C	
		μm	10^{-3} (in.)	μm	10^{-3} (in.)	μm	10^{-3} (in.)	μm	10^{-3} (in.)	μm	10^{-3} (in.)	μm	10^{-3} (in.)	μm	10^{-3} (in.)	μm	10^{-3} (in.)
Fe	Direct	5.0	0.200	7.8	0.300	4.5	0.180	6.1	0.240	2.8	0.110	7.5	0.290	13.1	0.510	9.7	0.380
	Corrected	3.0	0.120	5.8	0.230	2.5	0.097	4.1	0.160	0.8	0.031	5.5	0.210	11.1	0.430	7.7	0.300
Cr	Direct	3.4	0.130	5.0	0.200	3.1	0.120	4.5	0.180	2.4	0.093	5.0	0.200				
	Corrected	1.4	0.055	3.0	0.120	1.1	0.043	2.5	0.098	0.4	0.016	3.0	0.120				
Ni	Direct	2.5	0.098	4.0	0.160	1.9	0.074	3.8	0.150	8.9	0.350	13.1	0.510				
	Corrected	0.5	0.019	2.0	0.078	0.0	0.000	1.8	0.070	6.9	0.270	11.1	0.430				
Ta	Direct	5.6	0.220	7.5	0.290	4.1	0.160	5.5	0.210	4.4	0.170	7.4	0.290				
	Corrected	3.6	0.140	5.5	0.210	2.1	0.082	3.5	0.140	2.4	0.094	5.4	0.210				
Co	Direct									3.8	0.150	6.4	0.250	13.1	0.510	11.5	0.450
	Corrected									1.8	0.070	4.4	0.170	11.1	0.430	9.5	0.370
Si	Direct									4.7	0.180	2.8	0.110	13.9	0.540	9.4	0.370
	Corrected									2.7	0.110	0.8	0.031	11.9	0.460	7.4	0.290
Metallographic Measurement		.84	0.033	1.20	0.047	.69	0.027	.76	0.030								

Inset (within Braze/Stainless Steel columns): (Width from 99% to 1%)

zone, probably because of the lower extrusion temperature, 995°C (1825°F), as compared to 1065°C (1950°F) for the sleeve joints. The higher extrusion reduction ratio for the sleeve joint, 8:1 as compared to 5:1 for the tandem joint, apparently did not compensate for the increased diffusion at the higher temperature.

Brazed Joints - The thermal history of the cobalt base alloy brazed joints was complicated to the extent that any sort of post-braze diffusion analysis was impossible. The brazing cycle, which occurred over a temperature range of from 1180°C (2160°F) to 1230°C (2250°F) produced a liquid phase in the braze proper and considerable erosion of the tantalum and 316 stainless steel. Subsequent diffusion during the 1600 hour thermal cycle or 3000 hour thermal exposure at 730°C (1350°F) was dwarfed by the massive and variable melting and erosion during brazing.

A significant amount of the higher melting point tantalum was dissolved during the brazing process as shown by the electron beam microprobe linear scan for tantalum, Figure 19. Tantalum indications are observed across the entire large braze area. The metallographic section, Figure 20, shows the tongue and groove joint area traversed from bottom to top by the electron beam microprobe. The difficulty in determining post-braze diffusion is indicated by Figure 21 which is a high magnification microprobe scan for tantalum across the tantalum tongue-large braze interface. The arbitrary lower limit of 1% for tantalum is impossible to determine since islands of tantalum rich intermetallic compound extend throughout the braze area. Significant erosion of the stainless steel section of the brazed joint was indicated by microprobe scans for iron, Figure 22, which indicated an appreciable level of iron, 20-30%, in the iron free J-8400* braze alloy. Figure 23 shows microprobe scans for nickel and chromium, both of which are present in the stainless steel and the braze alloy. Figure 24 is a scan of cobalt and silicon elements that are limited to the braze alloy.
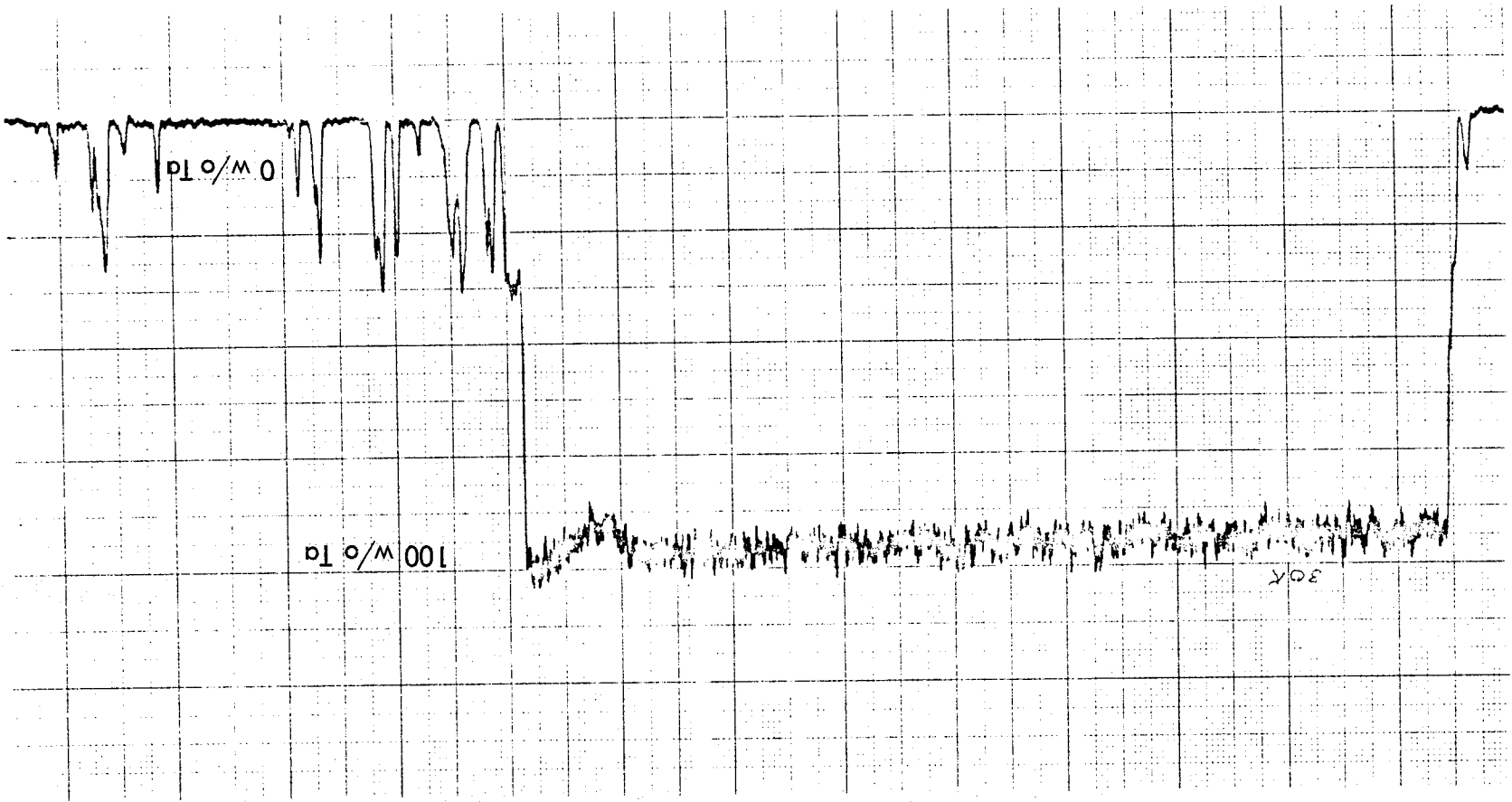
48

FIGURE 19. Low Magnification Electron Beam Microprobe Linear Scan for Tantalum Across Brazed Joint No. 11, As-brazed Condition

Astronuclear Laboratory

Tantalum → | |← Large Braze

5.5 μm
(0.210 x 10^{-3} inches)

FIGURE 21. High Magnification Electron Microprobe Linear Scan for
Tantalum Across Tantalum to Braze Interface
on Joint No. 11, As-brazed Condition

70 w/o Fe

0 w/o Fe
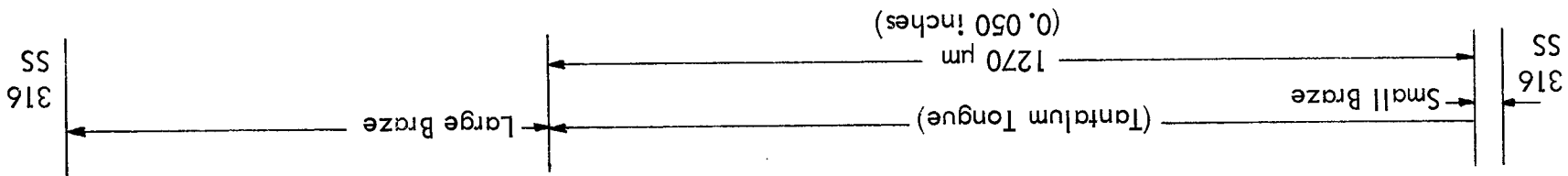
316
SS

Small
Braze

Tantalum Tongue

Large Braze

316
SS

FIGURE 22. Low Magnification Electron Beam Microprobe Linear Scan
for Iron Across Braze Joint No. 11, As-brazed Condition
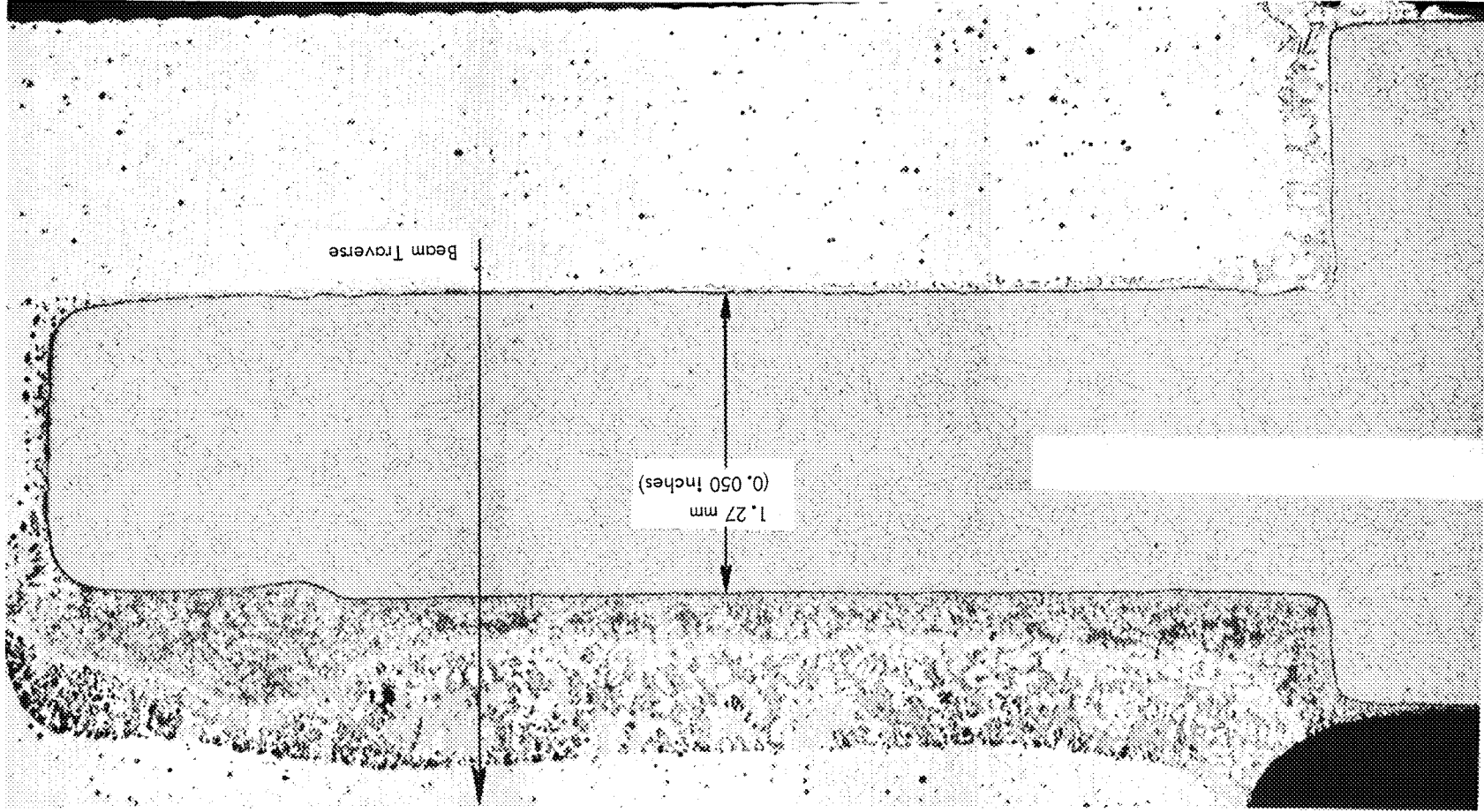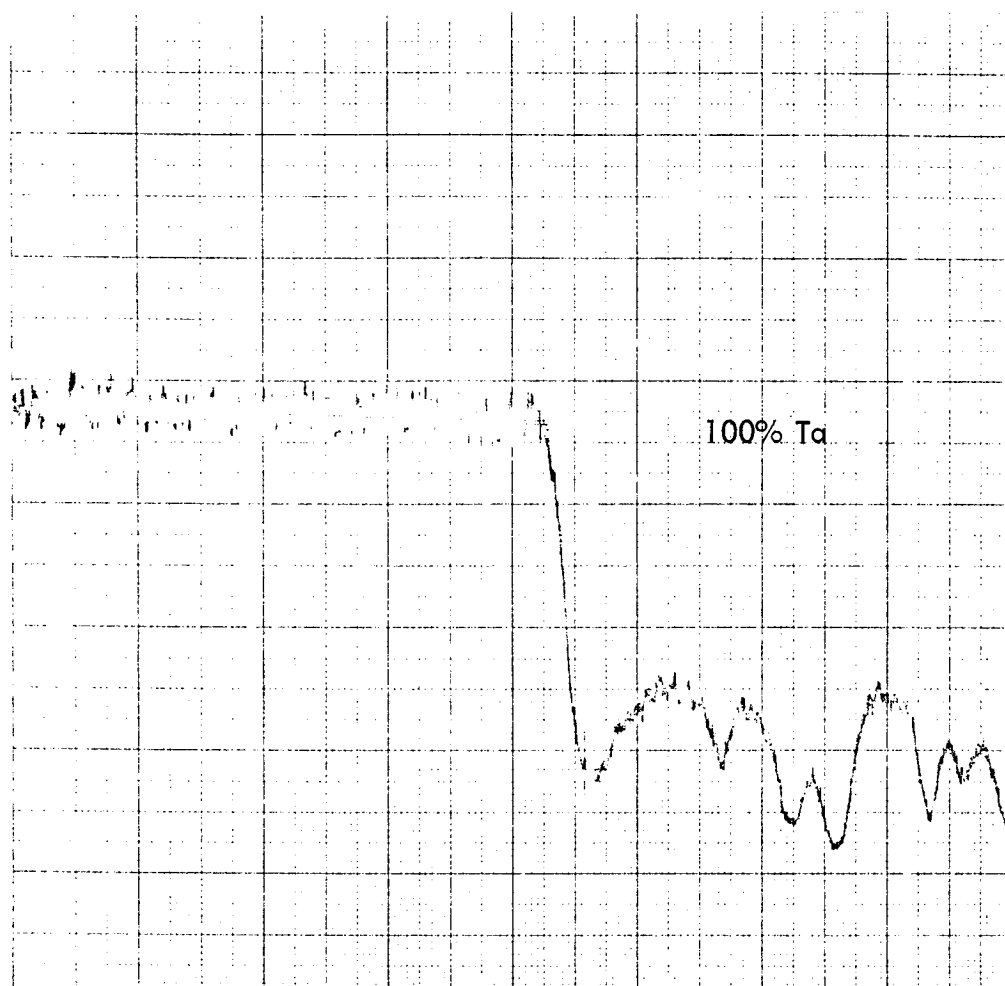
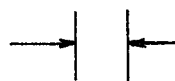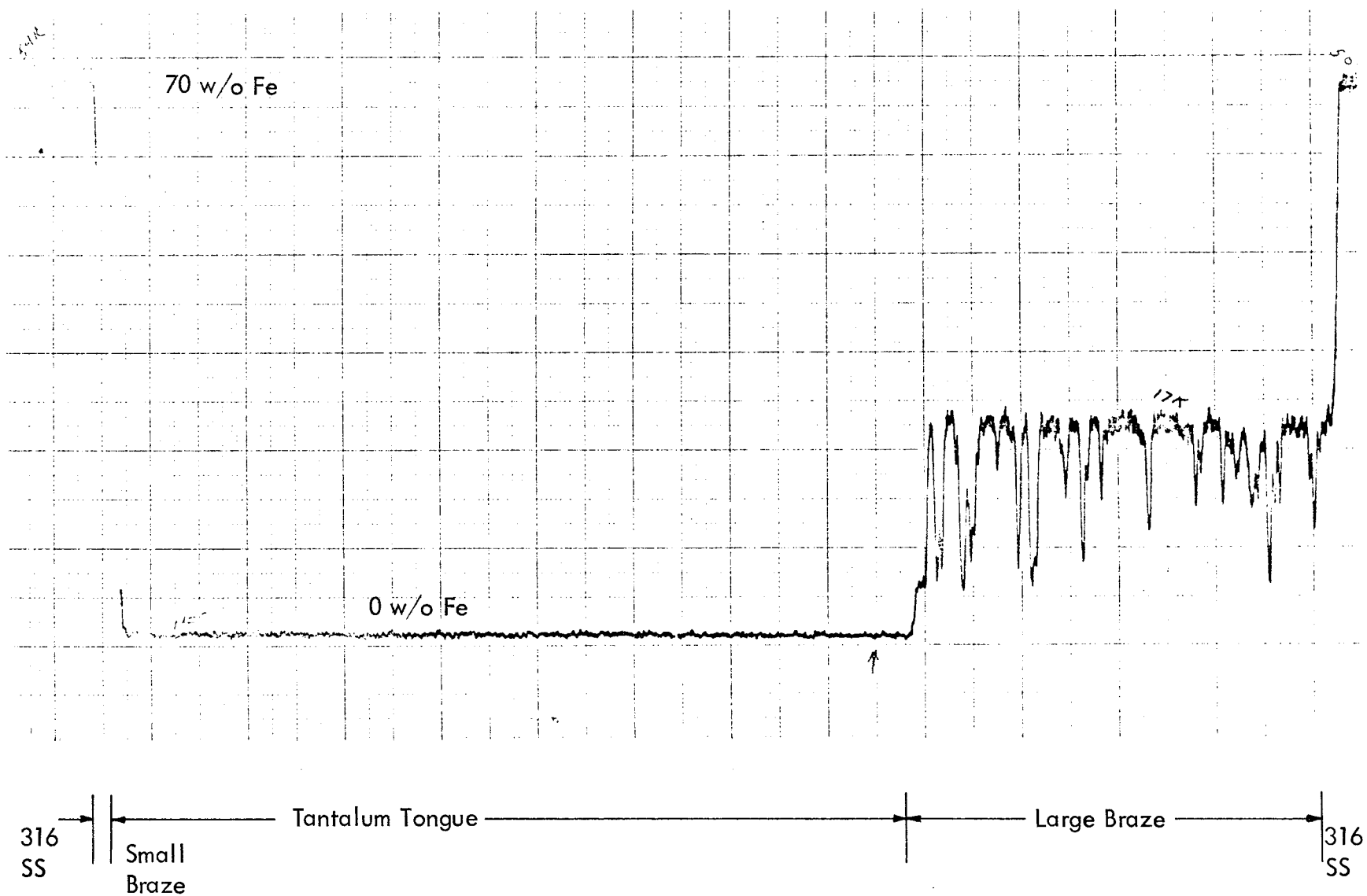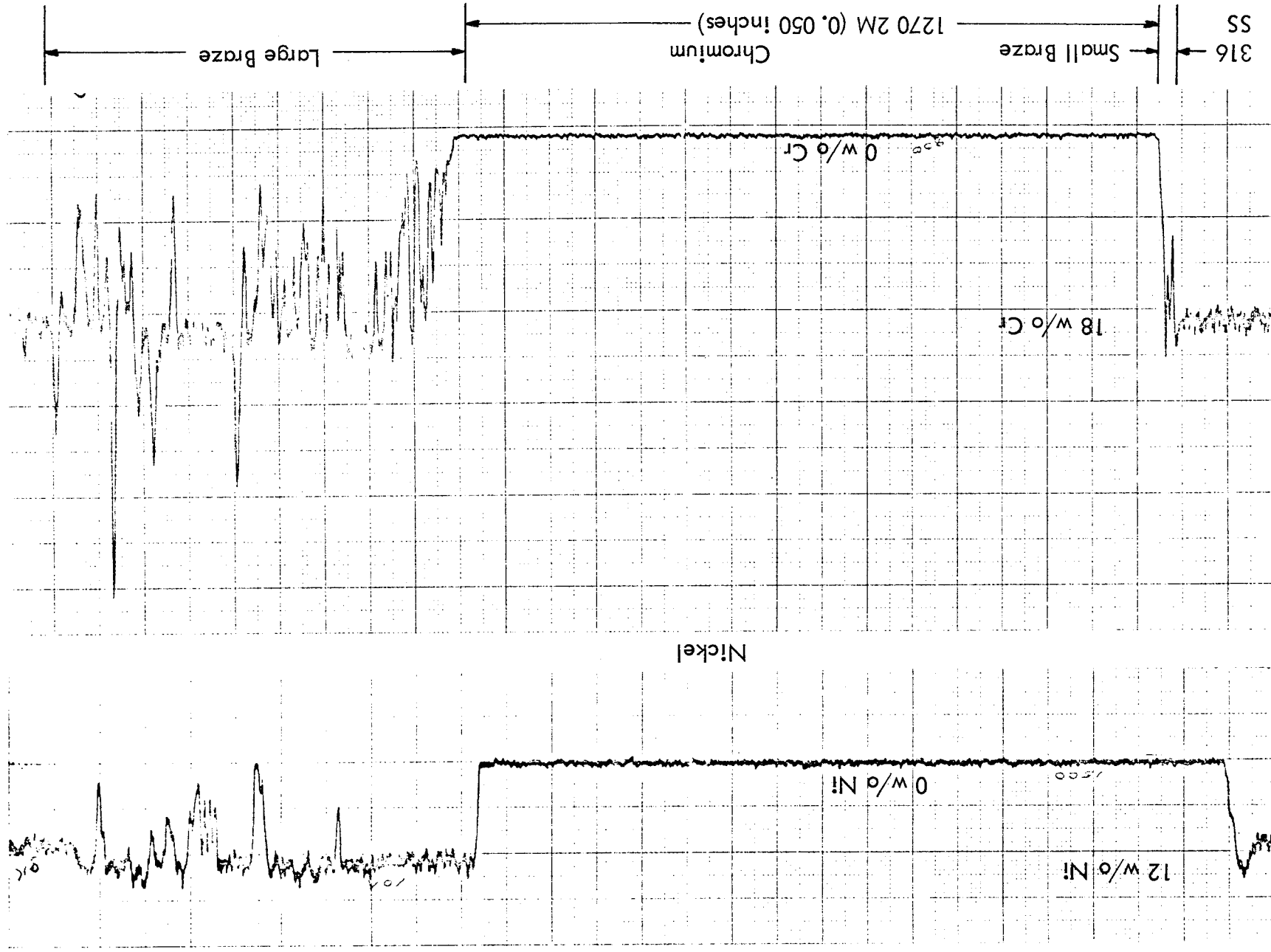FIGURE 23. Low Magnification Electron Beam Microprobe Linear Scans for Nickel and Chromium Across Braze Joint No. 11, As-brazed Condition
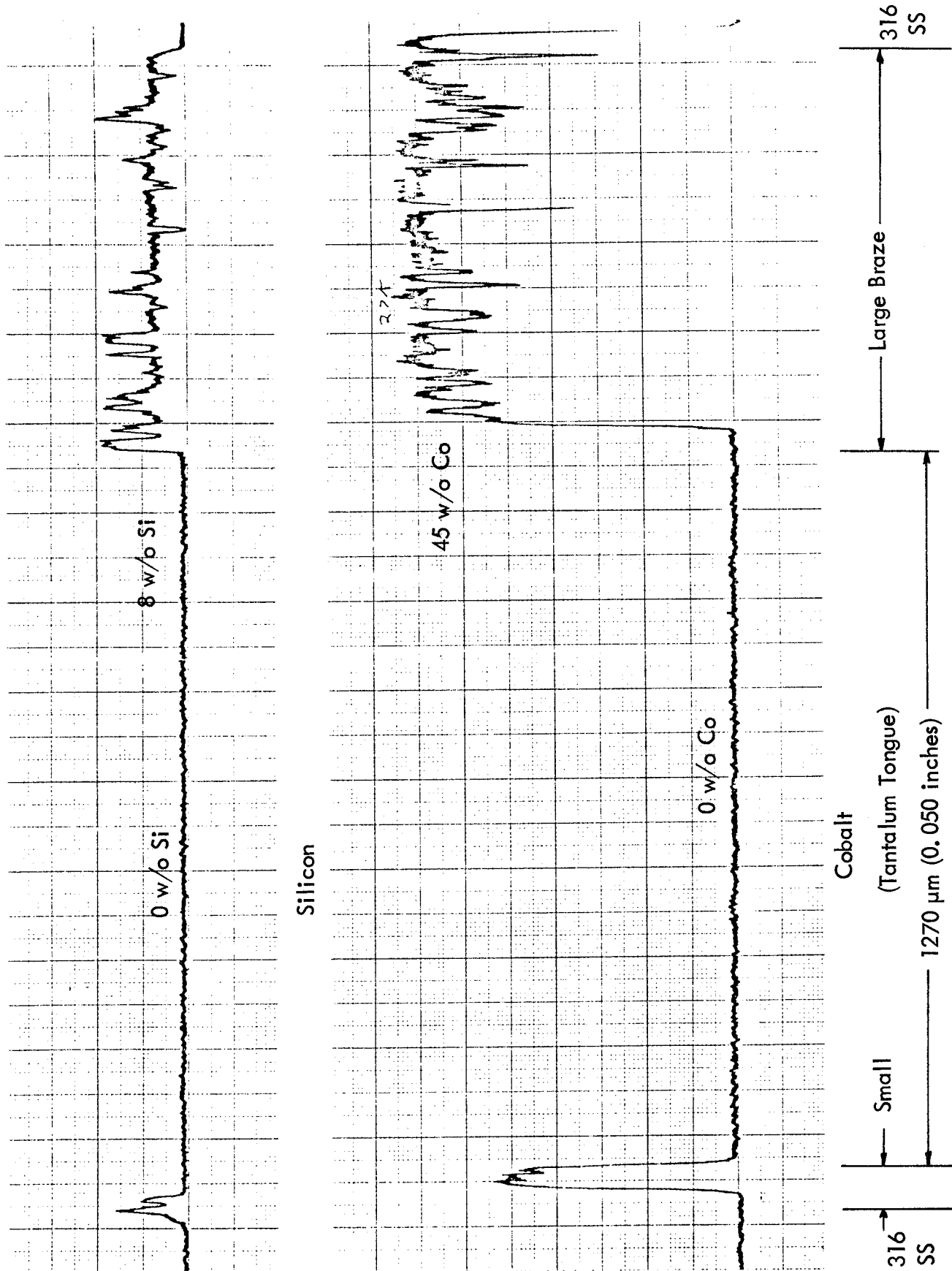
FIGURE 24. Low Magnification Electron Beam Microprobe Linear Scans for Silicon and Cobalt on Braze Joint No. 11, As-brazed Condition

54

Extrapolated Lifetime

Based on the assumption that bimetal bond properties are seriously degraded when the inter-diffusion zone exceeds 12.7 μm (0.5 x 10^{-3} inches)[2], an estimate may be made of the expected service life for tantalum-316 stainless steel joints at a temperature of 730°C (1350°F). A lifetime of 500 years is estimated on an as-fabricated maximum diffusion zone of 2.5 μm (0.1 x 10^{-3} inches) and predicting 10 μm (0.4 x 10^{-3} inches) for diffusion zone growth during service. The equation used and other time and temperature combinations are shown as follows:

$$D = K\,t^{1/2}$$

D = diffusion distance, μm

t = time, in hours

K = parabolic reaction rate constant** at 730°C (1350°F)
5.08 x 10^{-3} μm/$hr^{1/2}$ (2 x 10^{-7} in/$hr^{1/2}$)

Maximum temperature for 1000 hour life – 865°C (1590°F)

Maximum temperature for 10,000 hour life – 800°C (1480°F)

D. Microstructure and Hardness

A presentation of the as fabricated microstructure and hardness of all three types of bimetal transition joints was deferred to this section to more directly compare the "before and after thermal cycling" characteristics.

---

* 45 w/o Co, 21 w/o Cr, 21 w/o Ni, – 8 w/o Si – 3.5 w/o W 0.8 w/o B – 0.4 w/o C

**From Figure 17

Sleeve Joints

The thin interdiffusion zone of the as-extruded product can be measured in Figure 25 which is a longitudinal section view of sleeve joint No. 7. The effects of 100 thermal cycles, and in the case of Plan B specimen, an additional 1000 hour exposure at 730°C (1350°F) is shown in Figure 26. The formation of a considerable volume of sigma phase is observable in the 316 stainless steel due to the long exposure time at 730°C (1350°F). A comparative microhardness traverse across the bimetal interface is shown in Figure 27 for an as-extruded and thermal cycled sleeve joint. Considerable hardening for both the tantalum and 316 stainless steel is observed at the interface, probably due to thermal strain hardening during thermal cycling.

The hardness of the 316 stainless steel is much greater than the 145 DPH expected for solution treated and quenched material and reflects a partially work hardened condition following the 1065°C (1950°F) extrusion. The tantalum is also considerably harder, 180 DPH, than annealed high purity tantalum which will approach 70 - 80 DPH. The interstitial level of the tantalum section from sleeve joint No. 7 was 12 ppm carbon, 31 ppm nitrogen, and 53 ppm oxygen which is considered better than average commercial material.

All of the sleeve joint displayed bimetal joint separation at both ends of the tube section by the end of the 100 thermal cycles. Dye penetrant inspection was used to identify the defect, a summary of the results of which was shown in Table 7. Figure 28 is a longitudinal view of the flange end defect, which in Joint No. 6 extends .25 cm, (0.100 inch) along the bond length. The thermal strain has permanently increased the length of the stainless
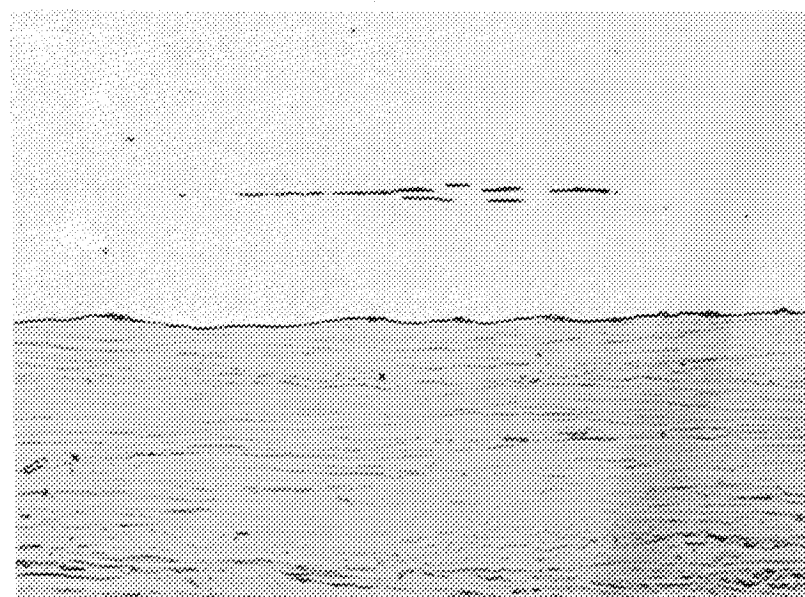
22,478A   400X

316 SS

25.4 µm
(0.001 inches)

Ta

22,478A   1500X

316 SS

0.84 µm
(.033 x 10^{-3} inches)

2.54 µm
(0.0001 inch)

Ta
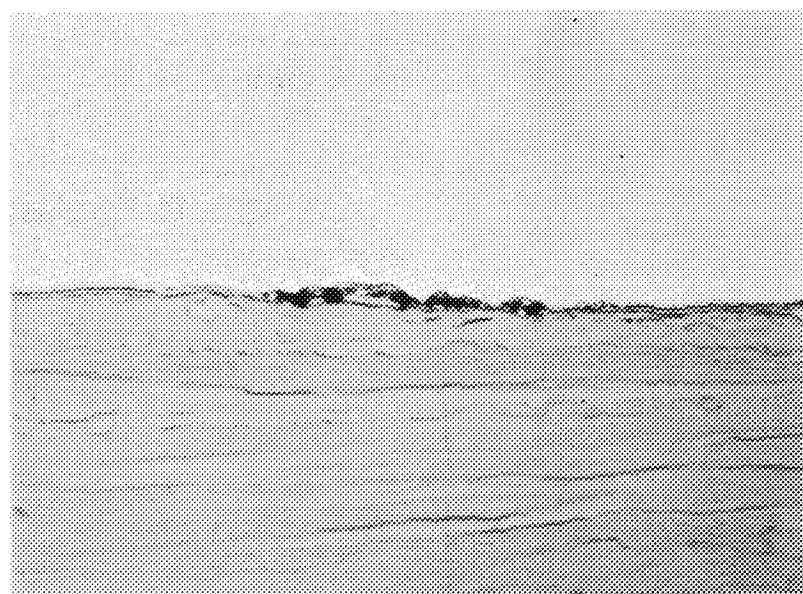
FIGURE 25. Longitudinal Section of Flanged Sleeve Joint No. 7
at Location "A" As-extruded
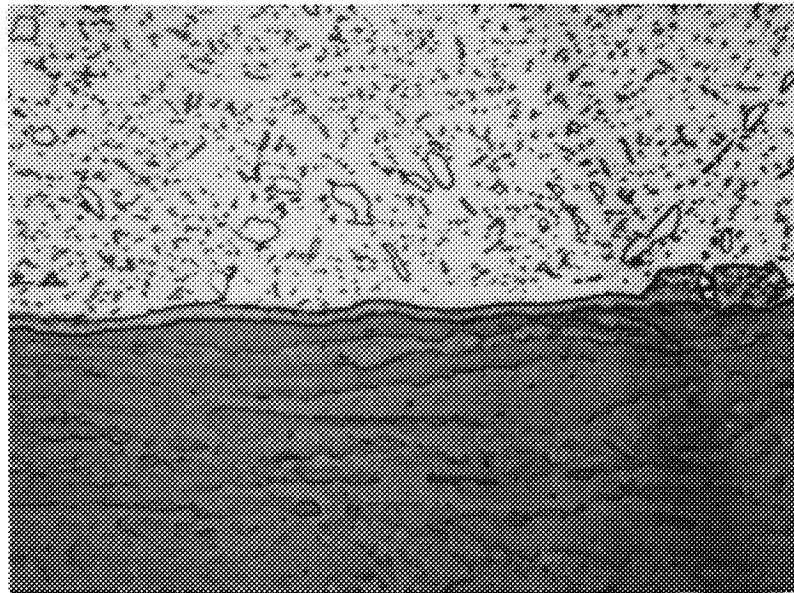
No. 8 Pressurized

316 SS   1.2 μm
          (0.047 x 10^{-3} inches)

          Plan B
          1600 Hours at 732°C
                    (1350°F)

Ta

23,336   1500X
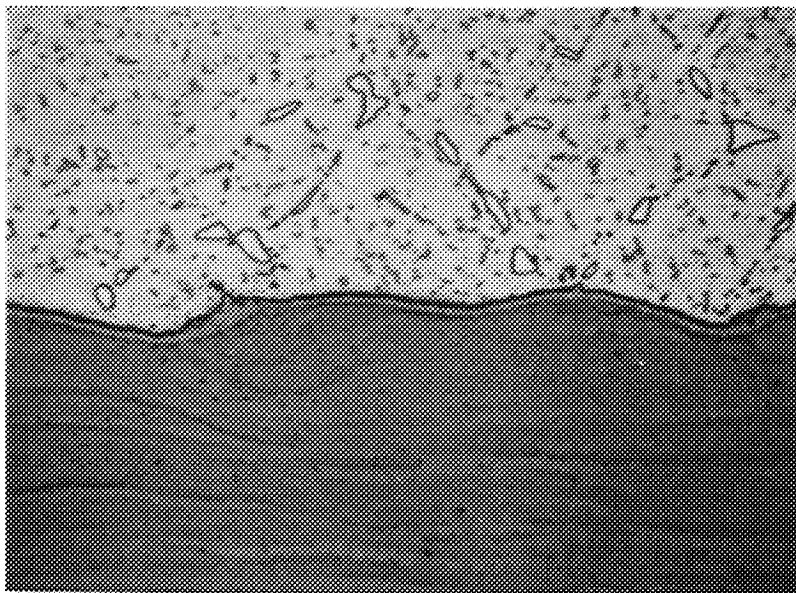
No. 2 Open

316 SS   0.93 μm
          (0.037 x 10^{-3} inches)

          Plan A
          600 Hours at 732°C
                    (1350°F)

Ta

23,335   1500X

FIGURE 26. High Magnification Comparison of Interdiffusion
Zone Growth in Thermal Cycled Sleeve Joints

No. 4, 100 Thermal Cycles, Plan A, Open Sleeve Joint
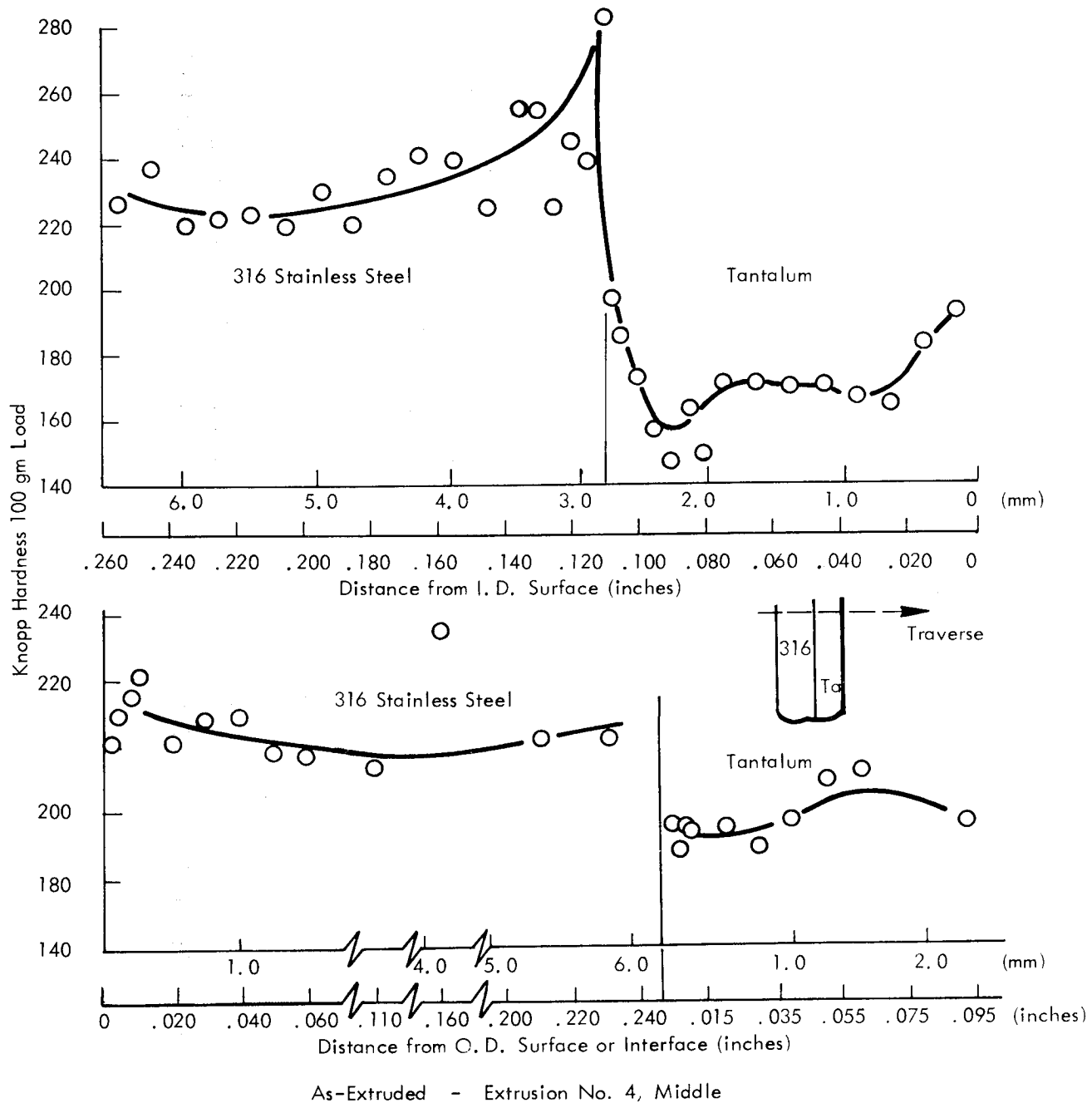
Figure 27. Comparison of As-Extruded and Thermal Cycled Hardness Traverses from Extrusion and Sleeve Joint No. 4, Longitudinal Sections

316 SS

Ta

23,334   Bond Rupture in Sleeve Joint No. 6   50X

316 SS

Tantalum

23,333   Sleeve Joint No. 2   50X

Flange

Flange Area

316 SS

254 μm
(0.010 inches)

FIGURE 28. Flange End Interface in Thermal Cycled Sleeve Joints
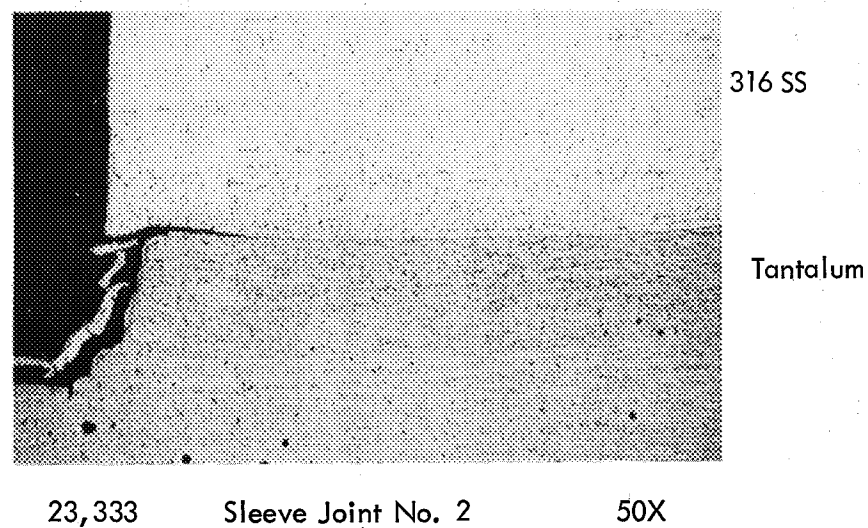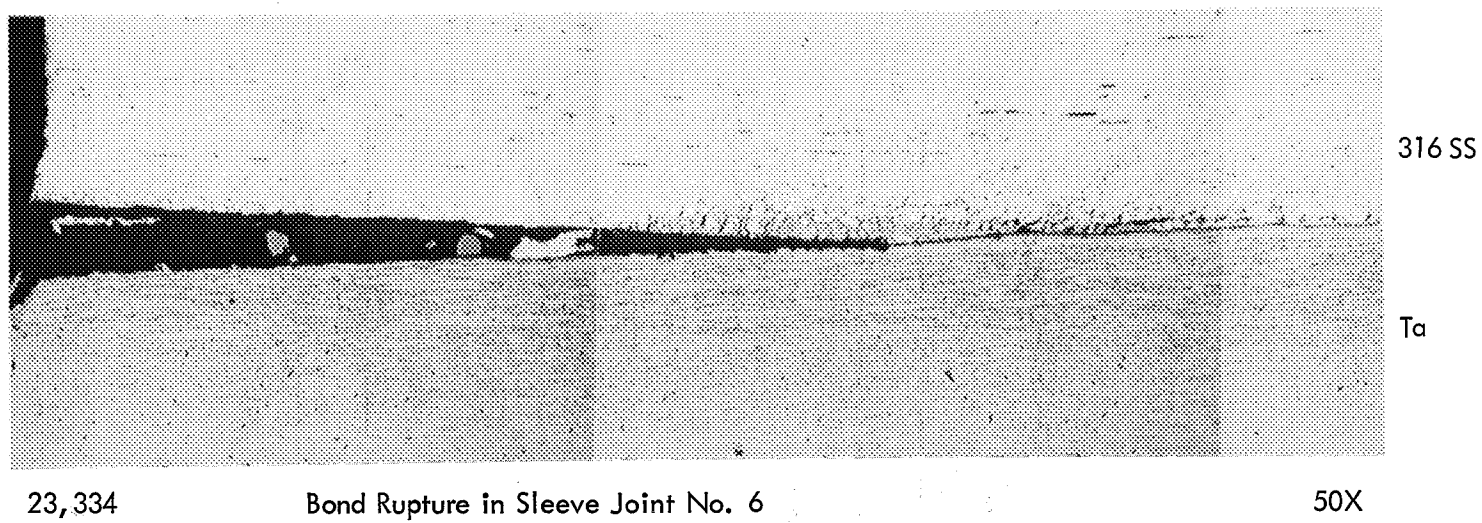
steel component as shown by the significant offset in the lower photograph in Figure 28.
A much deeper fissure   generally occurred at the end opposite the flange area as shown in
Figure 29.   The fissure   has propagated entirely in the stainless steel side of the sleeve joint
to a depth of nearly 0.63 cm, (0.250 inch).   A more extensive fissure in the counterbored
end of sleeve joint No. 4 which was also detected by ultrasonic inspection, was shown in
Figure 14.

Tandem Transition Joints

The critical structural area for tandem transition joints is considered the "feather edge"
bimetal overlap which occurs at the inside and outside diameter.   Figure 30 is an example of
a well bonded feather edge following 100 thermal cycles.   As noted in Table 7, the summary
of dye penetrant inspection results, 3 of the 4 thermal cycled tandem joints had no defects
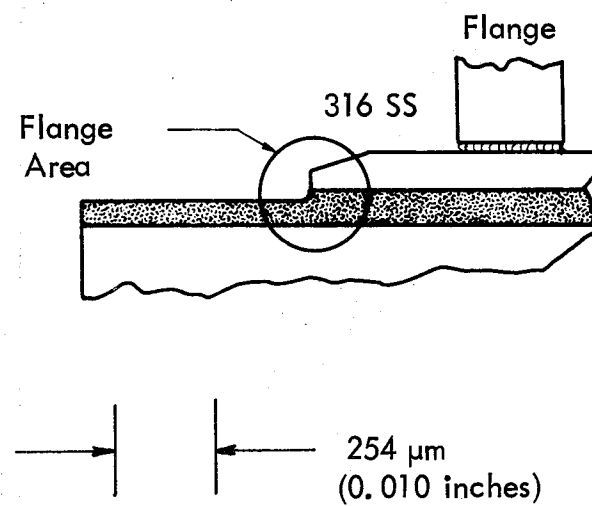on the outside diameter feather edge following 100 thermal cycles, but all had defects on
the inside diameter.

A comparison of the inside and outside diameter feather edge defects of tandem joints Nos. 7
and 8 is shown in Figure 31.   The fissures propagated through the stainless steel on the inside
diameter and through the tantalum on the outside diameter,similarly to the sleeve joint defects.

A higher magnification longitudinal section of as-extruded tandem joint No. 3 is shown
in Figure 32 which can be used to optically measure the diffusion zone width.   As was
discussed in the previous section on microprobe results, the diffusion zone observed in the
tandem transition joints was less than that of the sleeve joints.

Inside Diameter Counterbore Area

316 S. S.

Tantalum

254 μm (0.010 inches)

50X

23,336

316 SS

Ta

316 SS

Ta
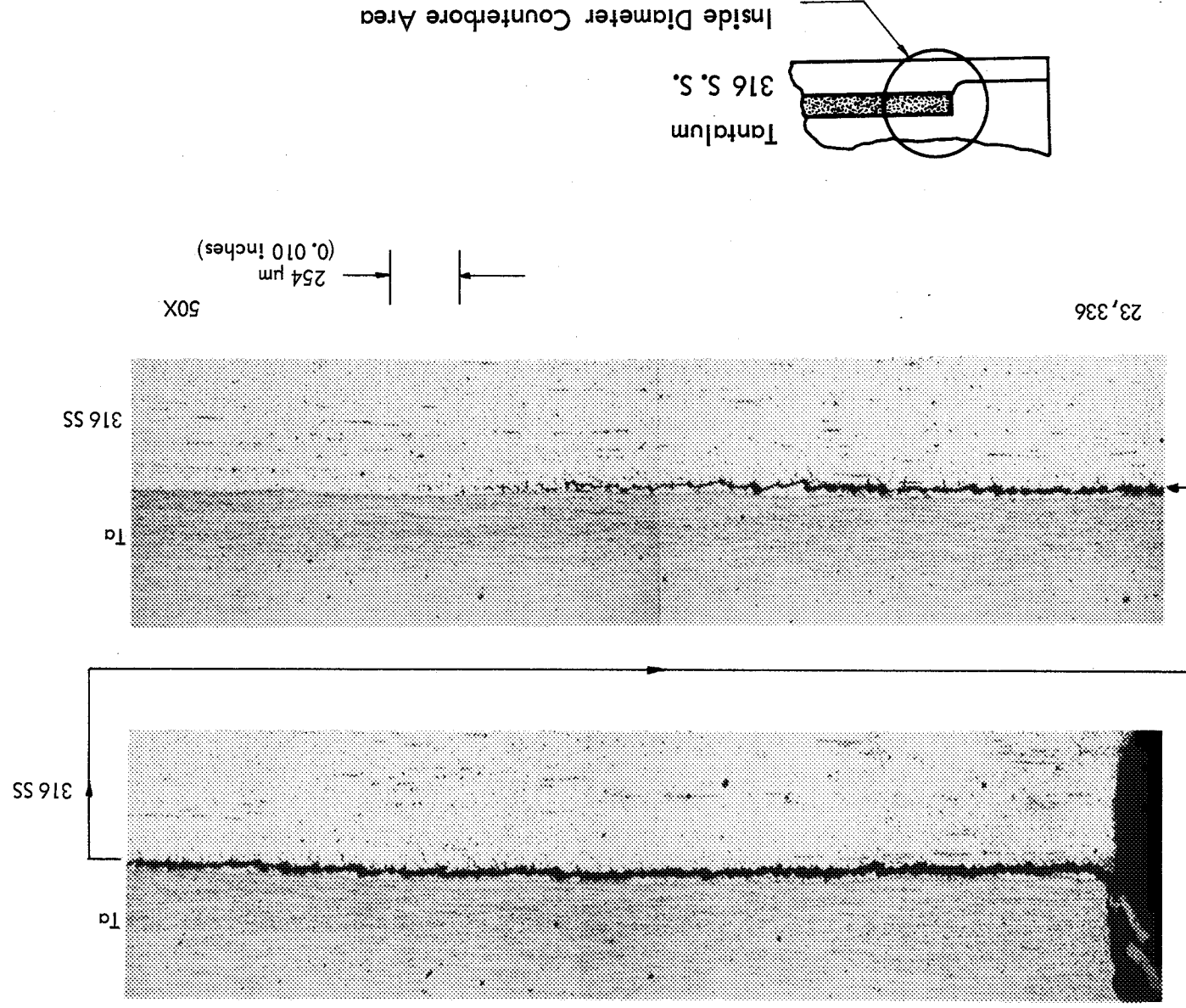
FIGURE 29. Bond Rupture Through Stainless Steel in Thermal Cycled Sleeve Joint No. 8, Counterbore Area
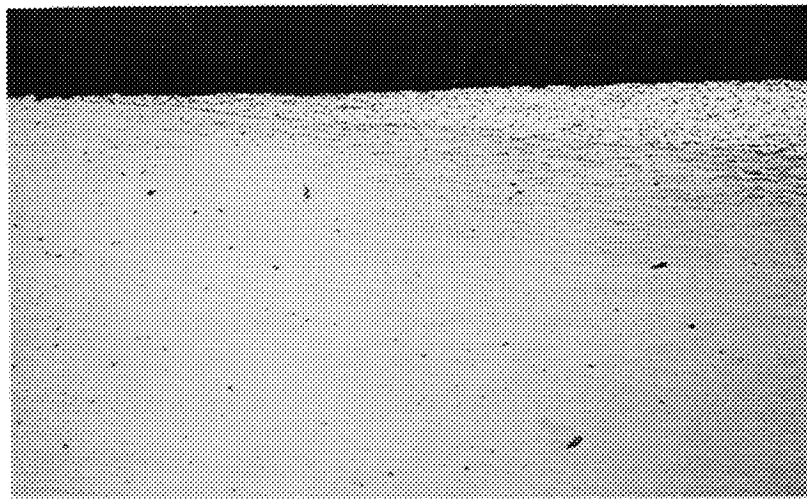
Outside Diameter
Feather Edge

316 SS

Ta

23, 332B   50X

Inside Diameter
Feather Edge

316 SS

Ta

23, 332A   50X
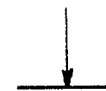
.254 μm
(0. 010 inch)

FIGURE 30.   Longitudinal Sections of Tandem Joint No. 11
Following Thermal Cycling Showing Well Bonded Feather Edge

Open
Tandem
Joint No. 7

Ta

316 SS

23,330 Inside Diameter Fissure in Stainless Steel Area   50X

Open
Tandem
Joint No. 8

316
SS

Ta

23,331 Outside Diameter Fissure in Tantalum Area   50X

. 254 μm
(0. 010 inch)

FIGURE 31. Longitudinal Sections of Tandem Joint Following
Thermal Cycling Showing Bond Line Fissures

316 S. S.

0.69 μm
(0.037 x 10^{-3} inches)
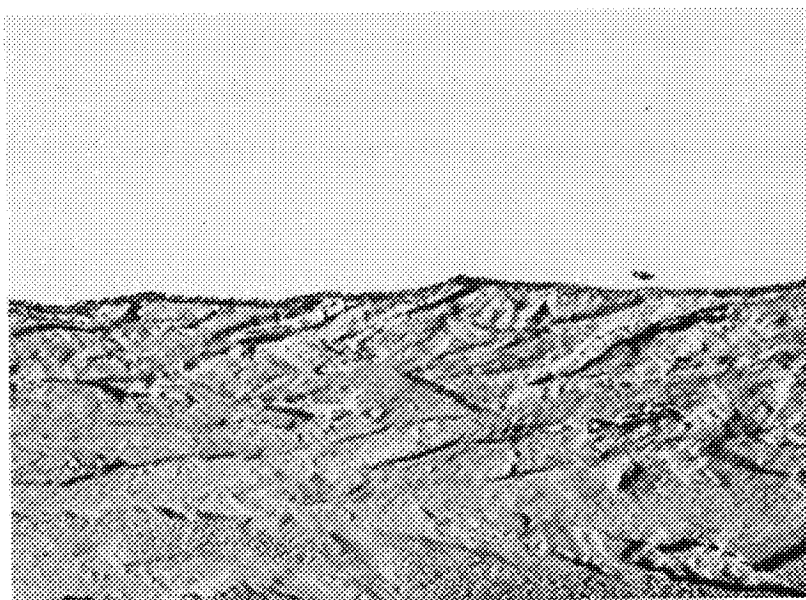
2.54 μm
(0.0001 inch)

Ta

22,492   1500X
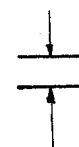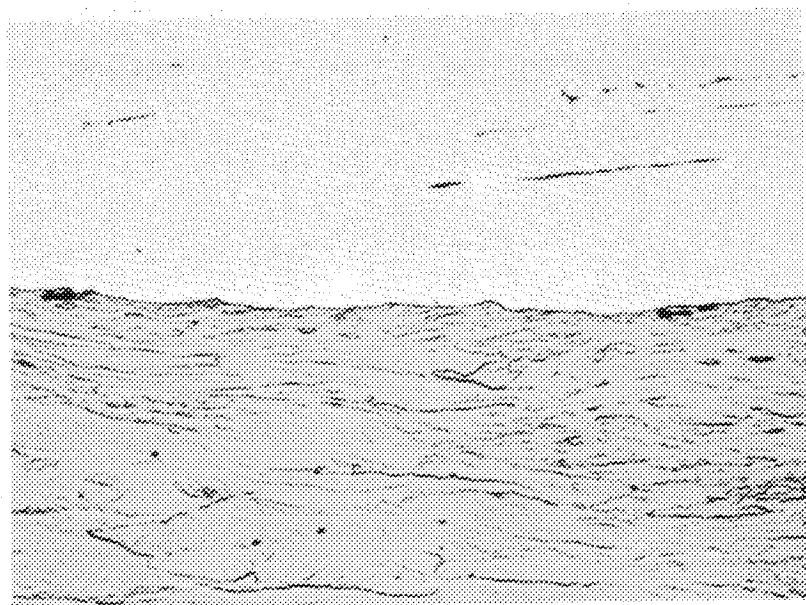
316 S. S.

25.4 μm
(0.001 inch)

Tantalum

Ta   316SS

22,492   400X
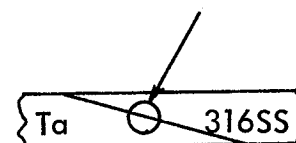
FIGURE 32.   Longitudinal Sections from Tandem Joint No. 3
in As-extruded Condition

Figure 33 shows longitudinal sections from two tandem joints following thermal cycling. As with the sleeve joints, a considerable volume of sigma phase is observed in the stainless steel. The diffusion zone width has not increased significantly following the thermal exposure as compared with the previous figure.

A hardness traverse for an as-extruded tandem joint is shown in Figure 34. Figure 35 provides a hardness comparison of the thermal cycled joints and also shows a marked difference between the pressurized and unpressured specimens,(pressurized transition joints were filled with helium to provide 1.72 MN/m^2 (250 psia) at 730°C, (1350°F), and unpressurized joints were open to vacuum). A similar lack of a hardness peak at the bimetal interface was observed for pressurized sleeve joints. Other than at the bimetal interface, no large increase in hardness was observed for the tantalum, which remains in a work hardened state from the 995°C (1825°F) extrusion temperature. As shown in Table 6, the interstitial chemical analysis for the tantalum layer was 14 ppm carbon, 23 ppm nitrogen, and 34 ppm oxygen which indicates a good commercial grade of starting material and a contamination-free extrusion process.

Brazed Joint

The J-8400* braze alloy transition joint which is vacuum brazed at temperatures from 1180°C (2160°F) to 1230°C (2250°F) provides a relatively thick 0.76 mm (0.030 inch) cast structure of complex microstructure. Figure 20, presented in the section on the electron beam microprobe results, is a composite longitudinal view of the entire tongue and groove brazed joint, with the tantalum in this case being the tongue section. Considerable erosion and dissolving of both the stainless steel and the tantalum occurs during the high temperature brazing operation producing a variety of phases during solidification and cooling to room temperature. Figure 36 is a a 400X magnification traverse of thick braze region of an as-brazed joint.

* J-8400 General Electric Company cobalt base braze.
  45 w/o Co - 21 w/o Cr - 21 w/o Ni - 8 w/o Si - 3.5 w/o W - 0.8 w/o B - 0.4 w/o C
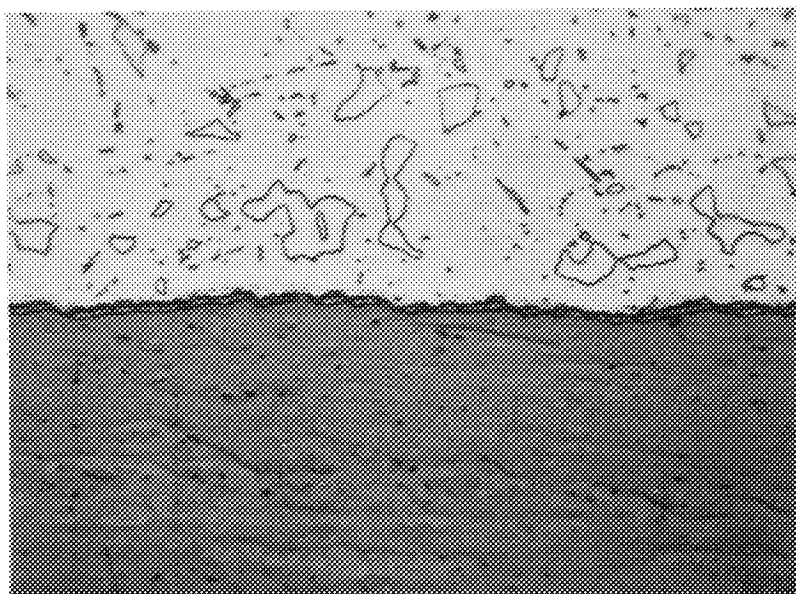
PLAN A
TANDEM JOINT
NO. 4

316 SS

0.42 μm
(0.017 x 10^{-3} inches)

Ta

23,329   600 Hrs. at 732°C (1350°F)   1500X
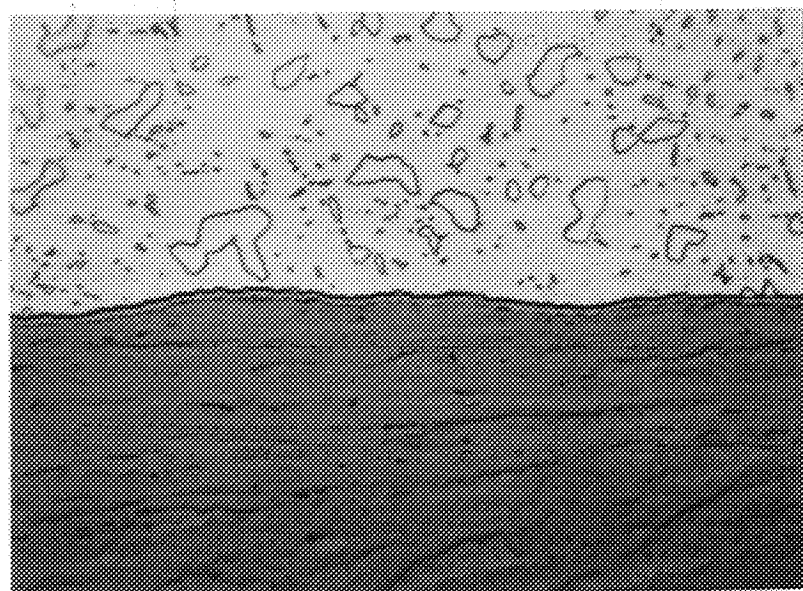
PLAN B
TANDEM JOINT
NO. 4

316 SS

0.76 μm
(0.030 x 10^{-3} inches)

Ta

2.54 μm
(0.0001 inch)

23,332   1600 Hrs. at 732°C (1350°F)   1500X

FIGURE 33.   High Magnification Comparison of Interdiffusion
Zone Growth in Thermal Cycled Tandem Joints
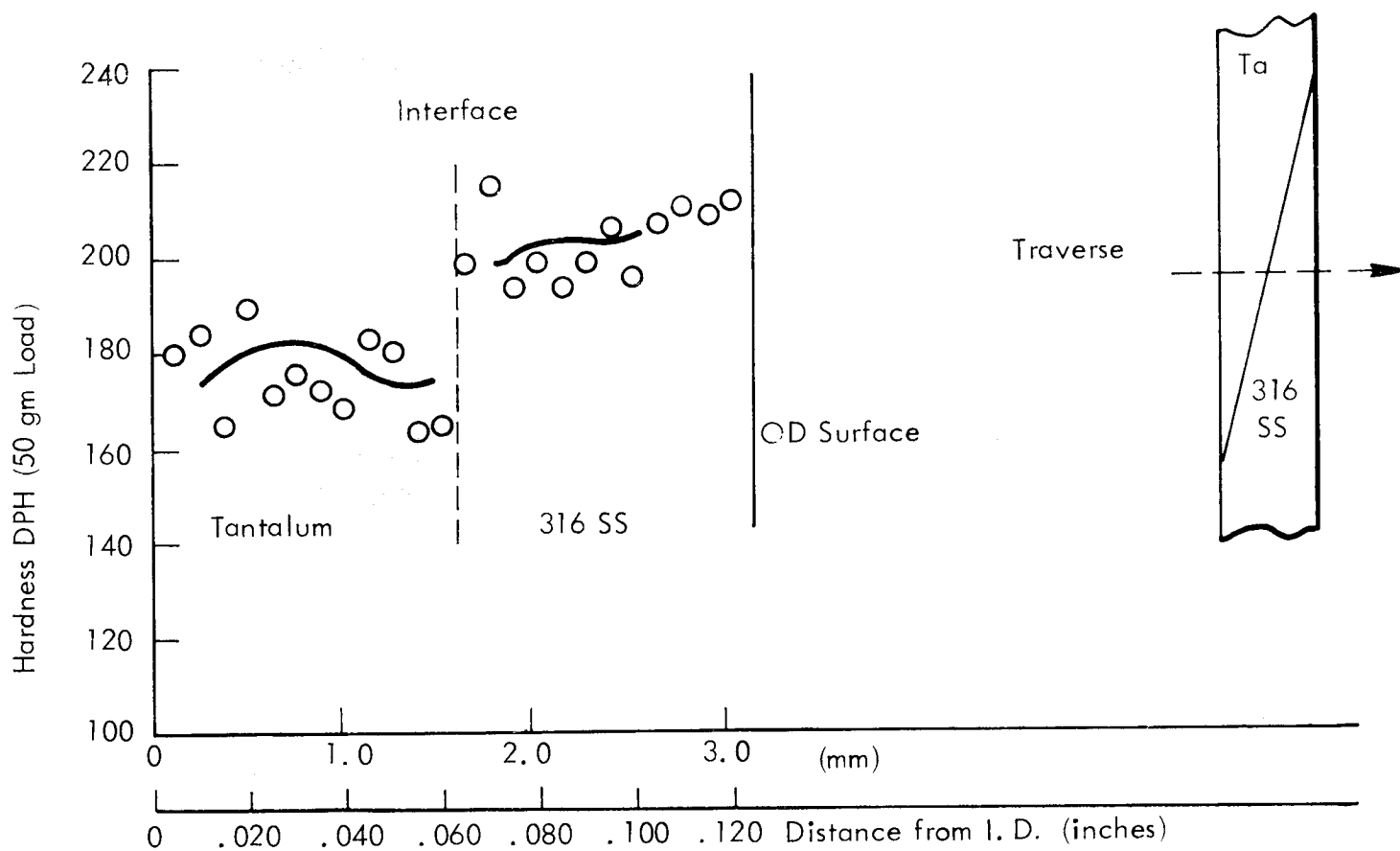
Figure 34. Tandem Joint No. 3, As-extruded Longitudinal Section

PRESSURIZED TANDEM JOINT NO. 6

OPEN TANDEM JOINT NO. 7

Distance from Inside Diameter
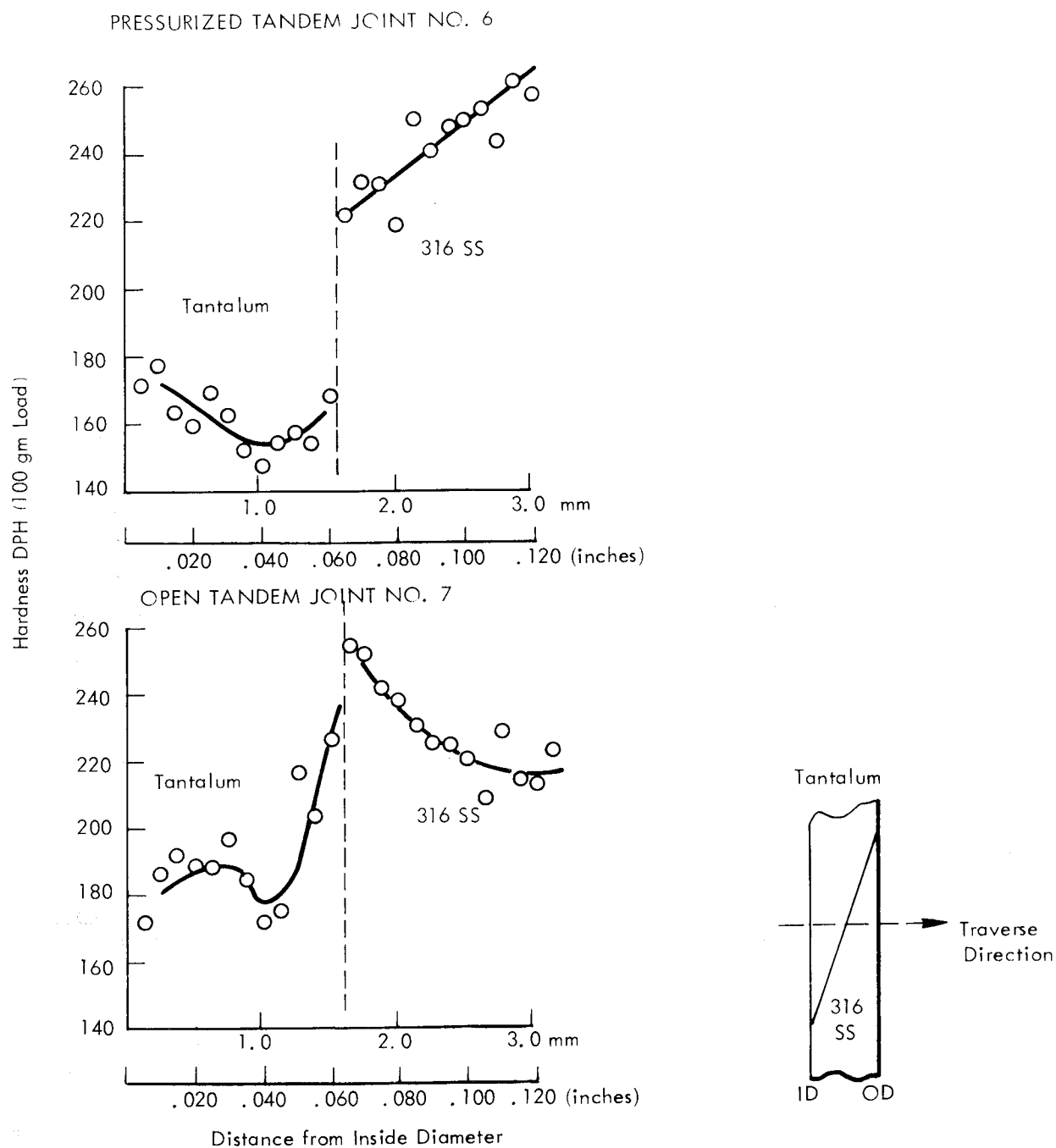
Figure 35. Hardness Traverse Across Wall Thickness of Thermal Cycled Tandem Joints
(Plan A)Comparing Pressurized and Open Specimens

21,711   400X
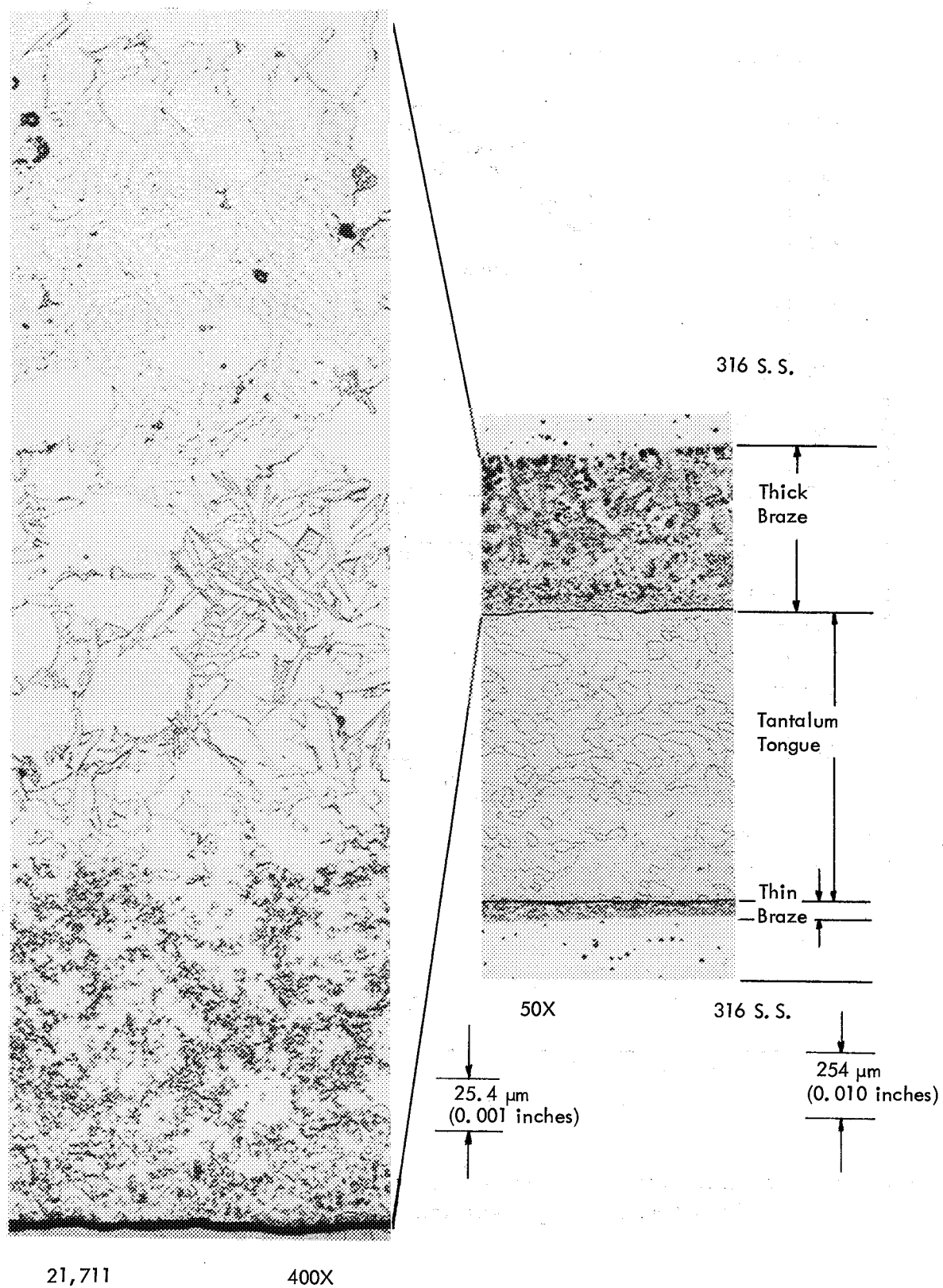
FIGURE 36. Braze Cross Section of As-brazed Joint No. 11 Longitudinal Section

A graded range of microstructure is evident from the tantalum area to the iron base, 316 SS. No attempt was made to identify by microprobe or x-ray diffraction the variety of micro-structures observed.

The effects of thermal exposure in the 730°C (1350°F) range produced a considerable volume of additional precipitation as shown by a comparison of Figure 37, the as-brazed micro-structure, and Figure 38, a section of brazed joint No. 11 exposed for 2000 hours at 730°C (1350°F). Precipitation occurs in the braze matrix and is apparently nucleated on existing precipitates. The rapid cooling rate 15°C (25°F) per minute from brazing temperature apparently retains a supersaturation of several alloying elements which precipitate at the 730°C (1350°F) test temperatures. Figures 37 and 38 are composed of 4 high magnification micrographs of the 0.76 mm (0.030 inch) braze zone shown in the composite Figure 36. The braze specimen exposed for 3000 hours at 730°C (1350°F) was similar to Figure 38.

A microhardness traverse of the braze joint did not show a significant increase in hardness following the precipitation inducing exposure at 730°C (1350°F) as shown by a comparison of Figures 39 and 40. A slight increase in stainless steel hardness was observed, due either to thermal strain hardening or the formation of sigma phase. The tantalum hardness remained low indicating negligible braze alloy penetration and a high purity braze environment. Interstitial chemical analyses of the tantalum components, Table 6, also indicated that no contamination and embrittlement of the tantalum component occurred.

316 S. S.

21,711   1500X

Tantalum

2.54 μm
(0. 0001 inch)
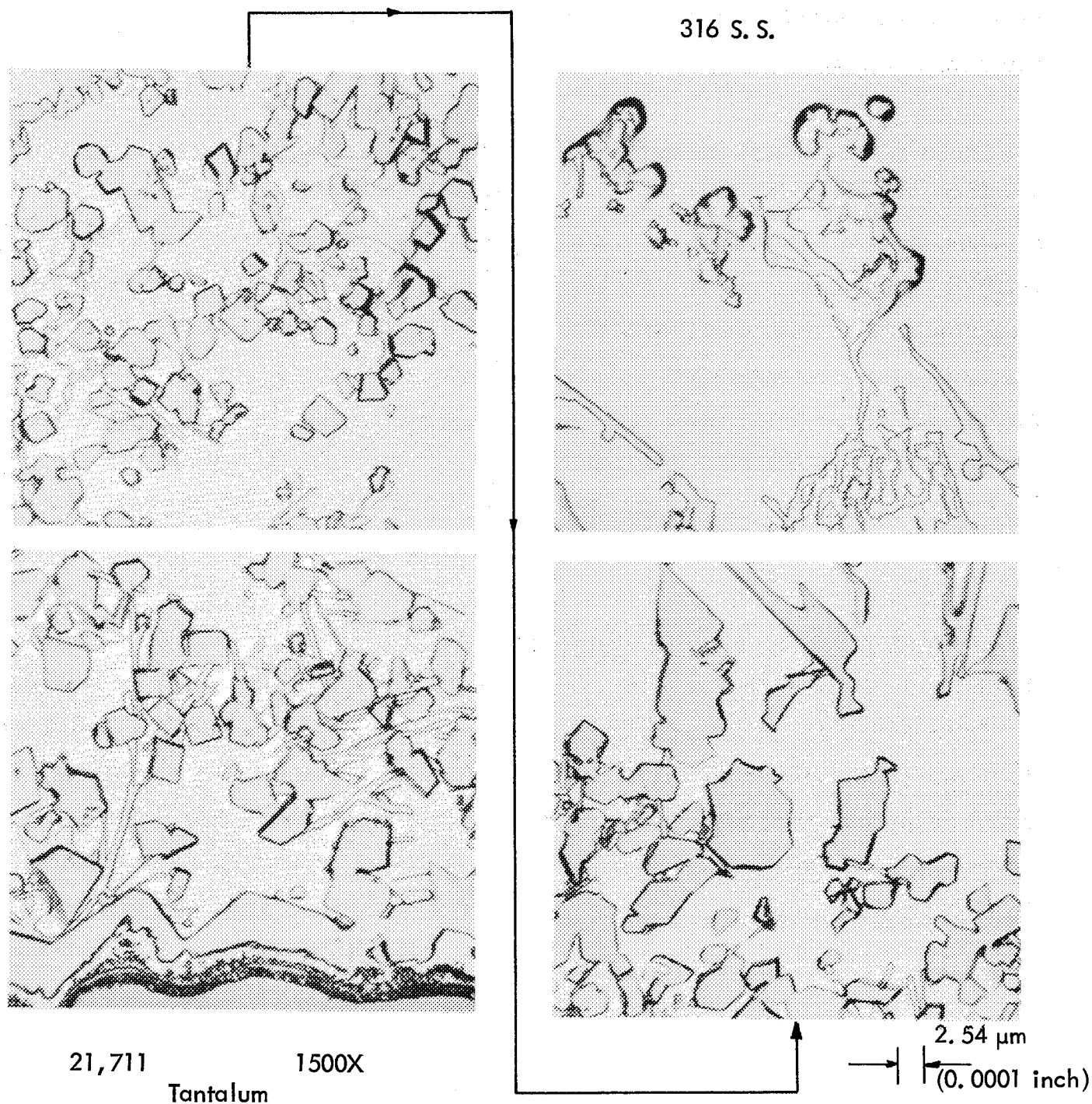
FIGURE 37.   As-brazed Joint Cross Section Joint No. 11

316 S. S.
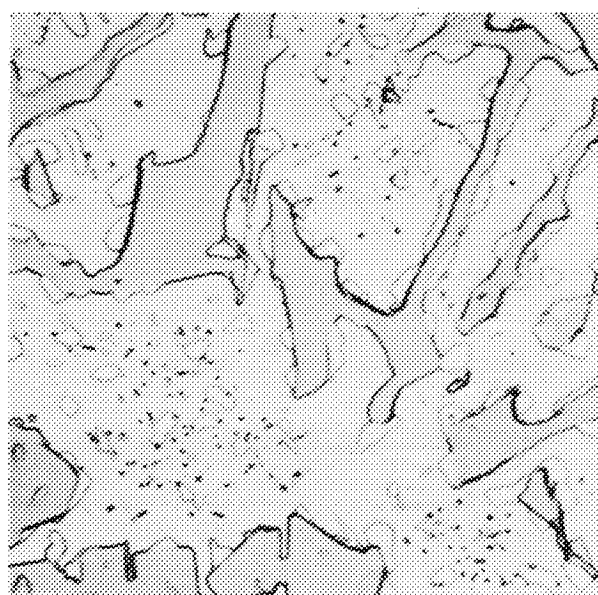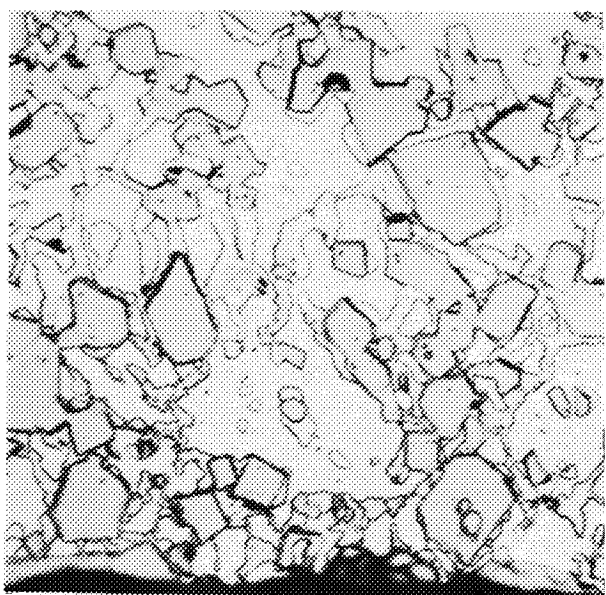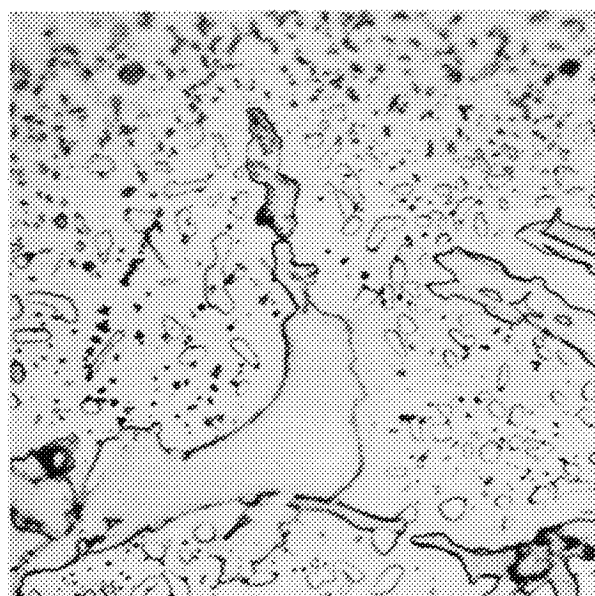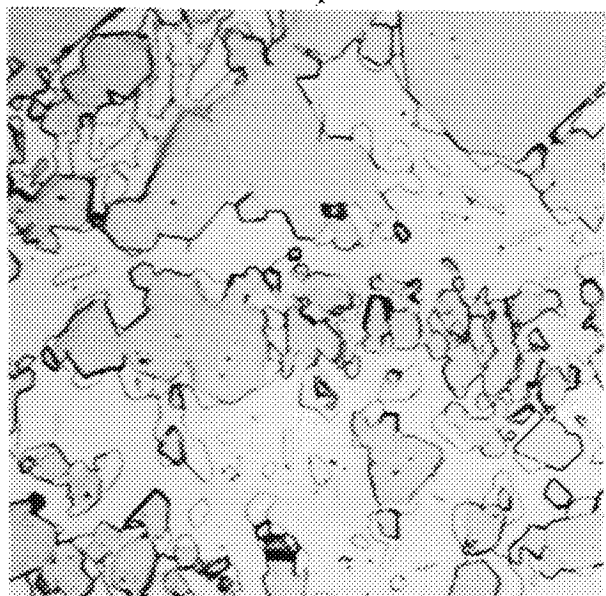
22,617   1500X
Tantalum

2. 54 μm   (0. 0001 inches)

FIGURE 38.   2000 Hours at 730°C (1350°F) (Braze Cross Section)
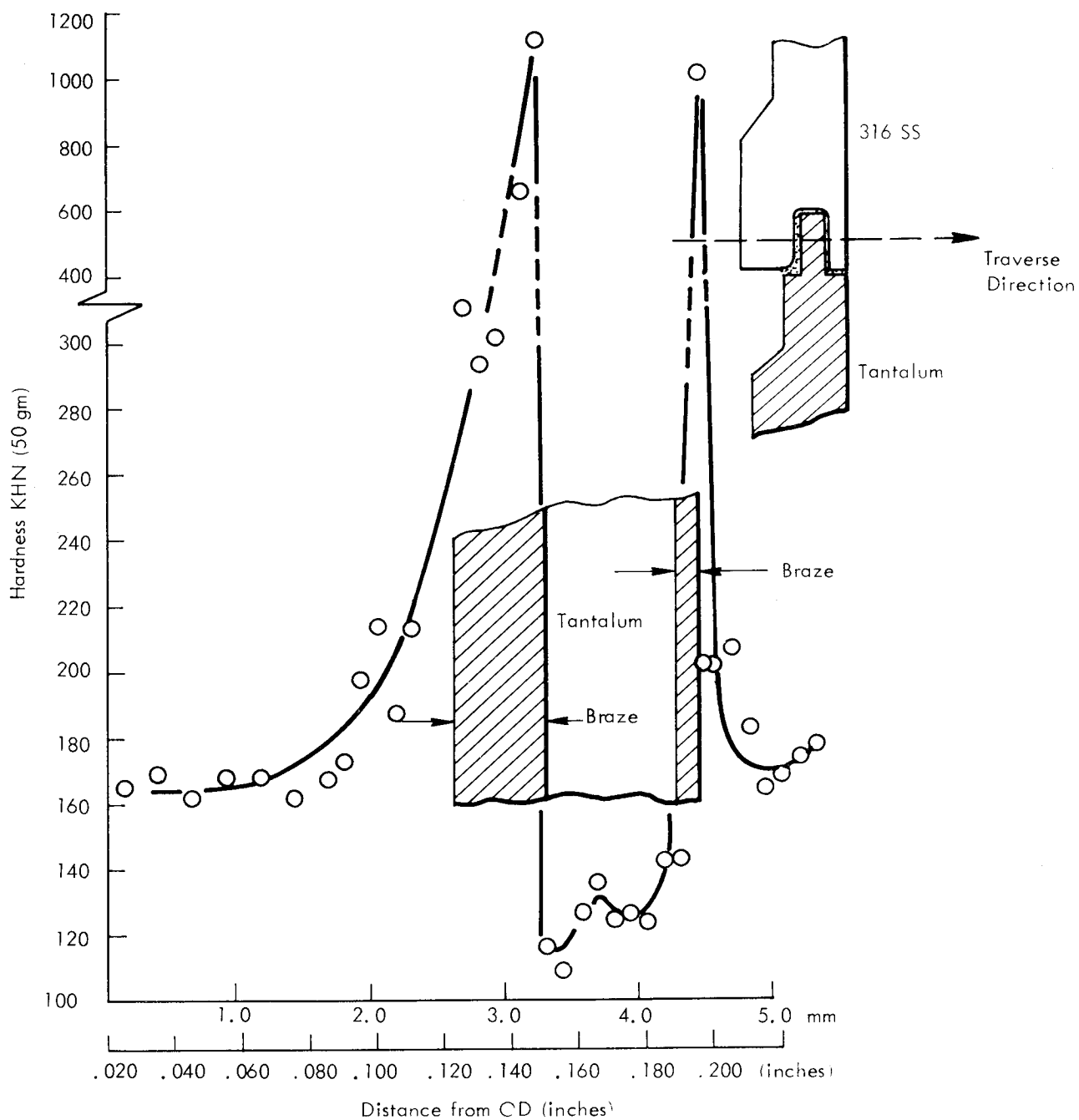
Figure 39. Hardness Traverse of As-Brazed Transition Joint No. 11

74
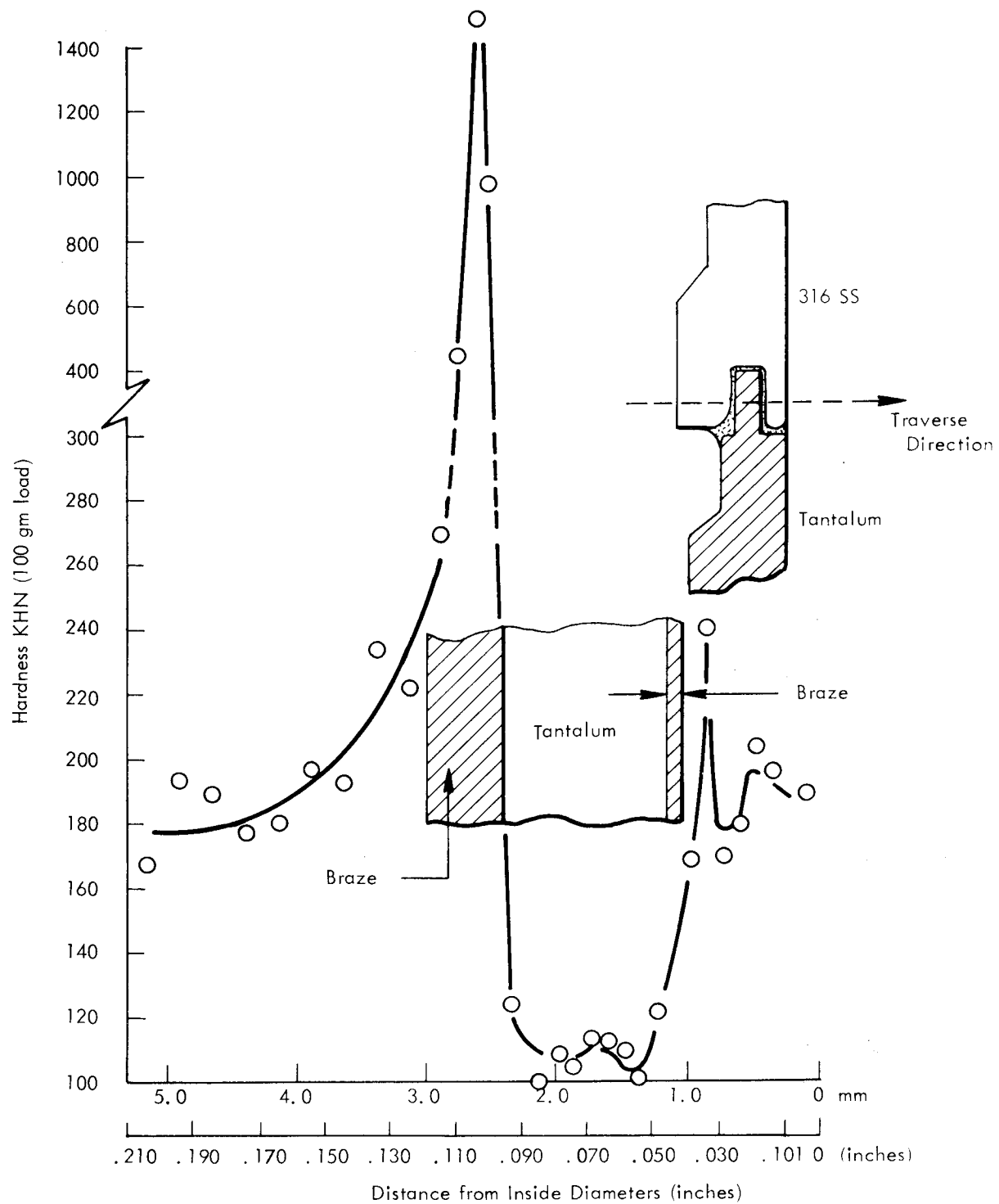
Figure 40. Hardness Traverse of Thermal Cycled Brazed Joint No. 15

E. Dimensional Changes

The coextruded tandem and sleeve joints experienced dimetral contraction in the stainless steel to tantalum transition area during thermal cycling. The sleeve joints additionally developed a cambered condition. The brazed transition joints were dimensionally stable throughout the thermal cycle tests.

Sleeve Joint - The severe distortion that occurred is shown in Figure 41, a photograph of specimen No. 6 following 100 thermal cycles. Prior to thermal cycling, the outside diameter surface was machined to size and diameter and camber dimensions were within 0.03 mm (± 0.002 inch). Table 10 compares before and after dimensions of the sleeve joint. The extreme ends or the reinforced flange area did not appreciably change in dimension but a severe diametral contraction was measured at the counterbored area where a transition from stainless steel to a bimetal bond occurs.

As was discussed in the fabrication description of the sleeve joints, the outside diameter of the initially cambered tubes was machined straight, producing a nonuniform wall thickness, which in the worst case, sleeve joint No. 5, varied from 7.7 mm (0.302 inch) to 5.2 mm (0.203 inch). As determined by radiograph, the tantalum portion of the total wall varied from 5.1 mm (0.200 inch) to 2.3 mm (0.090 inch). The possibility exists that the thermal cycle related cambering is produced by nonuniform shrinkage related to the tube wall nonuniformity, but no direct relation was observed. For instance, sleeve joint No. 4 displayed the worst camber, but both total wall thickness uniformity and tantalum to stainless steel ratio were better than average. Table 11 lists the total wall and tantalum portion variation in wall thickness for the flanged sleeve joints. In general, the better sleeve joints with the best dimensional properties were picked for the thermal cycle tests to avoid complications from nonuniform wall thickness.
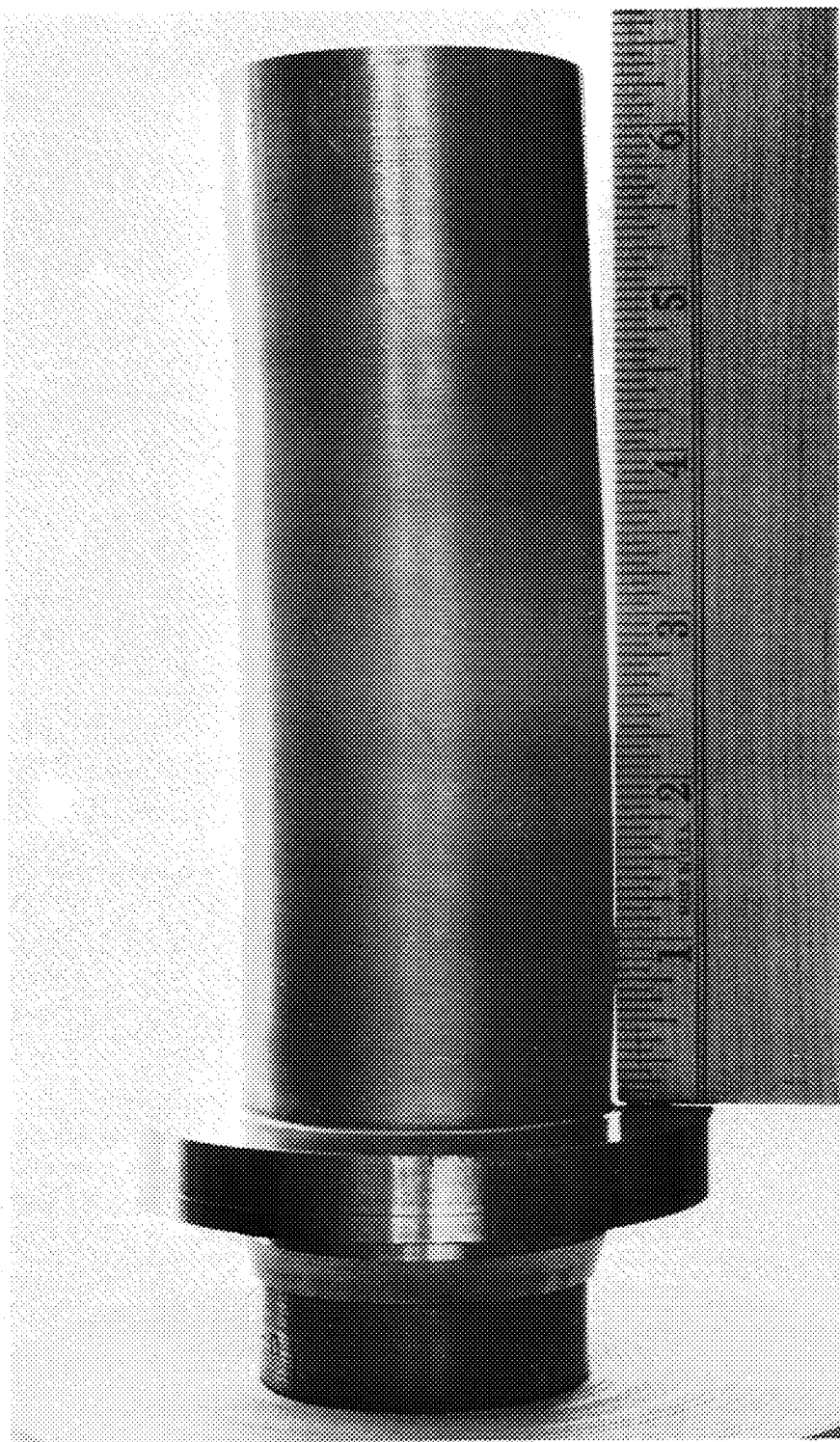
FIGURE 41. Sleeve Joint No. 6 Following 100 Thermal Cycles
Showing Severe Diametral Contraction and Camber

TABLE 10

Diameter Changes and Camber in Sleeve Joints After Thermal Cycling

SN	SN End			Necked Region			Center			
	Final	Initial	ΔX	Final	Initial	ΔX	Final	Initial	ΔX	
2	2.252	2.254	-.002	2.200	2.254	-.054	2.234	2.254	-.020	Inches
4	2.252	2.252	0	2.216	2.252	-.036	2.252	2.252	0	
6	2.252	2.254	-.002	2.250	2.254	-.004	2.264	2.254	+.010	
8	2.253	2.256	-.003	2.246	2.256	-.010	2.262	2.256	+.006	

SN	Tantalum End		
	Final	Initial	ΔX
2	1.886	1.886	0
4	1.972	1.970	+.002
6	1.956	1.954	+.002
8	1.870	1.869	+.001

SN	SN End			Necked Region			Center			
	Final	Initial	ΔX	Final	Initial	ΔX	Final	Initial	ΔX	
2	57.21	57.25	-.04	55.88	57.25	-1.47	56.74	57.25	-.51	mm
4	57.21	57.21	0	56.29	57.21	-.92	57.20	57.21	-.01	
6	57.21	57.25	-.04	57.15	57.25	-.10	57.50	57.25	+.25	
8	57.23	57.30	-.07	57.05	57.30	-.25	57.45	57.30	+.15	

SN	Tantalum End		
	Final	Initial	ΔX
2	47.90	47.90	0
4	50.09	50.04	+.05
6	49.68	49.63	+.05
8	47.50	47.47	+.03

2 - open 1600 hrs. at temperature
4 - open 600 hrs. at temperature
6 - pressurized, 600 hrs. at temp.
8 - pressurized 1600 hrs. at temp.

SN	Max. Dev. From ⊥	
	mm	inches
2	3.17	.125
4	5.08	.200
6	3.17	.125
8	4.06	.160

Max. Deviation from ⊥
SN End
Necked Region
Center
Tantalum End
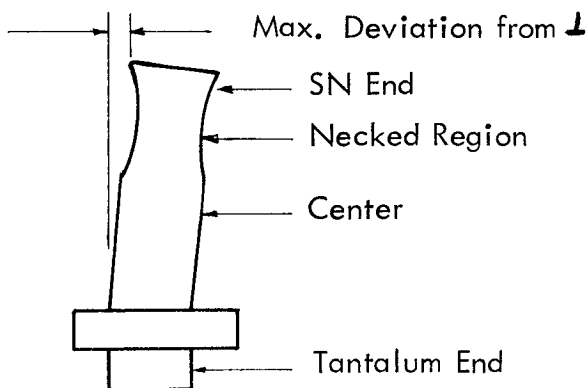
TABLE 11

Variation in Total Wall Thickness and in
Tantalum Thickness Near Center of Sleeve Joints

| SN | Millimeters | | | | Inches | | | |
| | Total Wall | | Tantalum | | Total Wall | | Tantalum | |
	Max.	Min.	Max.	Min.	Max.	Min.	Max.	Min.
2	67.8	64.3	44.4	34.3	.267	.253	.175	.135
4	68.1	63.2	53.3	49.5	.268	.249	.210	.195
5	76.7	51.6	50.8	22.9	.302	.203	.200	.090
6	66.3	64.8	43.2	35.6	.261	.255	.170	.140
7	66.8	64.8	39.4	36.8	.263	.255	.155	.145
8	68.8	63.2	41.9	34.3	.271	.249	.165	.135

Total Wall

Tantalum Thickness.
Radiograph Measurements

Sleeve Joint Transverse
Section, Near Center
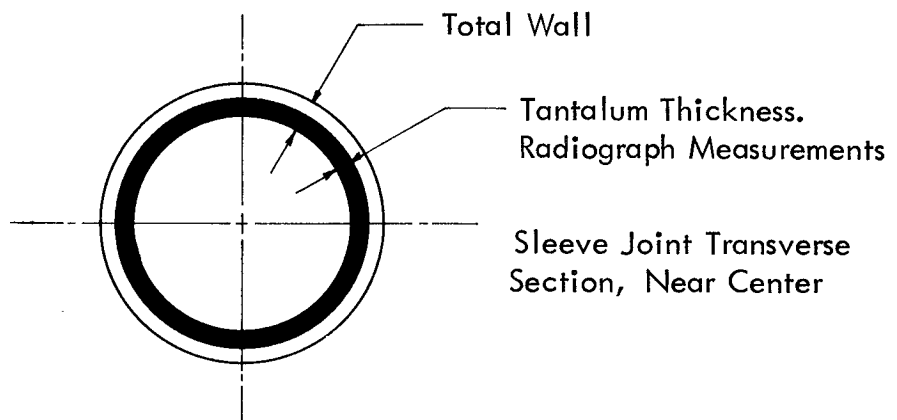
The internally pressurized specimens did not distort as severely as the open specimens. As listed in Table 10, specimens 6 and 8 were pressurized and specimens 2 and 4 were open. Also, specimen No. 2, which spent the longer time at temperature, (plan B specimens included a 1000 hour soak of 732°C (1350°F) prior to the last set of 10 thermal cycles), displayed a greater amount of contraction.

Tandem Joint - The similarly coextruded tandem transition joints also contracted dia-metrally at the tapered stainless steel to tantalum transition area. Table 12 lists the dimensional changes which were a maximum of 1.6 mm (1/16 inch). As with the sleeve joints, internal pressure during the thermal cycling minimized shrinkage.

A similar diametral contraction or necking phenomena was observed by Cameron[12] in the thermal cycling of larger 75 mm (3 inch) diameter columbium - 1% zirconium/316 SS tandem transition joints. A maximum diametral contraction of 2.6 mm (0.104 inch) was observed following 156 thermal cycles between 150° to 840°C, (300° to 1550°F) and 500 cycles between 780° to 870°C (1450° to 1600°F). As in these observations no leakage was observed in any of the thermal cycled specimens. Essentially no diametral change was observed in the tandem transition joints in areas farther from the bimetal interface.

Brazed Joint

As shown in Table 13, the braze joints had only minor dimensional changes either as a result of the thermal cycling or 1000 hour exposure to 732°C (1350°F).

TABLE 12

Diameter Changes in Tandem Joints After Thermal Cycling

SN	Millimeters			Inches			
	Final	Initial	ΔX	Final	Initial	ΔX	
6	51.00	50.98	+.02	2.008	2.007	+.001	316 SS O.D.
7	50.95	50.98	-.03	2.006	2.007	-.001	
8	51.00	51.00	0	2.008	2.008	0	
11	50.98	51.00	-.02	2.007	2.008	-.001	
6	50.85	50.98	-.13	2.002	2.007	-.005	Minimum O.D.
7	50.55	50.98	-.43	1.990	2.007	-.017	
8	49.33	50.98	-1.65	1.942	2.007	-.065	
11	50.60	50.98	-.38	1.992	2.007	-.015	
6	50.95	50.95	0	2.006	2.006	0	Tantalum O.D.
7	50.95	50.95	0	2.006	2.006	0	
8	51.00	51.00	0	2.008	2.008	0	
11	50.98	50.98	0	2.007	2.007	0	

Tantalum   316 SS

Tantalum OD   Minimum OD   316 SS OD
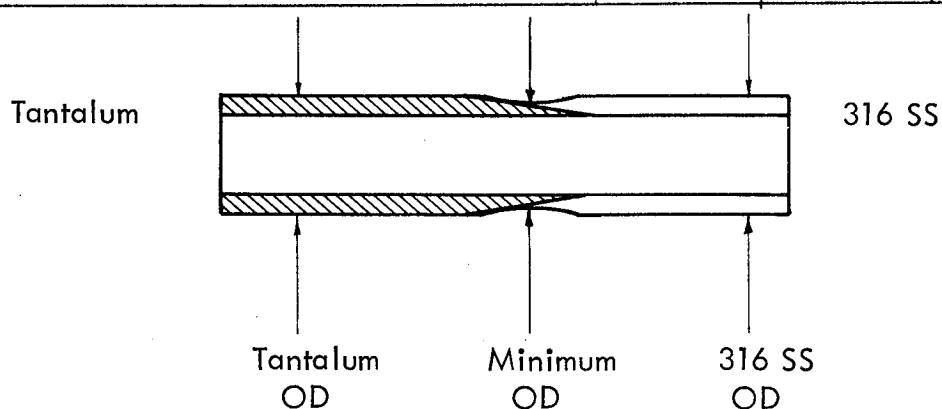
6   Pressurized, 600 hrs.at temperature.
7   Open, 600 hours at temperature.
8   Open, 1600 hours at temperature.
11   Pressurized, 1600 hrs. at temperature.

TABLE 13

Diameter Changes in Brazed Joints After Thermal Cycling

SN	Millimeters			Inches			Location
	Final	Initial	ΔX	Final	Initial	ΔX	
8	50.90	50.93	-.03	2.004	2.005	-.001	Tantalum O. D.
10	51.03	50.90	+.13	2.009	2.004	+.005	
15	51.10	51.10	0	2.012	2.012	0	
20	51.16	51.21	-.05	2.014	2.016	-.002	
8	49.35	49.28	+.07	1.943	1.940	+.003	Undercut Tantalum O. D.
10	49.02	48.97	+.05	1.930	1.928	+.002	
15	49.48	49.30	+.18	1.948	1.941	+.007	
20	49.12	49.40	-.28	1.934	1.945	-.009	
8	54.00	54.10	-.10	2.126	2.130	-.004	316 SS Ridge O. D.
10	53.44	53.49	-.05	2.104	2.106	-.002	
15	53.98	54.05	-.07	2.125	2.128	-.003	
20	53.92	54.00	-.08	2.123	2.126	-.003	
8	50.80	50.82	-.02	2.000	2.001	-.001	316 SS Sleeve O. D.
10	50.77	50.80	-.03	1.999	2.000	-.001	
15	50.77	50.88	-.03	1.999	2.000	-.001	
20	50.80	50.85	-.05	2.000	2.002	-.002	

Tantalum OD

Undercut Tantalum OD
316 SS Ridge OD

316 SS Sleeve OD
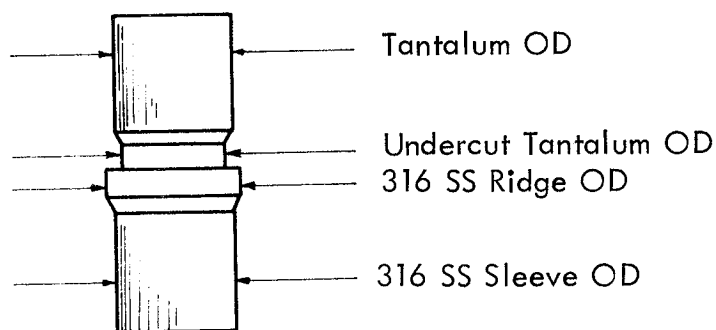
8 - Pressurized, 600 hours at temperature
10 - Open, 1600 hours at temperature
15 - Pressurized, 1600 hours at temperature
20 - Open, 600 hours at temperature

VII. SUMMARY OF RESULTS

- Both extruded and brazed bimetal transition joints, providing a 5 cm (2 inch) diameter connection between 316 stainless steel and tantalum, survived 100 thermal cycles from 120°C (250°F) to 730°C (1350°F) and remained helium leak tight. However, progressive bimetal bond deterioration was observed for the extruded joints as the thermal cycles continued. The deterioration was measured by liquid penetrant indications of fissures at the external surface bondline and by ultrasonic inspection. None of the defects led to a through leakage during the test program. All of the brazed joints displayed inside diameter liquid penetrant defects in the as-received condition, which did not enlarge significantly with thermal cycling and are probably indicative of braze shrinkage.

- Twelve transition joints were tested in all, providing a good overall estimate of process reproducibility.

- The coextruded sleeve and tandem transition joints displayed diametral contraction in the bimetal transition area as a result of thermal cycling. The sleeve joints also become cambered during the thermal cycling.

- The brazed transition joints had only minor dimensional changes during the thermal cycle tests.

- At the thermal cycling maximum temperature, 730°C (1350°F), no significant diffusion occurred during the 1600 hour total time at temperature to impair the bimetal bond strength. Based on the interdiffusion zone growth rates observed at 730°C (1350°F), a 500 year lifetime would be expected for 316 stainless steel-tantalum at this temperature were a maximum diffusion zone thickness the only consideration.

- Half of the transition joints were internally pressurized during thermal cycling to simulate operating pressures of 1.72 MN/m^2, (250 psig). The internal pressure had no adverse effect on bimetal bond durability and, in fact, minimized a diametral contraction phenomenon on the sleeve and tandem joints. These results indicate that the state of stress imposed by the overall system will affect the transition joint performance.

- Considerable effort was placed in developing an ultrasonic inspection technique since this was a nondestructive inspection technique that could be used to determine the progressive degradation of an interface as opposed to helium leak checking which can only indicate the case of complete bimetal joint failure. Ultrasonic inspection techniques

may also be used for "in service" inspection of assembled components. Good results were obtained in ultrasonic inspection in the sense that known defects of acceptable minimum size were determined in all three types of transition joints, and a slight progressive deterioration of bond quality was observed in the sleeve and tandem joint. Inspection difficulties with the small size braze joint, partly related to as-fabricated shrinkage voids which did not propagate during thermal cycling, prevented following any sort of braze joint degradation as a function of test time.

VIII. CONCLUDING REMARKS

- The brazed joints are the most durable based on the results of this evaluation program. It is important to consider, however, that the program was an economical approximation of the operational life of a SNAP-8 mercury boiler, and severe departures from the specific test condition, in terms of test environment or transition joint dimensions and materials, could alter the conclusions.

- One possible limitation of brazed transition joints is that very little strain can be accommodated in the braze area proper, and eventual braze joint failures may be sudden rather than the progressive deterioration observed in the extruded transition joints. However, as long as the low strain tolerance of the braze metal is realized and accommodated in the system design, the demonstrated in-service durability of brazed joint can be utilized.

- If fluid flow or mechanical restraint conditions require a constant diameter along the transition joint length, the tandem transition joint may offer positive advantages. The brazed joint has been most successful using a thickened tongue-and-groove transition section, and the sleeve joint inherently will have a stepped section where the bimetal components are turned and counterbored.

In summary, tantalum to 316 stainless steel transition joints brazed with cobalt base J-8400 filler were the best choice for cyclic operation under SNAP-8 conditions. For other system applications, however, the significant amount of favorable peripheral experience with tandem transition joints warrants their consideration for containment or structural applications.

VIII. REFERENCES

1. Hsia, Edward S., "Analysis and Testing of a Single Tube Mercury Boiler", General Electric Nuclear System Programs Space Div. GESP-650, NASA-CR-72897, September 1971.

2. Buckman, R. W., Jr., R. C. Goodspeed, "Evaluation of Refractory/Austenitic Bimetal Combinations", Westinghouse Astronuclear Laboratory, NASA CR-1516, WANL-PR-EE-004, August 1969, Contract NAS 3-7634.

3. Kass, J. N., D. R. Stoner, "Evaluation of Tantalum/316 Stainless Steel Bimetallic Tubing", Westinghouse Astronuclear Laboratory, NASA CR-1575, WANL-PR-PPP-001, Contract NAS 3-10601, June 1968.

4. Stoner, D. R., Final Report, "Joining Refractory /Austenitic Bimetal Tubing", Westinghouse Astronuclear Laboratory WANL-PR-(ZZ)-001, NASA-CR-72275, Contract NAS 3-7621, October, 1966.

5. "SNAP-8 Electrical Generation System Development Program, " NASA CR-72860, July 1971, Aerojet General Corporation, report on Contract NAS 3-13458.

6. Thompson, S. R., "Mercury Thermal Shock Testing of 2-1/2 Inch Diameter Bimetallic Joints for SNAP-8 Applications", Nuclear System Program Space Div., General Electric Co., Cincinnati, O., GESP-587, NASA CR-72829.

7. Spagnuolo, A. C., "Evaluation of Tantalum-to-Stainless Steel Transition Joints, " Lewis Research Center, Cleveland, O., NASA TM X-1540, 1968.

8. "Compact Thermoelectric Converter System Technology, " Quarterly Report, WANL-PR-(EEE)-048, August, 1972.

9. Friedman, Gerald I., Final Report, "Coextruded Tantalum - 316 Stainless Steel Bimetallic Joints and Tubing", NASA CR 72761, October 1970, Whittaker Corporation.

10. Thompson, S. R., J. D. Marble, and R. A. Ekvall, "Development of Optimum Fabrication Techniques for Brazed Ta/Type 316 SS Tubular Transition Joints", Nuclear Systems Programs Space Systems, General Electric, Cincinnati, Ohio, GESP-521, 1970. NASA CR-72746.

11. Ferry, P. B., and J. P. Page, "Metallurgical Study of Niobium/Type 316 Stainless Steel Duplex Tubing", NAA-SR-11191, January 5, 1966.

12. Cameron, Harry M., "Thermal Cycling Test on a 3-Inch Diameter Columbium-1 Percent Zirconium to 316 Stainless Steel Transition Joint", Lewis Research Center - Cleveland, Ohio, NASA-TMX-2118, November 1970.

DISTRIBUTION

NASA CR 121027

<div align="right">No. of Copies</div>

NASA-Lewis Research Center
21000 Brookpark Road
Cleveland, OH 44135

Attn:		
P. L. Stone, MS 105-1		10
E. J. Kolman, MS 500-313		1
N. T. Saunders, MS 105-1		1
C. P. Blankenship, MS 105-1		1
R. L. Davies, MS 106-1		1
R. W. Hall, MS 105-1		1
G. M. Ault, MS 3-13		1
M. J. Saari, MS 500-202		1
W. A. Paulson, MS 49-2		1
P. H. Lustig, MS 49-2		1
Report Control Office, MS 5-5		1
Library, MS 60-3		1
Technical Information Office, MS 3-11		1
Lewis Office of R&QA, MS 500-211		1

NASA Headquarters
Washington, DC 20546

Attn:		
RW/G. Deutsch		1
RWM/J. Gangler		1
NS-1/J. Lynch		1
NS-2/C. Johnson		1
NS-2/R. Anderson		1

NASA Scientific & Technical Information Facility   12
Attn: NASA Representative
Box 5700
Bethesda, MD

NASA Ames Research Center   1
Attn: Library
Moffett Field, CA 94035

NASA Flight Research Center   1
Attn: Library
P. O. Box 274
Edwards, CA 93523

NASA-Goddard Space Flight Center   1
Attn: Library
Greenbelt, MD 20771

Jet Propulsion Laboratory   1
Attn: Library
4800 Oak Grove Drive
Pasadena, CA 91103

NASA-Langley Research Center   1
Langley Station
Attn: Library
Hampton, VA 23365

NASA-Manned Spacecraft Center   1
Attn: Library
Houston, TX 77001

NASA-Marshall Space Flight Center   1
Attn: Library
Huntsville, AL 35812

NASA Western Operations Office   1
Attn: Library
150 Pico Blvd.
Santa Monica, CA 90406

AFSC   1
Aeronautical Systems Division
Attn: Library
Wright-Patterson Air Force Base, OH 45433

U. S. Atomic Energy Commission   1
Technical Information Service Extension
P. O. Box 62
Oak Ridge, TN 37831

U. S. Atomic Energy Commission
Attn: J. Simmons   1
       Library   1
Washington, DC 20545

U. S. Atomic Energy Commission
Attn: E. E. Hoffman   1
       Library   1
Germantown, MD 20767

Argonne National Laboratory   1
Attn: Library
9700 South Cass Avenue
Argonne, IL 60440

3

Battelle Memorial Institute
Attn: MCIC   1
       Library   1
505 King Avenue
Columbus, OH   43201

Brookhaven National Laboratory
Attn: Dr. D. H. Gurnsky   1
       Library   1
Upton, Long Island
New York 11973

AiResearch Manufacturing Company   1
Division of the Garrett Corporation
Attn: Library
Sky Harbor Airport
403 So. 36th Street
Phoenix, AZ   85034

AiResearch Manufacturing Company   1
Division of the Garrett Corporation
9851-9951 Sepulveda Blvd.
Los Angeles, CA   90009

AVCO   1
Research and Advanced Development Department
Attn: Library
201 Lowell Street
Wilmington, MA   01887

Battelle-Northwest Labs   1
Attn: Library
P. O. Box 999
Richland, WA   99352

General Electric Company   1
Missile and Space Vehicle Department
Attn: Library
3198 Chestnut Street
Philadelphia, PA   19104

General Electric Company   1
Vallecitos Atomic Laboratory
Attn: Library
Pleasanton, CA   94566

No. of Copies

General Electric Company   1
Technical Information Center
Building 700, Mail Drop U-32
Evendale, OH 45215

Gulf-General Atomics   1
Attn: Library
LaJolla, CA 92037

IIT Research Institute   1
Attn: Library
10 W. #5 Street
Chicago, IL 60616

Lawrence Radiation Lab   1
Attn: Library
Livermore, CA 94550

Los Alamos Scientific Laboratory   1
Attn: Library
Los Alamos, NM 87544

Materials Research and Development   1
Manlabs, Inc.
Attn: Library
21 Erie street
Cambridge, MA 02139

Materials Research Corporation   1
Attn: Library
Orangeberg, NY 10962

MSA Research Corporation   1
Attn: Library
Callery, PA 16024

National Research Corporation   1
Attn: Library
70 Memorial Drive
Cambridge, MA 02142

North American Rockwell Corporation
Atomics International Division
Attn: T. A. Moss   1
       Library   1
8900 DeSoto Avenue
Canoga Park, CA 91304

5

Sandia Corporation   1
Attn: Library
P. O. Box 5800
Albuquerque, NM 87116

Solar   1
Attn: Library
2200 Pacific Highway
San Diego, CA 92112

Southwest Research Institute   1
Attn: Library
3500 Culebra Rd.
San Antonio, TX 78228

TRW, Inc.
Attn: K. Sheffler   1
      Library   1
23555 Euclid Avenue
Cleveland, OH 44117

Cabot Corporation/Stellite Division
Attn: Library   1
1020 West Park
Kokomo, IN 46901

Union Carbide Corporation   1
Parma Research Center
Attn: Library
P. O. Box 6115
Cleveland, OH 44101

United Nuclear   1
Attn: Library
Grossland Road
Elmsford, NY 10523

Wah Chang Corporation   1
Attn: Library
Albany, OR 97321